

ON LOAD CORE LOSS MEASUREMENT AND ALLIED
PROBLEMS IN HIGHLY FLUXED TRANSFORMER CORES

Thesis presented to the University of London
for the award of the degree of Master of Philosophy

Riazul Haque
Department of Electrical Engineering,
Imperial College of Science and Technology,
London S.W.7

March, 1978

ABSTRACT

This thesis deals with the measurement of core loss in a loaded transformer at different loading conditions. This is in contrast to the measurement of core loss of a power transformer by open circuit test. The object of this work is to investigate the dependence of core loss on load power factor and from the results obtained it is shown that this loss is more sensitive to leading than to lagging reactive loads.

The approach is made towards direct measurement of the loss by the extraction of the excitation component of current from the input and output currents of the loaded transformer rather than by computation from input and output powers.

A survey of possible methods of extraction of the excitation current has been carried out and a comparison is made with the method developed. The errors and the limitations of each method have also been studied. The measurement of core loss at different load angles in a generator transformer designed to operate at high flux density is made by dynamometer wattmeter from the extracted excitation current and compared with measurement made with a modified electronic wattmeter using its multiplication characteristics. A three-phase wattmeter based on Hall effect multipliers has been designed to measure the core loss from a signal proportional to excitation current obtained by the method developed. Record of the instantaneous power as a periodic function of time and of the cyclic variation of flux linkage with current was obtained. Both showed perceptible variation with load power factor.

A novel technique for the synthetic full load testing of a three-winding transformer has been investigated. A practical method for measuring the core and copper losses of such a transformer at different loading conditions is discussed and tested. The rated voltage is impressed on one winding and the rated current is circulated in the other two windings without requiring sources of the rated power in this method of testing.

ACKNOWLEDGEMENT

The author wishes to express his sincere gratitude to his supervisor, Dr. P.H.G. Allen, for providing the inspiration behind the project, his keen interest, encouragement and advice during the course of the work described in this thesis.

Many colleagues have been particularly helpful. Discussions with them have invariably been both stimulating and useful, which improved the overall quality of this work.

The author is thankful to the technical staff of the Heavy Current Laboratory of the Department of Electrical Engineering, Imperial College, for their assistance and help. Thanks also due to Mrs Shelagh Murdock for typing this thesis and bringing it to a presentable form.

Finally, the author is grateful to his wife for her patience, and to the Trustees of the Wali Mohammed Fellowship for financial support provided for a part of the project.

TABLE OF CONTENTS

4.

	<u>Page</u>
Abstract	2
Acknowledgement	3
Table of Contents	4
<u>Chapter One:</u> Introduction	9
1.1 General	9
1.2 Nature of the Problem	10
1.3 Previous Work on the Problem	12
1.4 Summary of the Present Work	15
<u>Chapter Two:</u> Measurement of Iron Loss by Open Circuit Test in a Highly Fluxed Three-Phase Three-Limb Core-Type Transformer	17
2.1 Power Measurement in a Polyphase System	17
2.2 The Three-Phase Magnetic Core and Phase Excitation Currents	17
2.3 Possible Connections for Core Loss Measurement by the Two-Wattmeter Method	19
2.4 Power Relation in the Three-Wattmeter Method of Core Loss Measurements	23
2.5 Numerical Computation of Power Relations	24
2.6 Experimental Results	26
2.7 Effect of the Wattmeter Error	27
2.8 Effect of the Neutral Connection on the Measurement of Core Loss by Open Circuit Test	30
<u>Chapter Three:</u> The Excitation Current and its Separation from the Main Currents of a Loaded Transformer	32
3.1 Introduction	32
3.2 Relation between Excitation Current and Main Currents	34
3.3 Essentials for Methods of Separation	36
3.4 Methods of Separation of Excitation Current	36
3.4.1 Direct Differential Method	37
3.4.1.1 Theoretical Basis	37
3.4.1.2 Experimental Considerations	38
3.4.1.3 Errors and Limitations of Direct Differential Method	40

	<u>Page</u>
3.4.2 The Current Transformer Differential Method	40
3.4.2.1 The Method	40
3.4.2.2 Inherent Errors	43
3.4.2.3 Error Evaluation	44
3.4.2.4 Operational Errors	49
3.4.2.5 Dependence of Errors on Operating Conditions	50
3.4.2.6 Modification of Errors	52
3.4.2.7 Current Transformers and the Present Test	53
3.4.2.8 Use of Compensated Current Transformers	60
3.4.2.9 Use of Current Sensors	60
3.4.2.10 Use of a Single Current Transformer	61
3.4.3 Series Resistance Differential Method	62
3.4.3.1 The Method	62
3.4.3.2 Effects of R_A and R_B on the Impedance of the Transformer	63
3.4.3.3 Effects of Ratio and Phase Angle Error of an Isolating Transformer	66
3.4.3.4 Flexibility of the Method	66
<u>Chapter Four:</u> Possible Methods of Measurement of Core Loss on Load; their Comparison, Choice and Limitation	68
4.1 Core Loss	68
4.2 The Core Loss Current	69
4.3 Equivalent Circuit with Eddy Current and Hysteresis Loss	70
4.4 Computation of Core Loss	72
4.5 Independence of Power on the Harmonics in the Currents and Voltages	74
4.6 Methods used in Core Loss Measurement	77
4.6.1 Measurement with Dynamometer Wattmeter	77
4.6.2 Measurement with VAW Meter Model 102	78
4.6.3 Measurement with a Hall Effect Wattmeter	80
4.6.4 Derivation of Core Loss from the Instantaneous Power Loss	81
4.6.5 Core Loss Display through Dynamic Hysteresis Loss Loop	82

	<u>Page</u>
<u>Chapter Five:</u> Three-Phase Electronic Wattmeter using Hall Effect Multipliers	88
5.0 Introduction	88
5.1 Hall Effect	89
5.1.1 Explanation of the Hall e.m.f.	89
5.1.2 Magnitude of the Hall e.m.f.	89
5.2 The Wattmeter	91
5.2.1 The Advantages	91
5.2.2 The Limitations	92
5.3 Criteria of Circuit Design	93
5.3.1 Frequency Dependence of Series Resistor R_S	96
5.3.2 Frequency Dependence of the Magnetizing Coil Circuit	96
5.3.3 Phase Shift Error	97
5.3.4 Manufacturer's Data for the Multipliers	98
5.4 Sources of Error in Multiplier Output and Their Elimination	98
5.4.1 Introduction	98
5.4.2 Errors due to Coupling	99
5.4.3 Error due to Non-Linearity	100
5.4.3.1 Imbalance Error	100
5.4.3.2 Feedback Error	101
5.4.3.3 Magneto Resistance Error	102
5.4.3.4 Rectifying Contact Error	102
5.4.4 Errors due to Operating Conditions	102
5.5 Final Balancing Circuit	103
5.6 The Summation of Signals	105
5.6.1 The Subtraction	107
5.6.2 The Summation Circuit	107
5.7 Calibration of Wattmeter	109
5.8 Power Consumption of Wattmeter	111
5.9 Correction for Power Consumed in the Wattmeter	112
5.10 Sensitivity of Wattmeter	112
<u>Chapter Six:</u> Experimental Arrangements and Test Results	116
6.1 The Transformer and its Characteristics	116
6.1.1 Core	116
6.1.2 Search Coils	116

	<u>Page</u>
6.1.3 Main Windings	118
6.1.4 Rating	118
6.2 Parameters for Core Loss Measurements	119
6.3 Experimental Arrangements	119
6.4 Measurement of Load Power Factor	122
6.5 Core Loss Tests and Test Results	123
6.5.1 Open Circuit (no-load) Test for the Measurement of Core Loss	123
6.5.2 Direct Differential Current Method	123
6.5.3 Current Transformer Differential Method	125
6.5.4 Series Resistance Differential Method	128
6.6 Additional Results	136
6.6.1 Excitation Current and Load Power Factor	136
6.6.2 The Magnetizing Current and Load Power Factor	137
6.6.3 The Core Material Characteristic Angle and Load Power Factor	137
6.6.4 The Input Current and Load Power Factor	138
6.7 Additional Tests	140
6.7.1 Simulation of Operating Conditions	140
6.7.2 Short Circuit and Impedance Test	141
<u>Chapter Seven:</u> Synthetic Loading of Transformer and Measurement of Losses	144
7.1 Introduction	144
7.2 Theoretical Considerations	146
7.3 Experimental Resolution	148
7.4 Concept of Load Power Factor	151
7.4.1 Correction Factor for Phase Angle Meter Reading	154
7.5 Test Arrangements	157
7.5.1 Computation of Core Loss	158
7.6 Tests on Micro Transformer	162
7.6.1 Winding Connections	162
7.6.2 Open Circuit Test	165
7.6.3 Core Loss Measurement under Load Conditions	165
7.6.4 Computation of Core Loss from Instantaneous Power Loss	166
7.6.5 Dynamic Hysteresis Loops	168
7.6.6 Synthetic Load Test	168

	<u>Page</u>
7.7 Factors affecting Synthetic Loading and the Computation of Core Loss	174
7.7.1 Geometrical Considerations	174
7.7.2 Transfer of Power between Two Circuits	176
7.7.3 Waveform Distortion of Current and Voltage	177
7.8 Effectiveness of Synthetic Test	178
<u>Chapter Eight:</u> Conclusions and Suggestions for Future Work	179
8.1 Open Circuit Test	179
8.2 Extraction of Excitation Current and On-Load Core Loss Measurement	180
8.3 Simulation of the On-Load Conditions in the Transformer by Synthetic Test	182
<u>References</u>	184

CHAPTER ONEINTRODUCTION1.1 GENERAL

Rising material costs have changed significantly the old concept of the design superiority of a transformer based on efficiency and designers are now compelled to think of designs such as can give, e.g. optimum output to weight ratio, as in applications such as generator transformers or power transformers close to the generating station where the annual cost of energy losses is comparable with the interest on the capital involved in improving the efficiency beyond a certain limit. This change of emphasis leads to designs which run the core well into saturation and use winding conductors at high current density. While extensive research is being carried out into better but equally economical materials, new techniques are also being developed for better utilization of existing ones.

One outcome of this research is new methods of core construction providing ducts in the core parallel to the laminations for better transfer of generated heat^{1.1,1.2} to the cooling medium and modification in the flow paths of the latter. The use of sulphur hexafluoride instead of mineral oil as a cooling medium due to its comparable insulation characteristic at pressures above atmospheric pressure is a new innovation in this field. The better understanding of the flux distribution around joints, especially around the middle limb joint^{1.3} and of the effect of the joint angle on the flux distribution have initiated the change in the joint angle. Similar investigations have paved the way for the introduction of electrostatic shielding rings around end windings for better distribution of

electric field stress^{1.4}. The degree of control over annealing of laminations after slitting and cutting and the replacement of insulated clamping bolts for limb laminations by glass fibre binding straps giving adequate and uniform pressure over the entire limb and also the elimination of the risk of core bolt failure^{1.5} are some of the other new techniques being adopted by transformer manufacturers.

The size of generators increases with every new "generation" of stations. This is partly due to the economic fact that at higher ratings the cost is not a linear function of the output, and partly due to the turbine size, which is increasing with that of the boilers of nuclear power stations. The concept of fewer but larger power houses has also affected the size of these equipments and the research carried out in the field of slotless generators^{1.6} has provided an opportunity to see these machines in the GW range in the near future. There is every prospect that the transformer being an integral part of the station will also increase in size, and to keep the physical dimensions minimum, the operating flux densities will also increase to the optimum limits.

1.2 NATURE OF THE PROBLEM

Recently, some three-phase, three-limb core type generator transformers designed to operate at a peak flux density of 1.8 T and rated at around 500 MVA have been installed at certain CEGB stations^{1.7}. Some complaints of overheating have been registered in these units. There is a possibility of high core temperatures occurring under operating conditions when the system is exciting the generator with

MVAR, e.g. during the night when the system presents a capacitive load to the generator and transformer^{1.8}. Under these conditions, if the generator terminal voltage is kept constant and the transformer output voltage is matched with the system by tap changer adjustment, a high voltage per turn condition exists in the high voltage winding and the transformer core experiences a high flux density. In the later installations the peak nominal flux density of the transformer has been reduced to 1.7 T to protect against damage due to core overheating.

Since most generator and power transformers undergo a considerable change of load factor and load power factor during each day's cycle of operation, it was considered useful to study the variation of core loss with the change in the load power factor, especially when leading. The possible introduction of generators with doubly wound rotors which could ultimately eliminate synchronous condensers from the system implies that the transformer in such a system, especially generator transformers, may well have to handle power factors as low as 0.2 leading.

The measurement of core loss of a transformer connected to such a system leads to a number of problems, the basic one being to handle a very large power flow when the transformer is loaded and the measurement of core loss is required under such conditions. Secondly, no standard technique is available for simulating such behaviour of a transformer operating at leading power factor in a manufacturer's test rig.

1.3 PREVIOUS WORK ON THE PROBLEM

Most of the work done in the measurement of power loss in magnetic materials is either based on the measurement of power loss in a single lamination^{1.9-1.13} or for a batch of laminations^{1.14}. Although these works contributed towards a better understanding of the subject, due to very complex behaviour of magnetic materials and the dependence of their losses on so many factors, the research is far from complete.

With the increase in the operating flux density, loss measurement problems arise due to flux waveform distortion. To investigate the behaviour under such conditions much work has been done in the past but limited to the sample laminations only and no real attempt has been made on actual core. If, however, the investigations are made on an actual core, the flux waveform is always assumed as sinusoidal and pure. The investigation of the power loss in a sample lamination or a batch of them at higher flux densities has been done both on the basis of distorted waveform^{1.15,1.16} and by its reduction to a sinewave using feedback. If a sinusoidal voltage is applied to an excitation circuit having resistance and leakage reactance, this will give rise to a distorted flux and hence induced voltage. Therefore, if a similarly distorted voltage is applied to the circuit, the induced voltage will be sinusoidal. This is the basic principle used to produce a sinusoidal flux for iron loss at high flux density by controlling the flux waveform above a certain limit when it does not remain pure. This was achieved by MacFarlane and Harris^{1.17} through feedback control while Cocks and N. Nagy^{1.18} made use of a harmonic generator to inject the necessary harmonics into the sinusoidal input voltage waveform to

distort it such that the induced voltage waveform and hence the flux waveform became sinusoidal.

In an assembled core, there are certain factors which depend on the material characteristics and can thus easily be understood by a knowledge of the material's behaviour when it is subjected to varying magnetic fields of high intensity and usually the manufacturer's data give ample information in this respect. There are, however, certain factors which belong to the built up core and their effects are not measureable when a single lamination is tested. It is a well known fact that in the case of an eddy current loss, the calculated and measured values differ significantly. Similarly, the power loss in an assembled core is considerably higher than the computed value based on measurements made on a sample of the material from which the core is fabricated. Past experimental work on this has checked the redistribution of flux in the different parts of the core with changing loading conditions, by employing search coils^{1.19}. Since cores were not subjected to such limiting flux density as at present, the investigation was not applicable to the present situation.

With the advances in computation techniques, much work has been carried out on the analysis of the leakage flux of the transformer and of the losses due to eddy currents produced by this flux^{1.20-1.22}. Since a major part of this leakage flux has its direction transverse to the lamination plane, it can cause severe local loss and core heating, even production of the hot spot. Extensive work has been done to predict quantitatively these losses on a theoretical basis^{1.23-1.25}. A recent paper^{1.26} describes an

attempt to investigate the loss due to this flux experimentally by the development of a special rig suitable to accommodate a large size core member to be subjected to a flux at right angles to the lamination plane, thus simulating the condition of leakage flux near the vertical edges of the transformer core where the possibility of the occurrence of hot spot is maximum. This rig, however, does not simulate the conditions the transformer experiences with varying load power factor.

While numerical methods are an excellent tool for design improvement and take into account a number of variables, there has still been no method by which the actual core loss could be measured while the transformer is in actual operation. Owing to the measurement difficulties, the only method employed so far on full size transformers is the measurement of core temperatures, which is done by embedded thermo-junctions. These temperature measurements can give a fair approximation of core loss by the initial rate of temperature rise, but cannot be related directly to actual core loss under steady state operation as there may be other factors which could change the overall temperature of the transformer including that of the core.

Swampillai^{1.27} measured the local loss in a simple core structure using a Hall probe to establish the Poynting Vector, a method proposed by Allen^{1.28}. Measurement of the d.c. output by galvanometer led to problems and errors were introduced into the field strength measurements due to its dependence on the relative position of the Hall probe. A later attempt^{*} improved the accuracy

* Third year undergraduate project by J.C. Steed, 1974, Department of Electrical Engineering, Imperial College of Science and Technology, London.

of the method by amplifying the field strength signals prior to their multiplication through an integrated multiplier.

Ali^{1.29} tried to measure the instantaneous core loss of the three-phase, three-limb transformer used in this work by the method described in Section 4.6.1. Due to inherent errors in the use of current transformers, the results could not be related as functions of load power factor due to their inconsistency.

1.4 SUMMARY OF THE PRESENT WORK

The present work was initially based on 1.29, to investigate whether improvements can be made in the method which, owing to its flexibility, can be adapted to any type or rating of transformer without affecting its operational parameters. This was attempted first by using a better accuracy class of current transformers but without any significant improvement in the results. A thorough investigation reveals that as far as the magnitude of the extracted excitation current is concerned, it is within the limits of acceptability, but its phase relation affects the measurements significantly and thus the conventional "generation" of current transformers cannot be used for this purpose.

Investigation is done on the other possible methods for extraction of the excitation current from a loaded transformer and a method, with practically no magnitude error in the extracted signal corresponding to the excitation current and without any phase shift, is developed. This signal is processed through an electronic wattmeter to give an output proportional to the transformer core loss and also through a three-channel wattmeter using Hall effect

multipliers which have been developed and tested especially for the purpose.

An attempt is made to develop a synthetic method of simulating the full load conditions in a transformer without transfer of rated power and thus to measure the copper and core losses at varying load power factor. The test performed on a three-phase transformer does show the dependence of core loss on load power factor, but the results do not agree closely with those obtained from actual load test. The same test is also performed on a "micro transformer"^{1.30} having the per unit leakage reactance characteristics of a generator transformer (0.09 p.u.) and the results show a very close agreement with those obtained from actual load test, thus proving its suitability as a development test and of the core loss measurement method in type tests in the manufacture of power transformers.

CHAPTER TWOMEASUREMENT OF IRON LOSS BY OPEN CIRCUIT TEST IN A
HIGHLY FLUXED THREE-PHASE THREE-LIMB CORE-TYPE TRANSFORMER2.1 POWER MEASUREMENT IN A POLYPHASE SYSTEM

According to Blondel's theorem^{2.1} the number of complete elements required to measure the total power in a polyphase system is one fewer than the number of wires in the system. This is stipulated regardless of the wave form, frequency and the degree of symmetry of the system. The same theorem is applied in principle when the core loss in a three-phase three-limb transformer is measured by open circuit test using the two-wattmeter method. However, the test is performed at the rated frequency and the wave shape of the applied voltage is kept sinusoidal as far as possible. The two-wattmeter method of core loss measurement is acceptable to B.S. 171.

2.2 THE THREE-PHASE MAGNETIC CORE AND PHASE EXCITATION CURRENTS

The three-limb core of a three-phase transformer is magnetically asymmetric, as the central limb has an equivalent magnetic path much shorter than the outer limbs. This magnetic asymmetry causes an inequality in the magnitudes of the phase excitation currents and also introduces a phase shift from the symmetrical position. At high flux density both factors, i.e. inequality in magnitude and shift in phase, are quite significant. Brailsford^{2.2} has derived the theoretical equations for these currents in terms of magnetic path lengths and applied voltages. These equations can therefore be related to the flux density to

which the core is subjected for a core of fixed dimensions.

Letting the magnetic path lengths for the three limbs be ℓ_1 , ℓ_2 and ℓ_3 where $\ell_1 = \ell_3$ and $\ell_2/\ell_1 = k$, the excitation currents be I_1 , I_3 and I_2 for the two outer and centre windings respectively, then the modulus of the current in each case according to Brailsford analysis is given by:

$$I_1 = I_3 = \frac{V\ell_1}{3\sqrt{3} \omega A |\mu|} \sqrt{(7+k+k^2)} \quad (2.1)$$

$$I_2 = \frac{V\ell_1}{3\sqrt{3} \omega A |\mu|} (1 + 2k) \quad (2.2)$$

where A = area of cross-section of core, which is assumed the same for limbs and yokes.

$|\mu|$ = modulus of permeability vector μ .

ω = angular frequency.

$V = V_{12}$, $V_{23} = a^2V$ and $V_{31} = aV$ - here $a = -\frac{1}{2} + j\sqrt{3}/2$

The no-load currents therefore bear the following relation

$$I_1 : I_2 : I_3 = 1 : \frac{1 + 2k}{\sqrt{(7 + k + k^2)}} : 1$$

The above relationship is independent of everything except k , the ratio of magnetic path length of the centre limb to that of the outer limbs. Since $I_1 + I_2 + I_3 = 0$, their phasors may be drawn to form a closed triangle. The phase angle between these will remain fixed for any applied voltage and thus flux density. The relative phase of this system of currents with respect to the system of line or phase voltages will, however, change with the flux density.

The transformer tested has $k = 0.436$, and thus the calculated ratio of the excitation currents on the basis of the above equations was 1:0.68:1. The transformer was excited to its working flux density of 1.8 T and the ratio of the currents as measured was 1:0.69:1.

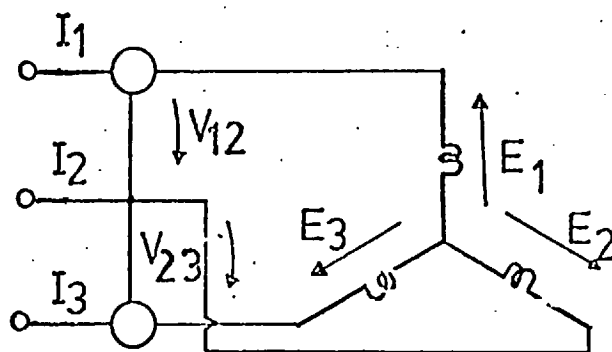
The above results show that these equations can well be utilized to calculate the core power losses for comparison with the actual measurements.

2.3 POSSIBLE CONNECTIONS FOR CORE LOSS MEASUREMENT BY THE TWO-WATTMETER METHOD

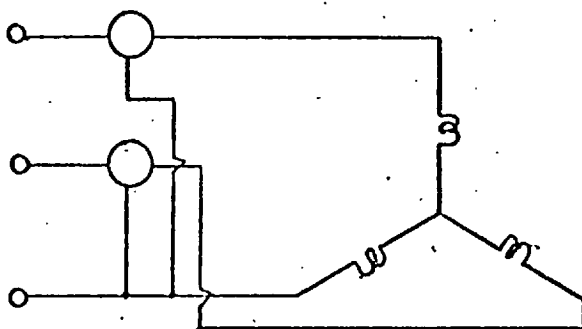
When the core loss is measured by the two-wattmeter method there are three possible connections that can be employed as shown in Fig. 2.1. The power in the circuit for any of these connections, which will be indicated by the wattmeters, can be given by the product of the current flowing through the current coil circuit and the complex conjugate of the voltage across the potential coil of the wattmeter.

Since the currents and voltages are being treated as complex quantities, it is convenient to assign a complex value to the permeability of the core material, as the relations connecting the electrical characteristics of the coil with the components of vector permeability of the core can then be much simplified^{2,3}. Thus the relation between the field strength vector \underline{H} and the flux density vector \underline{B} will be $\underline{B} = \underline{\mu} \underline{H}$ where $\underline{\mu}$ is the vector permeability bearing real and imaginary components $\underline{\mu} = \mu' - j\mu''$. If ϕ is the phase angle between V and I , then $\tan \phi = \mu' / \mu''$ and $\cos \phi = \mu'' / |\mu|$ where $|\mu|$ is the modulus of $\underline{\mu}$ and $\cos \phi$ is the power factor of the core material at flux density B_{\max} , the amplitude of \underline{B} .

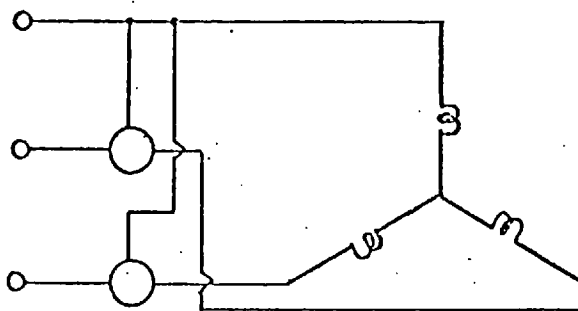
Consider the circuit condition Fig. 2.1(a) when the current coils of the wattmeters are in the "outer" phases. The powers P_{12} and P_{32} can be given as stated earlier by the product



(a)



(b)



(c)

FIG. 2.1

Possible connections for power measurement in a three-phase system by two-wattmeter method.

of the current and complex conjugates of voltage, i.e. V_{12} and I_1 for P_{12} and $-V_{23}$ and I_3 for P_{32} . Thus

$$P_{12} = \frac{V^2 \ell_1}{6\sqrt{3} \omega |\mu|^2 |A|} \left[\sqrt{3} \mu''(2+k) - \mu'(4-k) \right] \quad (2.3)$$

and

$$P_{32} = \frac{V^2 \ell_1}{6\sqrt{3} \omega |\mu|^2 |A|} \left[\sqrt{3} \mu''(2+k) + \mu'(4-k) \right] \quad (2.4)$$

The total power = P

$$= P_{12} + P_{32} = \frac{V^2 \ell_1}{6\sqrt{3} \omega |\mu|^2 |A|} 2\sqrt{3} \mu''(2+k) \quad (2.5)$$

P_{12} and P_{32} are the readings which would be indicated in the wattmeters in watts. The Volt-Amps in the two cases, if denoted by S_{12} , S_{32} can be given by the products of the moduli of currents and voltages, such that:

$$S_{12} = V_{12} I_1 = \frac{V^2 \ell_1}{3\sqrt{3} \omega A |\mu|} \sqrt{(7+k+k^2)} \quad (2.6)$$

$$S_{32} = V_{32} I_3 = S_{12}$$

The power factor angles, ϕ_{12} and ϕ_{32} , under which these wattmeters are working, i.e. the phase angle between voltages and currents, can be given by Watts/Volt-Amps, or

$$\cos \phi_{12} = \frac{\sqrt{3} \mu''(2+k) - \mu'(4-k)}{2|\mu| \sqrt{7+k+k^2}} \quad (2.7)$$

$$= \frac{\sqrt{3} (2+k) - (4-k) \tan \phi}{2\sqrt{7+k+k^2}} \cos \phi \quad (2.8)$$

and

$$\cos \phi_{32} = \frac{\sqrt{3} (2+k) + (4-k) \tan \phi}{2\sqrt{7+k+k^2}} \cos \phi \quad (2.9)$$

Because of the low power factor of the core material in the range of flux density to which the transformer core is subjected, the algebraic sum is the difference of two wattmeter readings. This

condition is also true for the balanced and symmetrical system when the power factor is below 0.5 where one of the instruments will give negative reading. If three sets of readings in the later case are taken using each of the connections shown in Fig. 2.1 this will give identical readings and their difference will be the same. However, in the present case when there is asymmetry in the phase relation between currents and voltages of each phase and also the current magnitudes are not the same, the three sets of readings will give entirely different results and of course the individual wattmeter readings in each set will be greater than the total iron loss of the transformer.

The above equations for power, if expressed in terms of the ratio of wattmeter reading to total power, P (algebraic sum of both wattmeter readings), can be reduced as under:

$$\frac{P_{12}}{P} = \frac{1}{2} - \frac{(4-k)}{2\sqrt{3}(2+k)} \tan \phi \quad (2.10)$$

$$\frac{P_{32}}{P} = \frac{1}{2} + \frac{(4-k)}{2\sqrt{3}(2+k)} \tan \phi \quad (2.11)$$

Similarly, for the other wattmeter connections shown in Fig. 2.1 the resultant equations in ratio form are:

$$\frac{P_{15}}{P} = \frac{3\sqrt{3} + (1+2k)\tan \phi}{2\sqrt{3}(2+k)} \quad (2.12)$$

$$\frac{P_{23}}{P} = \frac{(1+2k) [\sqrt{3} - \tan \phi]}{2\sqrt{3}(2+k)} \quad (2.13)$$

$$\frac{P_{21}}{P} = \frac{(1+2k) [\sqrt{3} + \tan \phi]}{2\sqrt{3}(2+k)} \quad (2.14)$$

$$\frac{P_{31}}{P} = \frac{3\sqrt{3} - (1+2k)\tan \phi}{2\sqrt{3}(2+k)} \quad (2.15)$$

The power factor under which each wattmeter is working can similarly be deduced:

$$\cos \phi_{13} = \frac{3\sqrt{3} + (1 + 2k)\tan \phi}{2\sqrt{7 + k + k^2}} \cos \phi \quad (2.16)$$

$$\cos \phi_{23} = \frac{1}{2} \left[\sqrt{3} - \tan \phi \right] \cos \phi \quad (2.17)$$

$$\cos \phi_{21} = \frac{1}{2} \left[\sqrt{3} + \tan \phi \right] \cos \phi \quad (2.18)$$

$$\cos \phi_{31} = \frac{3\sqrt{3} - (1 + 2k)\tan \phi}{2\sqrt{7 + k + k^2}} \cos \phi \quad (2.19)$$

2.4 POWER RELATION IN THE THREE-WATTMETER METHOD OF CORE LOSS MEASUREMENTS

When the core loss is measured by the three-wattmeter method, each wattmeter measuring the power input to one phase, the algebraic sum of the three represents the total core loss.

The equations for such a case on the same basis can be developed as previously and the resultant equations given by:

$$\frac{P_1}{P} = \frac{(5+k) - \sqrt{3}(1-k)\tan \phi}{6(2+k)} \quad (2.20)$$

$$\frac{P_2}{P} = \frac{1 + 2k}{3(2+k)} \quad (2.21)$$

$$\frac{P_3}{P} = \frac{(5+k) + \sqrt{3}(1-k)\tan \phi}{6(2+k)} \quad (2.22)$$

Similarly, the power factors at which the wattmeters are working, which is also the power factor of each circuit, is given by:

$$\cos \phi_1 = \frac{(5+k) - \sqrt{3}(1-k)\tan \phi}{2\sqrt{7+k+k^2}} \cdot \cos \phi \quad (2.23)$$

$$\cos \phi_2 = \cos \phi \quad (2.24)$$

$$\cos \phi_3 = \frac{(5 + k) + \sqrt{3}(1 - k)\tan \phi}{2\sqrt{7 + k + k^2}} \cos \phi \quad (2.25)$$

2.5 NUMERICAL COMPUTATION OF POWER RELATIONS

On the basis of the foregoing equations for power loss measurement, numerical results computed and plotted against the peak flux density, as shown in Figs. 2.2(a), (b) and (c), clearly indicate that for the two-wattmeter method:

1. The power to be indicated by each wattmeter in one set of connections is different from that indicated by other sets.
2. With increasing flux density, the rate of increase of individual wattmeter indications (given by the slope of each curve) is sharper and is different for each set.
3. Since the difference of the two wattmeter indications plotted on the basis of the ratio to the total power is the total core loss, its magnitude in relation to the actual indications of the wattmeters is negligibly small and decreases as flux density increases.
4. For connections 'a' (Fig. 2.1) when the wattmeters are connected in the "outer" phases, the magnitudes of the wattmeter indications are large compared to the other two connections. The small difference of two large indications is more susceptible to error than the same difference of two smaller indications. Thus, connections 'a' are worst in the case of the two-wattmeter method and connection 'c', where

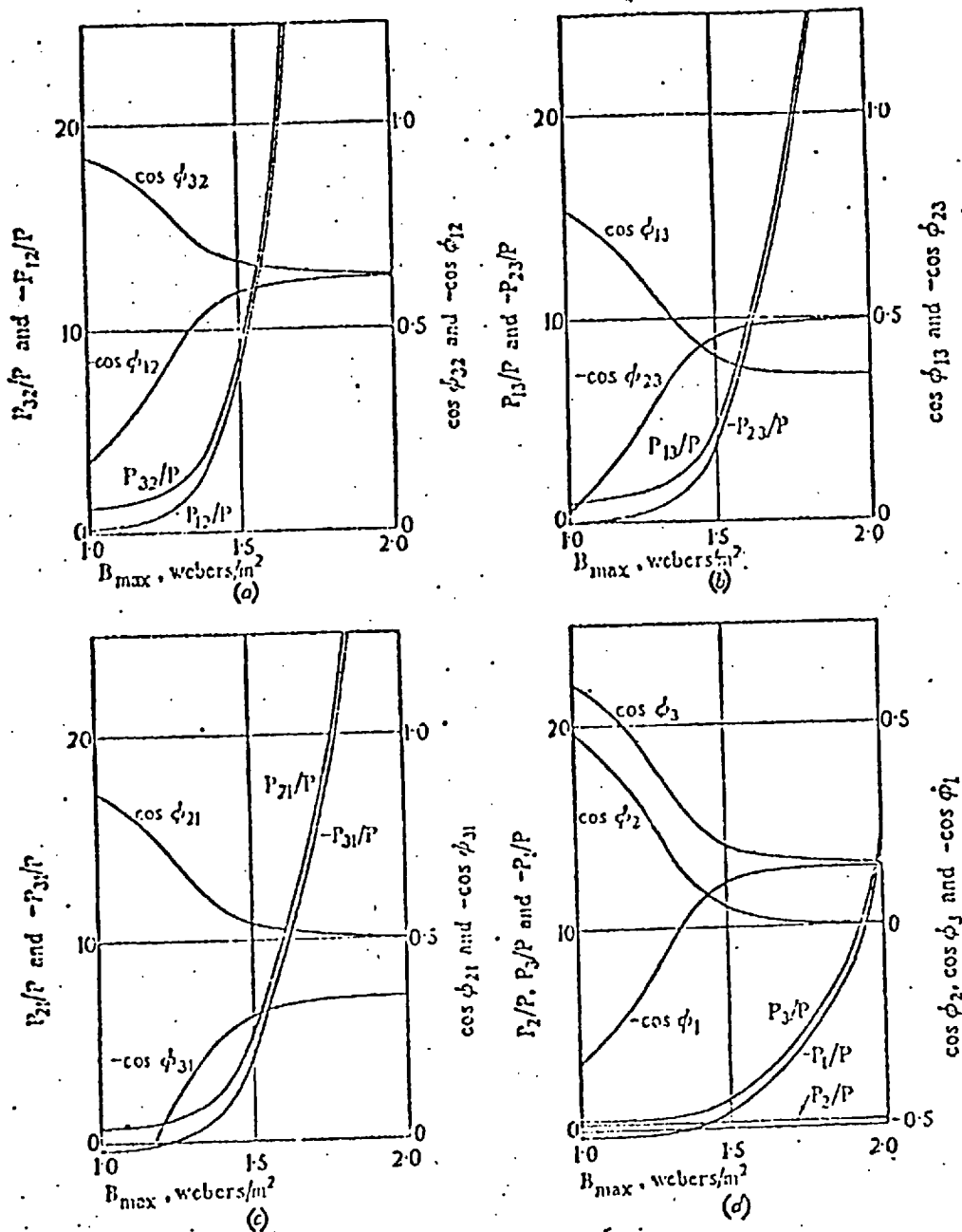


FIG. 2.2

Power ratios and relative wattmeter power factors for a typical core.

Diagrams (a), (b) and (c) correspond to diagrams (a), (b) and (c) of Fig. 2.1. Diagram (d) corresponds to measurement by three-wattmeter method.

(From Ref. 2.2.)

the indications of the individual wattmeter are almost half those of case 'a', the best.

Fig. 2.2(d) shows the curves for measurement by the three wattmeter method. The computation has been made on the basis of equations (2.20) to (2.25). These curves show that the individual wattmeter indication is far less than any of the two-wattmeter method. These indications do not change sharply with the flux density and for the middle phase, it is practically constant as the phase angle between current and voltage is equal to the material phase angle. This also shows that as the flux density increases, the first phase starts returning power to the source. This method is therefore best for measurement of core loss on open circuit test for a three-phase three-limb transformer working at high flux density, as each individual wattmeter indication is small and therefore the relative algebraic summation is large.

Since even distribution transformers are now designed, for economic reasons, at flux densities well above 1.5 T the two-wattmeter method for measurement of core loss for such transformers is not recommended and if it has to be adopted for some reason the connection shown in Fig. 2.1(c) should be used. Standard industrial practice is, however, the opposite to this^{2.4} and the connection of Fig. 2.1(a) is commonly used. As shown in 2.6, this indicates lower total core loss than actual.

2.6 EXPERIMENTAL RESULTS

Open circuit core loss measurements were made by two- and three-wattmeter methods. In the former case, the three

possible connections as shown in Fig. 2.1 were used separately and the results are shown in Table 2.1 for flux density 1.8 T. These results show that the measurement by two-wattmeter method which falls nearest the three-wattmeter value uses connections 'c' of Fig. 2.1 while the connection 'a' of Fig. 2.1 give 5.5% low reading and that 'b' of Fig. 2.1, 3.4% high reading.

The magnitude of the excitation current and its phase relation with induced voltage was also checked as shown in Fig. 2.3.

To check the validity of the power equations, the supply connections of the outer limbs were interchanged and it was observed that individual losses are associated with the lines and not with the limbs. The negative reading was still indicated by the 'red' phase and the total core loss was practically unaffected. This referred to measurement made by three-wattmeter method.

2.7 EFFECT OF THE WATTMETER ERROR

Measurements made by either method show that at high flux density the positive-reading wattmeter works at lagging power factor while the negative-reading wattmeter works at leading one. This means that if the wattmeter has an inductive pressure circuit the positive-reading wattmeter will indicate high while the negative-reading wattmeter will indicate low, so that the total observed power, being the difference of the two readings, will be high.

Although its effect on any method of measurement will be the same, the observation error may be greater when the individual readings are large relative to their difference and hence on this consideration also, the three-wattmeter method will be best.

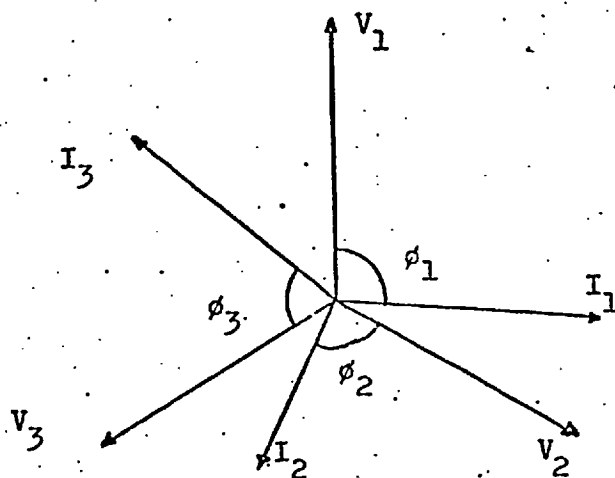


FIG. 2.3

Phasor diagram of a three-phase, three-limb transformer at high flux density with isolated neutral.

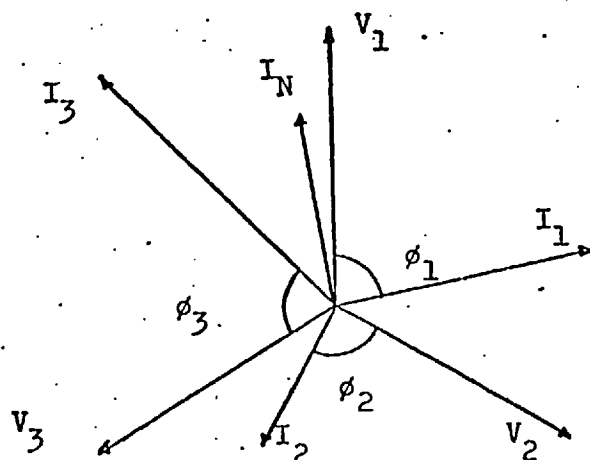


FIG. 2.4

Phasor diagram as Fig. 2.3, but neutral connected to the source's neutral.

$V_1 = V_2 = V_3 = \text{phase voltage.}$

	I_1	I_2	I_3	ϕ_1	ϕ_2	ϕ_3
Fig. 2.3	- 8.4A	5.8A	8.4A	95°	86°	70°
Fig. 2.4	- 8.4A	4.9A	10.4A	80°	91°	76°

Wattmeter Connections	Power measured in circuit number	Meter reading Watts	Core loss Watts
Two wattmeter Fig. 2.1(a)	P_{12}	- 930	210
	P_{32}	1140	
Two wattmeter Fig. 2.1(b)	P_{13}	640	230
	P_{23}	-410	
Two wattmeter Fig. 2.1(c)	P_{21}	-335	225
	P_{31}	560	
Three wattmeter	P_1	-115	222.5
	P_2	50	
	P_3	287.5	

TABLE 2.1

Comparison of power measurement by two-wattmeter and three-wattmeter methods at peak flux density 1.8 T.

2.8 EFFECT OF THE NEUTRAL CONNECTION ON THE MEASUREMENT OF CORE LOSS BY OPEN CIRCUIT TEST

Due to the asymmetry of the no-load currents in a three-phase three-limb transformer, as shown in Fig. 2.3, the neutral connection plays an important role in the measurement of core loss. The problem can be analysed by resolving the currents into symmetrical components. When the transformer neutral is isolated, there is no return path for the zero-phase sequence currents and thus they do not exist in either coil or the line. However, when the transformer neutral is either grounded or connected to the neutral of the source, these currents will appear in the line and the neutral current will be equal to three times the zero-phase sequence current in each phase^{2.5}. When these currents flow in each phase, the resultant phase current is given by the vectorial sum of positive and zero sequence currents which apart from altering the magnitude as compared with the case of isolated neutral, also shifts their phase positions. Phasor diagram Fig. 2.4 shows the position of the excitation currents with respect to phase voltages and neutral currents, and should be compared with Fig. 2.3. The core loss when measured with neutral connected shows an increase (11.3% rise in core loss was observed in the case of transformer tested at 1.8 T) over that with isolated neutral. This explains why manufacturers never use a neutral connection when measuring core loss, an effect noticed but never explained. A further observation worth quoting is that due to the change in phase relations between currents and voltages, the wattmeter reading for each phase was significantly changed. The 'red' phase wattmeter which, as shown in Table 2.1, reads negative gives a positive

reading and the central limb, 'yellow' phase reading becomes negative. It is clear from Fig. 2.4 that this is because the phase angle between current and voltage of this phase is more than quadrature.

To verify the above results, a thermal check was made by locating two thermally lagged thermometers at two different places on the yoke and noting their temperatures over a period of 3 hours while the transformer was operated open circuited with isolated neutral and, later, with neutral connected. The ambient temperature in both cases was very close and to avoid the sudden changes in the ambient conditions, the laboratory doors were kept closed with a controlled air circulation. A check on the ambient temperature was also made during the test. When the rise in temperature was plotted against time, both the initial rate of temperature and final temperature rise in the case of neutral connection were about 10% greater than without neutral connection, agreeing very closely with the results measured by wattmeter.

CHAPTER THREETHE EXCITATION CURRENT AND ITS SEPARATION FROM
THE MAIN CURRENTS OF A LOADED TRANSFORMER3.1 INTRODUCTION

The excitation current of a transformer is defined as "the current which maintains the excitation"^{3.1}. Presumably, by rate of change of "excitation" is meant the flux linkage which, together with the resistive potential drop, is in a transformer equal to the applied voltage when referred to either winding.

Due to the non-linearity of the core material magnetic characteristics, a component of this current is considered to meet the energy loss in the core. The excitation current is, therefore, considered as having two components, a power component corresponding practically to all core losses and a reactive or wattless component responsible for the reversible magnetisation of the core.

Since the transfer of energy in a transformer is accomplished at the expense of excitation current, the exact measure of this current is of fundamental concern for the measurement of the power component and thus the core loss of the transformer. The basic equivalent circuit of a two winding unity ratio transformer is shown in Fig. 3.1. Here,

R_1 and R_2 = Primary and secondary winding resistances,

X_{1l} and X_{2l} = Primary and secondary winding leakage reactances,

E_1 and E_2 = Induced voltages in the primary and secondary windings, $E_1 = E_2$,

V_1 = Primary impressed voltage,

V_2 = Secondary terminal voltage,

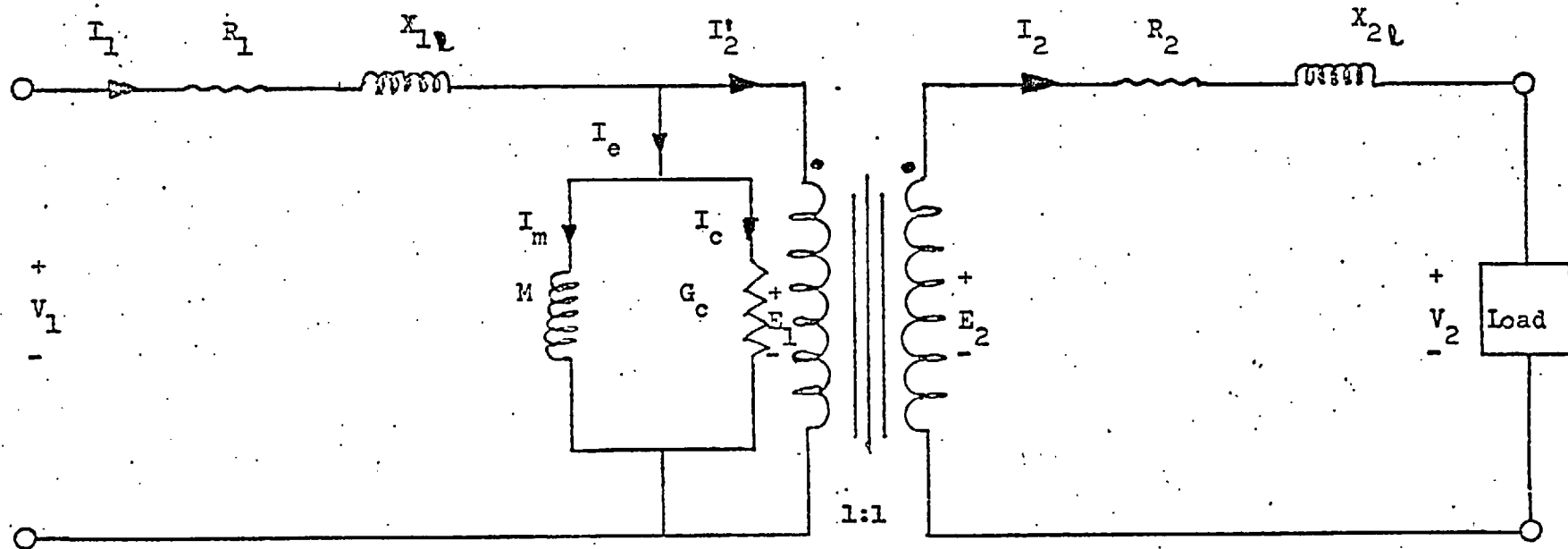


FIG. 3.1

A basic equivalent circuit of a two-winding unity ratio transformer.

- I_1 = Primary current,
 I_2 = Secondary current,
 I_e = Excitation current,
 M = Magnetizing inductance,
 G_c = Conductance giving core loss.

The currents relation of this transformer can be given by:

$$I_1 = I_m + I_c + I_2' \quad (3.1)$$

$$= I_e + I_2' \quad (3.2)$$

$$= I_e + I_2 \quad (3.3)$$

I_c is the component of excitation current, I_e , which accounts for the core loss and can be given by:

$$I_c = G_c E_1 \quad (3.4)$$

From the nature of the eddy currents and hysteresis effects, this component is not generally a linear one but depends mainly on the induction, frequency and the nature of the magnetic material, i.e. the conductance G_c is not a fixed parameter but is variable with the above factors. This is also true of M , the magnetising inductance.

3.2 RELATION BETWEEN EXCITATION CURRENT AND MAIN CURRENTS

In open circuit conditions, when no secondary current flows, the primary circuit current is wholly attributable to the excitation, provided there is no circulating current within the windings due to any parallel connections, in which case an additional current will accompany this current to counter the effects of the circulating current. The division of excitation

current into its power and reactive components is, however, not a major problem in this case and the estimation of core loss can easily be made.

In the case of a transformer connected to a power system, it is sometimes not even possible to associate the excitation current with a particular winding, especially when:

1. The unit interconnects the systems at different voltages to exchange power between them, each system having its own generators and loads.
2. A generator transformer connects the machine to the system and the latter excites the machine with MVAR, i.e. leading reactive load condition on the transformer.

The magnetomotive force which maintains the main flux in the core in steady state operation is the resultant of both primary and secondary currents acting in opposition and (required by Lenz's Law) to magnetise the core in the direction decided by the "right-hand rule". Also, the excitation current has a direct relation with the resultant magnetomotive force (assuming constant permeability in the working range of the transformer). The excitation current can therefore only be separated if the instantaneous difference of these two currents is taken. In view of the above it is difficult to state which winding is supplying the excitation current at a particular instant, i.e. L.V., H.V. or both, therefore the concept of mutual participation in maintaining the magnetizing flux is best considered.

3.3 ESSENTIALS FOR METHODS OF SEPARATION

Methods of separation of excitation current from the main currents must take into account the instantaneous values of both currents, i.e. H.V. and L.V. Also, the resultant current thus obtained must bear the same relation to the induced voltage when referred to either of the windings as in the open circuit test. This can be achieved by taking either the instantaneous difference directly or the difference of effects produced by these currents. The effects considered in this work are magnetic and ohmic voltage drop. Although there are always some possibilities of introduction of errors due to the devices, i.e. current transformer and linear resistor, which sense these effects owing to their own energy losses, there appears to be no alternative method which can be employed when the direct differential method is not applicable. The ultimate aim is to obtain either the excitation current or a signal proportional to the excitation current in magnitude and in phase so that its power and reactive components in relation to the induced voltage can be measured and thus core loss can be computed.

3.4 METHODS OF SEPARATION OF EXCITATION CURRENT

On the basis of the discussion in Section 3.3, the following methods of extraction of excitation current from the input and output currents of the transformer have been used in this work and a detailed study is made of the errors and limitations of each method:

1. Current difference by direct differential method.

2. Current difference by magnetic effects using current transformers differentially.
3. Voltage difference proportional to the current by ohmic voltage drop effects using series/resistance differential method.

3.4.1 Direct Differential Method

3.4.1.1 Theoretical basis

When the primary and secondary windings have the same number of turns, the primary and secondary voltages induced by the resultant mutual m.m.f. are equal and the load component of the primary current equals the load current. The equivalent circuit of such a transformer is shown in Fig. 3.2.

The e.m.f. (E) induced in the secondary is the vector sum of secondary terminal voltage (V_2) and leakage impedance voltage drop due to load current (I_L) while the impressed voltage (V_1) is the vector sum of the induced voltage and the leakage impedance voltage drop due to the primary current ($I_e + I_L'$). The excitation current is the vector sum of the core/loss current which is in phase with the induced voltage and the magnetising current in quadrature to the induced voltage. This circuit has the same electrical characteristics as the actual transformer with the following assumptions:

1. The effect of capacitance in the windings is negligible.
2. The effective resistances and leakage reactances are constant.

3. The magnetic conditions in the core are determined by the frequency and flux and therefore core loss and excitation current depend upon frequency, magnitude and wave form of the induced voltage.
4. A given m.m.f. due to either winding produces the same effects in the core irrespective of the arrangement of the winding around the core.
5. The excitation current is represented by its fundamental component.

The equivalent circuit of Fig. 3.2 can be used to replace the actual transformer in the circuit of which the transformer is a part provided a single connection between a primary terminal and the secondary terminal of the same relative polarity does not alter the conditions in the circuit^{3.2}.

3.4.1.2 Experimental considerations

If the excitation current is neglected, the unity ratio transformer supplying power to a load can be connected as shown in Fig. 3.3, with the primary and secondary terminals of same polarity connected together. The connection will not change the conditions in the circuit. The one to one turn ratio transformer is thus equivalent to a simple series impedance connected in the circuit, in part of which magnetomotive forces of equal magnitude but opposite sense cancel each other.

To account for the excitation current, the circuit can be connected as shown in Fig. 3.4. The current flowing to the

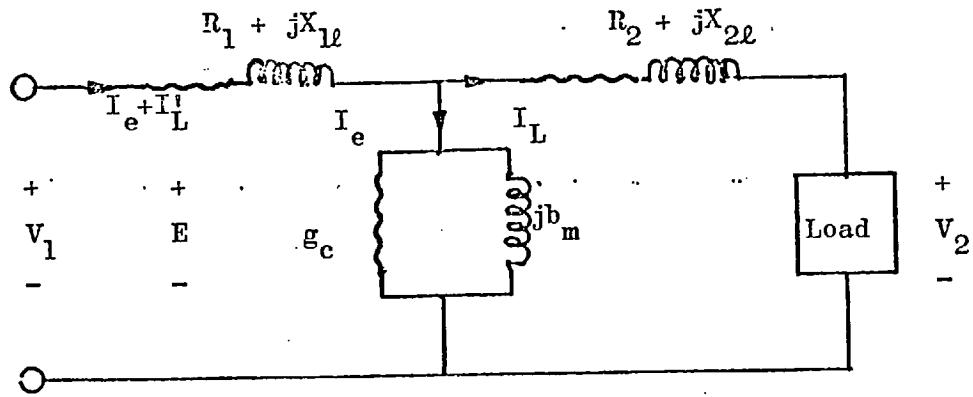


FIG. 3.2 Equivalent circuit of a 1:1 ratio transformer.

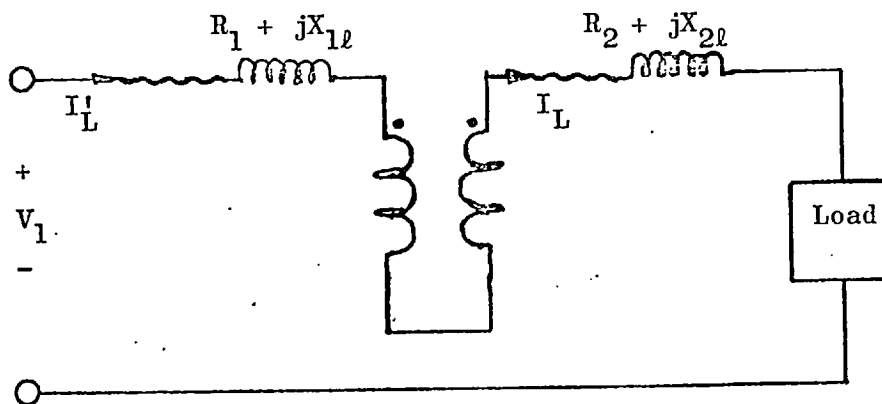


FIG. 3.3 A 1:1 ratio transformer as a series impedance in a circuit, if exciting current is neglected.

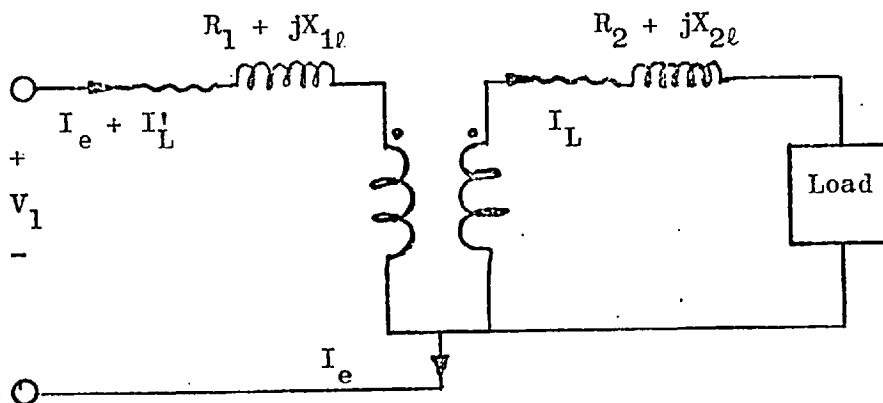


FIG. 3.4 A 1:1 ratio transformer with terminals of the same polarity, connected together and to the source's neutral to separate the exciting current.

neutral from the common connection between the windings will be the excitation current and can thus be used in the computation of core loss by splitting it into its power and reactive components.

3.4.1.3 Errors and limitations of direct differential method

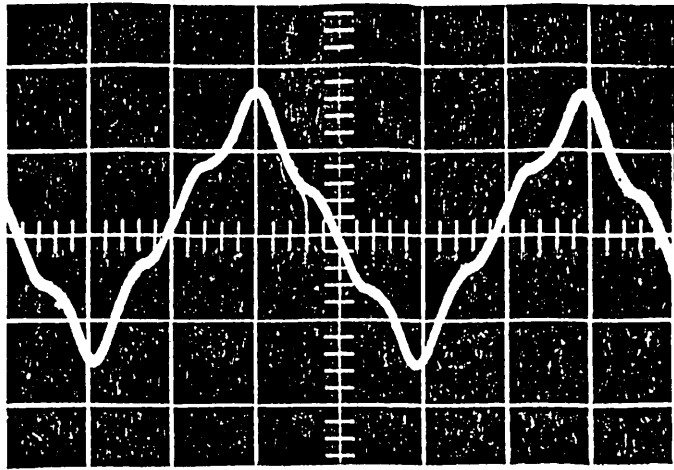
The amplitude and phase relation of the excitation current of the test transformer extracted by this method was compared with the excitation current taken in the no load test. There is an agreement for magnitude, phase relation and wave shape as shown in Figs. 3.5 and 3.6.

This method, however, has the serious limitation that it can only be applied to unity ratio transformers, which if three-phase, must be star-star connected. It is a good technique for development purposes where the quality of certain steels with respect to core configuration is to be checked or different core/winding configurations are to be compared. This method can, however, not be used for large production transformers as they seldom have unity ratio windings.

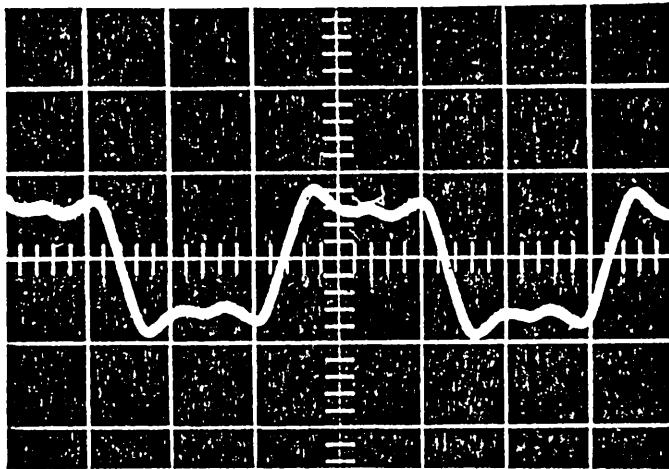
3.4.2 The Current Transformer Differential Method

3.4.2.1 The method

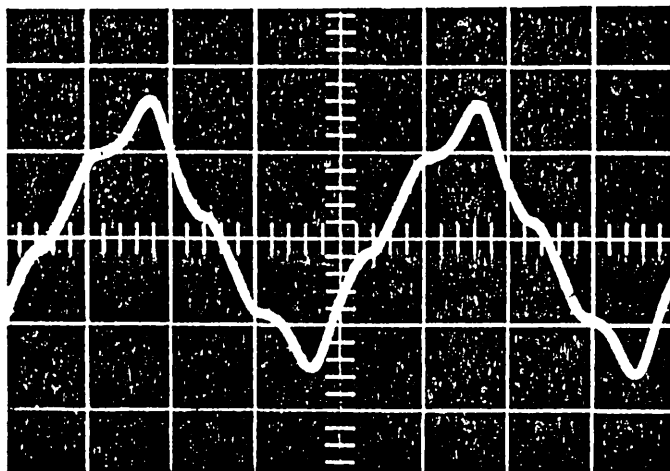
The excitation current can be extracted by connecting differentially the secondaries of two current transformers, the primaries of which are connected in the input and output circuits of the test transformer. The method was first employed by Ali^{3.3} using two 1:1 ratio current transformers for the measurement of



(a)



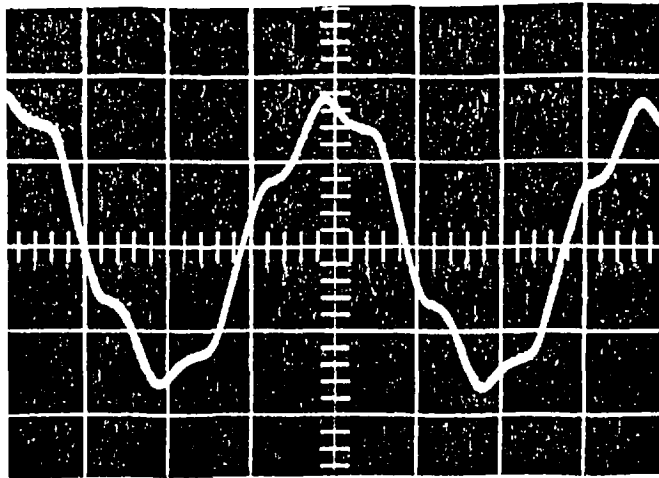
(b)



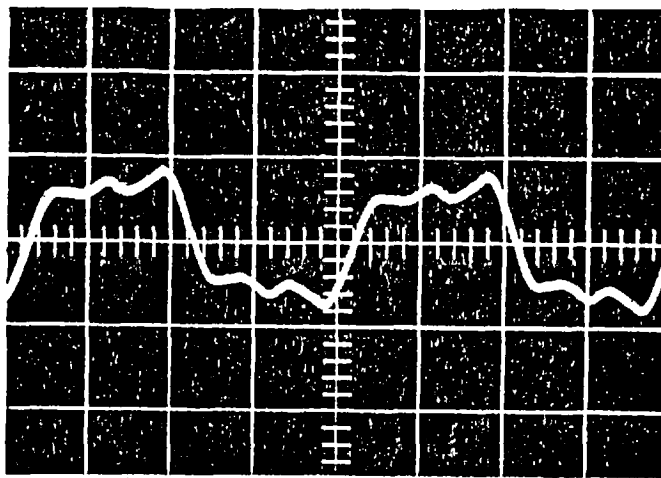
(c)

FIG. 3.5

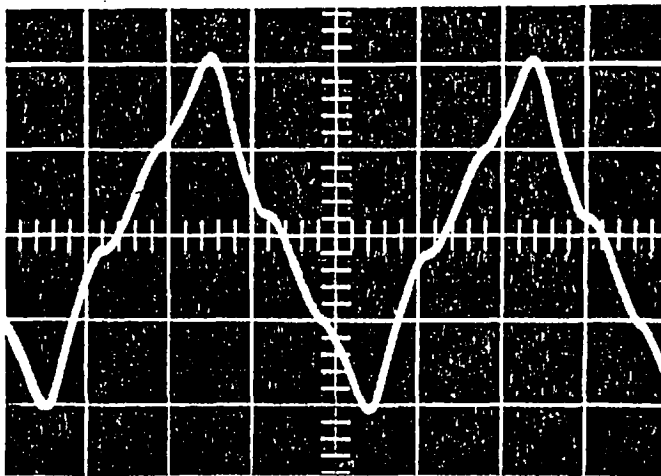
Oscillograms of the excitation current of the three-phase test transformer with open circuited secondary. Waveforms (a), (b) and (c) correspond to 'Red', 'Yellow' and 'Blue' phase respectively.



(a)



(b)



(c)

FIG. 3.6

Oscillograms of the excitation current extracted by direct differential method. Waveforms correspond to phases as in Fig. 3.5.

the core loss with varying load power factor but certain inherent errors of the current transformers and some operational limitations were ignored in the work and while core loss measurement did show a dependence on load power factor, the variation in loss was not realistic.

This method was also employed in the present work for comparison and improvement purposes by using better accuracy class of transformers (Class AL instead of Class CM used in the previous work) as specified under B.S. 3938, and the results thus obtained are shown in Section 6.5.3. The errors and limitations associated with this method are discussed in this Chapter.

3.4.2.2 Inherent errors

According to B.S. 3938, a current transformer is defined as a device for the transformation of current and under normal operating conditions the current in the secondary is substantially proportional to the current in the primary winding, differing from it in phase by an angle which is approximately zero for appropriate connections.

In designing current transformers, while ample care is taken in the selection of the core material and of working flux density so that the above condition may be met, nevertheless in a practical C.T., regardless of the core material, the maintenance of the induced flux requires the expenditure of exciting ampere turns. This excitation m.m.f. although very small compared to that in a power transformer, introduces errors in magnitude (ratio error) and phase relation (phase error) of the secondary ampere turns with

respect to primary ampere turns. When the C.T. is used merely to measure the magnitude of the current in a circuit, e.g. to operate an ammeter, the only factor to minimize is the ratio error, the phase error being of no significance. In the case of a C.T. being used in conjunction with power or energy measuring instruments, both of these errors become of great importance and the secondary quantity must be proportional, and should maintain the same phase relationship to the primary quantity.

The estimation of these errors has been made on the assumption of ampere turn balance between both sides of the transformer and has been expressed in a number of parameters, e.g. self and mutual inductances^{3.4}, turns and current ratios^{3.5}, or percentage ratio error in terms of ratio correction factor^{3.6}. The analysis made here is on the basis of percentage ratio error and phase angle error in terms of primary current and power factor of the secondary burden.

3.4.2.3 Error evaluation

Fig. 3.7 represents the phasor diagram of a C.T. when the overall secondary circuit power factor is lagging. Here,

$N_p I_p$ & $N_s I_s$ = Primary and secondary ampere-turns respectively,

$N_p I_e$, $N_p I_w$ & $N_p I_m$ = Excitation, power and magnetizing ampere-turns respectively,

R_s = Sum of the resistances of burden and secondary winding,

X_s = Sum of the reactance of burden and leakage reactance of secondary winding,

α = Overall secondary circuit phase angle,

β = Phase error, i.e. phase difference between the primary and secondary ampere-turns,

ϕ = Angle between excitation ampere-turns and power loss ampere-turns. This is a characteristic of the material and depends on the flux density at which the C.T. is operating,

γ = Ratio error which is the difference between the primary and secondary ampere-turns,

E_s = Secondary induced voltage,

Φ = Magnetizing flux.

Resolving $N_p I_p$ parallel and perpendicular to $N_p I'_p$:

$$N_p I_p \cos \beta = N_p I'_p + N_p I_m \sin \alpha + N_p I_w \cos \alpha \quad (3.5)$$

and

$$N_p I_p \sin \beta = N_p I_m \cos \alpha - N_p I_w \sin \alpha \quad (3.6)$$

Squaring both sides of equation (3.5) and (3.6) and adding

$$\begin{aligned} (N_p I_p)^2 &= N_p^2 I_p'^2 + 2N_p I_p' (N_p I_m \sin \alpha + N_p I_w \cos \alpha) \\ &\quad + (N_p^2 I_m^2 + N_p^2 I_w^2) \end{aligned} \quad (3.7)$$

Dividing both sides of equation (3.7) by N_p^2 :

$$I_p^2 = I_p'^2 + 2I_p' (I_m \sin \alpha + I_w \cos \alpha) + (I_m^2 + I_w^2) \quad (3.8)$$

Now denoting turns ratio, $N_s/N_p = K_t$ and current ratio

$$I_p/I_s = K_c,$$

$$N_p' = I_s K_t$$

Dividing equation (3.8) by I_s^2 and replacing the appropriate terms with K_t and K_c ,

$$K_c^2 = K_t^2 + \frac{2K_t}{I_s} (I_m \sin \alpha + I_w \cos \alpha) + \frac{1}{I_s^2} (I_m^2 + I_w^2) \quad (3.9)$$

or

$$K_c^2 = K_t^2 \left[1 + \frac{2}{I_s K_t} (I_m \sin \alpha + I_w \cos \alpha) + \frac{1}{I_s^2 K_t^2} (I_m^2 + I_w^2) \right] \quad (3.10)$$

Now $I_m^2 + I_w^2 = I_e^2$ and since $I_e^2 \ll K_t^2 I_s^2$, the root of the expression in the square bracket can be taken $\approx 1 + \frac{I_m \sin \alpha + I_w \cos \alpha}{K_t I_s}$.

Equation (3.10) can therefore be written as:

$$K_c^2 \approx K_t^2 \left(1 + \frac{I_m \sin \alpha + I_w \cos \alpha}{K_t I_s} \right)^2 \quad (3.11)$$

so:

$$K_c \approx K_t + \frac{I_m \sin \alpha + I_w \cos \alpha}{I_s} \quad (3.12)$$

Similarly, from equations (3.5) and (3.6)

$$\tan \beta = \frac{N_p I_m \cos \alpha - N_p I_w \sin \alpha}{N_p I_p' + N_p I_m \sin \alpha + N_p I_w \cos \alpha} \quad (3.13)$$

Further simplification of equation (3.13) within a reasonable accuracy can be made as

$$\tan \beta = \frac{N_p I_m \cos \alpha - N_p I_w \sin \alpha}{N_p I_p'} \quad (3.14)$$

Since angle β is kept as small as possible to minimise the phase error and since $I_p' = I_s \frac{N_s}{N_p}$

$$\beta \approx \frac{I_m \cos \alpha - I_w \sin \alpha}{I_s \times \frac{N_s}{N_p}} \text{ radians} \quad (3.15)$$

In equation (3.12) K_c gives the ratio between actual primary and secondary currents. In practice, these currents are seldom equal to the nominal or rated value and, therefore, rated or nominal current ratio $K_n = I_{pn}/I_{sn}$ is introduced to make the correction at a given current ratio as the manufacturer's guaranteed errors are based on the rated value of I_{pn} and I_{sn} .

The ratio error, according to B.S. 3938, is specified in percentage, and is expressed as:

$$\% \text{ R.E. at } I_p = \left(\frac{K_n I_s - I_p}{I_p} \right) \times 100\% \quad (3.16)$$

or

$$\% \text{ R.E. at } I_p = \left(\frac{K_n - K_c}{K_c} \right) \times 100\% \quad (3.17)$$

By substituting for K_c in equation (3.12)

$$\% \text{ R.E. at } I_p = \frac{\left[K_n - K_t - \left\{ (I_m \sin \alpha + I_w \cos \alpha) / I_s \right\} \right]}{K_c} \times 100\% \quad (3.18)$$

Equation (3.18) can be rearranged and expressed as

$$\% \text{ R.E. at } I_p = -100 \left(\frac{I_m \sin \alpha + I_w \cos \alpha}{I_p} \right) + 100 \left(\frac{K_n - K_t}{K_c} \right) \% \quad (3.19)$$

The second term of the right-hand side of equation (3.19) is independent of the operating flux density and the quality of core material. This term is often used in designing current transformers.

If K_n is made equal to K_t , the % R.E. can be given by:

$$\% \text{ R.E. at } I_p = -100 \left(\frac{I_m \sin \alpha + I_w \cos \alpha}{I_p} \right) \% \quad (3.20)$$

Equations (3.12) and (3.14) are the basic equations of the current transformer by which the behaviour of the errors with respect to the secondary burden and secondary overall power factor can easily be seen. The following are the special operating conditions worth considering.

1. Unity power factor of the current transformer secondary circuit when $\alpha = 0$:

$$K_c \approx K_t + \frac{I_w}{I_s} \quad \text{and} \quad \beta \approx \frac{I_m}{I_s} \text{ (radians)}$$

2. Maximum leading or lagging power factor of current transformer secondary circuit when $\alpha = \pi/2$:

$$K_c \approx K_t + \frac{I_m}{I_s} \quad \text{and} \quad \beta \approx -\frac{I_w}{I_s} \text{ (radians) for inductive burden,}$$

and $K_c \approx K_t - \frac{I_m}{I_s}$ and $\beta \approx + \frac{I_w}{I_s}$ (radians) for capacitive burden.

3. Condition of maximum ratio error.

When $\alpha = \phi$, a condition when secondary ampere-turns and primary ampere-turns are in direct antiphase with each other. The phase angle error = 0, but ratio error is maximum.

$$K_c \approx K_t + \frac{I_e}{I_s}$$

4. Condition of maximum phase angle error.

For the leading power factor of the burden of the current transformer, a condition will exist when $\alpha = (90 - \phi)$, the ratio error will be negligible as $K_c \approx K_t$ and phase angle error will be maximum and can be given by:

$$\beta_{\max} = I_e \sqrt{K_T^2 I_s^2 - I_e^2}$$

3.4.2.4 Operational errors

The burden of the current transformer is specified in volt-amps at rated secondary current and a specific power factor. (According to B.S. 3938, for measuring C.T.s the burden is specified at unity power factor.) In practice the burden usually has a reactive component, generally inductive due to measuring instrument coils and those of protective relays. This difference in the actual burden power factor to that of standard, has a great influence on the C.T. error. Furthermore, the magnitude of the burden also affects these errors and the common practice of using a C.T. having higher rated burden than the actual burden with a view to obtaining

better performance may in fact increase the overall errors^{3.7}. A thorough investigation in respect of the above points and of the influence of the actual circuit parameters on the errors is therefore necessary before using a current transformer in a circuit. The burden offered by the wattmeter used in this work is $\approx 10\%$ of the rated burden of the one current transformer. Since two C.T.s were connected in differential mode which is an unusual case of C.T. operation, it can be assumed that burden is faced by the C.T. connected to the circuit supplying excitation current to the transformer under test, but there could be a situation when both of the C.T.s share this burden. In such a situation the prediction of errors will be more difficult.

Since it was not possible to obtain a set of C.T.s with rated burden matching the wattmeter, nor was it possible to obtain another wattmeter to match the burden of C.T.s, available set of C.T.s and wattmeter was used. The prospect of increasing the burden by providing an external impedance in series with the meter still exists, but this would introduce an additional correction factor in the wattmeter reading.

3.4.2.5 Dependence of errors on operating conditions

In contrast to a voltage transformer, the current transformer is subjected to a variable induction and thus its errors are not constant over the entire range of operation. The primary current is determined by whatever conditions exist in the network into which the primary winding of C.T. is connected and every variation in the primary current alters the magnitude of the impressed

p.d. necessitating a corresponding change in the induced voltage and, with this, in the main flux. This in turn changes the size and shape of the triangle formed by I_e , I_m and I_c which are the dominant factors in producing the ratio and phase angle errors. If these errors are plotted against flux density, it is shown^{3.8} that the percentage ratio error change is a minimum over the working range of flux density for an overall unity power factor of the burden, a situation rarely encountered in practice; on the other hand, the phase angle error at the same overall power factor of burden changes significantly with the flux density. It is, however, remarkably consistent at low lagging power factor, again a condition seldom occurring in a practical application, especially in a measuring circuit.

Since the flux density is directly proportional to the secondary current and therefore to the primary current (to the same degree of approximation as the error equations), the dependence of the errors on the overall burden phase angle and secondary current can easily be checked from these curves. The other useful method of approximation of these errors is the Mollinger and Gewecke C.T. diagram^{3.9}. These methods, however, show the behaviour of a single current transformer connected in circuit. For a number of current transformers connected to a network, the estimation is rather difficult and for the present test it becomes more complicated as both the C.T.s are working at different flux densities and are connected differentially.

3.4.2.6 Modification of errors

Over the years, a number of successful attempts have been made to reduce C.T. errors. Some of these are basically made to reduce the ratio error, as from equation (3.17) if K_c is made equal to K_n for some specific operating conditions, by making K_t slightly less than K_n , it is possible to minimize the percentage ratio error for specific operating conditions. This will not, however, affect the phase error appreciably. The adjustment of K_t can be done by providing fractional turns in a number of ways^{3.10}.

It is sometimes more important to have minimum phase angle error than minimum ratio error as, for example, when power is measured by a dynamometer wattmeter connected through a current transformer and especially at a very low load power factor. (The present application is a most suitable example of a completely new way of using current transformers.) Some of the methods employed for such corrections are associated with design rather than with operation and, although very ingenious, can become less effective under operating conditions other than those specified by the designer. To meet this end, use was made of auxiliary circuits and compounding devices^{3.11} on the one hand and of better core materials^{3.12} on the other.

On the basis of the previous discussions/references and error equation, it is clear that:

1. Both errors depend on secondary current and secondary overall power factor including burden.
2. Both errors change differently with the change in operating conditions and therefore it is not possible that

correction made for one error will also affect the other in the same way. It is in fact common for certain correction methods to reduce one error but increase the other.

In view of the above, the output with minimum errors can only be obtained if a C.T. is designed on such basis that the errors should remain minimum ones over a maximum range of operation or be designed specifically for the particular circuit in view, i.e. metering, protection or integrated circuit for energy measurement. It is a general practice that C.T.s are designed separately for metering or protection not on the grounds of errors but to meet other requirements as specified in B.S. 3938. Metering transformers are, however, used in energy measurements and since power is generally supplied to the consumers within a range of certain power factor, the energy metered is corrected by a certain factor on the basis of the C.T. error.

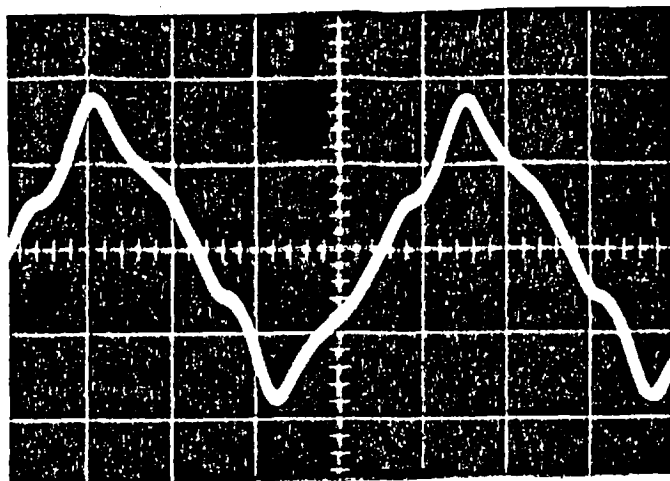
3.4.2.7 Current transformers and the present test

The C.T.s used in the present work are type AL and type CM according to B.S. 3938. In each case the primary is wound around the transformer with 12 turns in the case of type AL and 8 in type CM to give a unity ratio with highest rated winding. Comparing the current ratings of these windings with the excitation current of the test transformer, the C.T.s are being operated at very low flux density which is the range of maximum error as the errors vary approximately inversely as the square of the ampere-turns. The basic reason for more percentage errors at low burden current is the fact that I_e does not reduce proportionally with the reduction in the primary current, i.e. the ratio between I_e and I_p does not

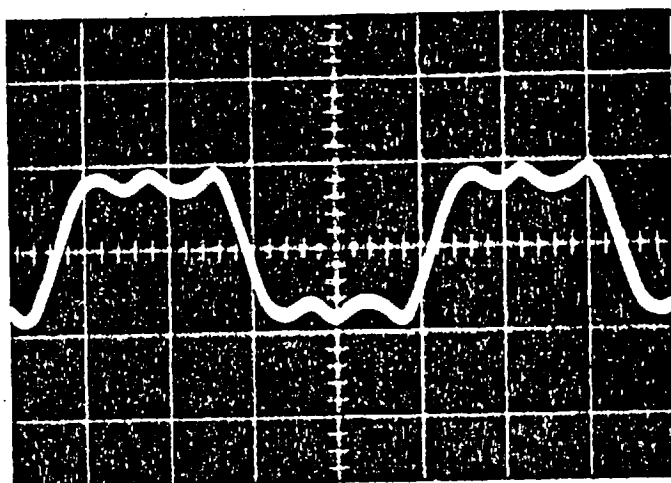
remain the same. Although the primary winding is made symmetrical around the transformer housing, for a uniform induction in the core, the housing being rectangular causes the concentration of ampere turns at some section and thus core in operation experiences a non-uniform induction throughout its magnetic length. The errors under such conditions would be considerably different from those specified by the manufacturers according to the accuracy clause. Park^{3.13} made a number of tests with respect to the position of primary conductors when passed through the window of C.T. and results showed that errors do vary with the location of the primary conductor.

In view of the above operating constraints, the C.T.s used to perform this test to a reasonable accuracy should have a minimum phase error and the burden presented by the instrument must match the rated burden of the C.T.s. Since the excitation current separated from the input and output currents bears a nearly quadrature relation with the induced voltage, any dynamometer wattmeter connected to such a circuit will be more susceptible to give erroneous reading for very small phase angle error than for the ratio error.

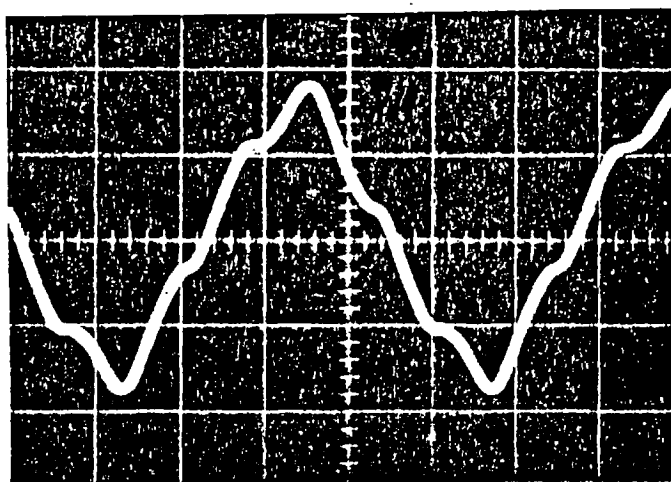
Fig. 3.8 shows oscillograms of excitation current of the test transformer separated by this method using unity ratio C.T.s and Fig. 3.9 using 2:1 ratio transformation. The latter being taken on a scale X2. The waveforms are identical, showing an excellent agreement in corresponding phases. When these are compared with the no-load current waveform, Fig. 3.5, there is agreement as far as the waveforms are concerned but there is, if anything, a slight



(a)



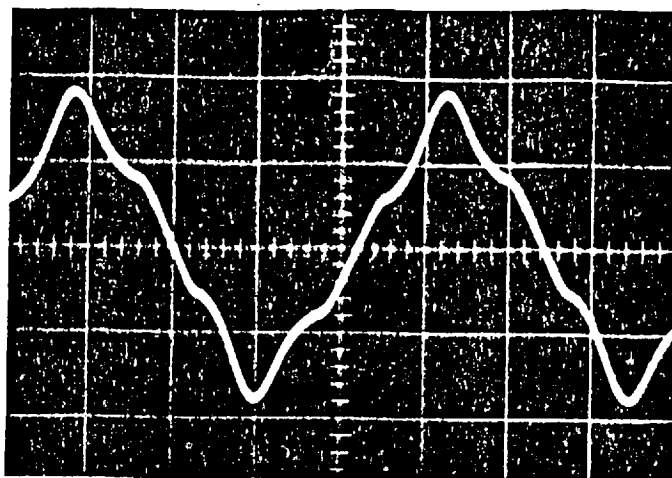
(b)



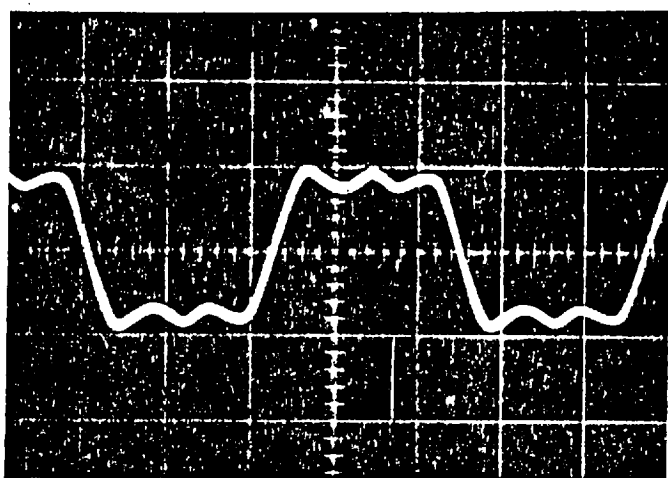
(c)

FIG. 3.8

Oscillograms of the excitation current extracted by the current transformer differential method, employing unity ratio. Waveforms correspond to phases as in Fig. 3.5.

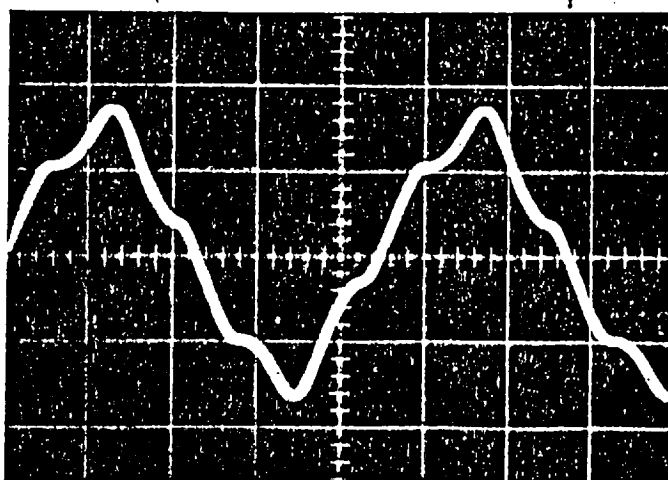


(a)



(b)

oscillograms
up side down



(c)

FIG. 3.9

Oscillograms of the excitation current extracted by the current transformer differential method, employing 2:1 ratio. Waveforms correspond to phases as in Fig. 3.5.

difference in magnitude. This is considered due to the cumulative errors of both current transformers. Due to the introduction of phase error in the secondary ampere turns of the current transformer, the differential ampere-turns are not truly representative of the excitation current of the test transformer as far as their phase relation is concerned. The core loss thus measured does not agree with the measurement made by open circuit test and by the other method used to make measurement under loaded condition. The trend of variation of core loss with load phase angle is also not similar to that shown by other methods. Rather, typically at lagging load power factor the loss measured increases rapidly with decreasing power factor and even if the copper and iron losses of the test transformer are computed from the difference between input and output power, no agreement is obtained.

The measurement taken from the same pair of current transformers but temporarily wound-on primary and permanently wound secondary windings interchanged, even differ from each other for the same load angle. Fig. 3.10 shows the variation of core loss with the load angle measured using type AL unity ratio current transformers with firstly primary as inserted turns and secondary wound, and, secondly, primary wound and secondary inserted. The trend of variation of core loss with load angle is similar in both cases, but the magnitudes differ widely.

Table 3.1 shows the measurements taken for three different conditions at the same load angles. The first two represent the conditions as specified for Fig. 3.10 and the third, using current transformation ratio 5:1 with both windings permanently wound.

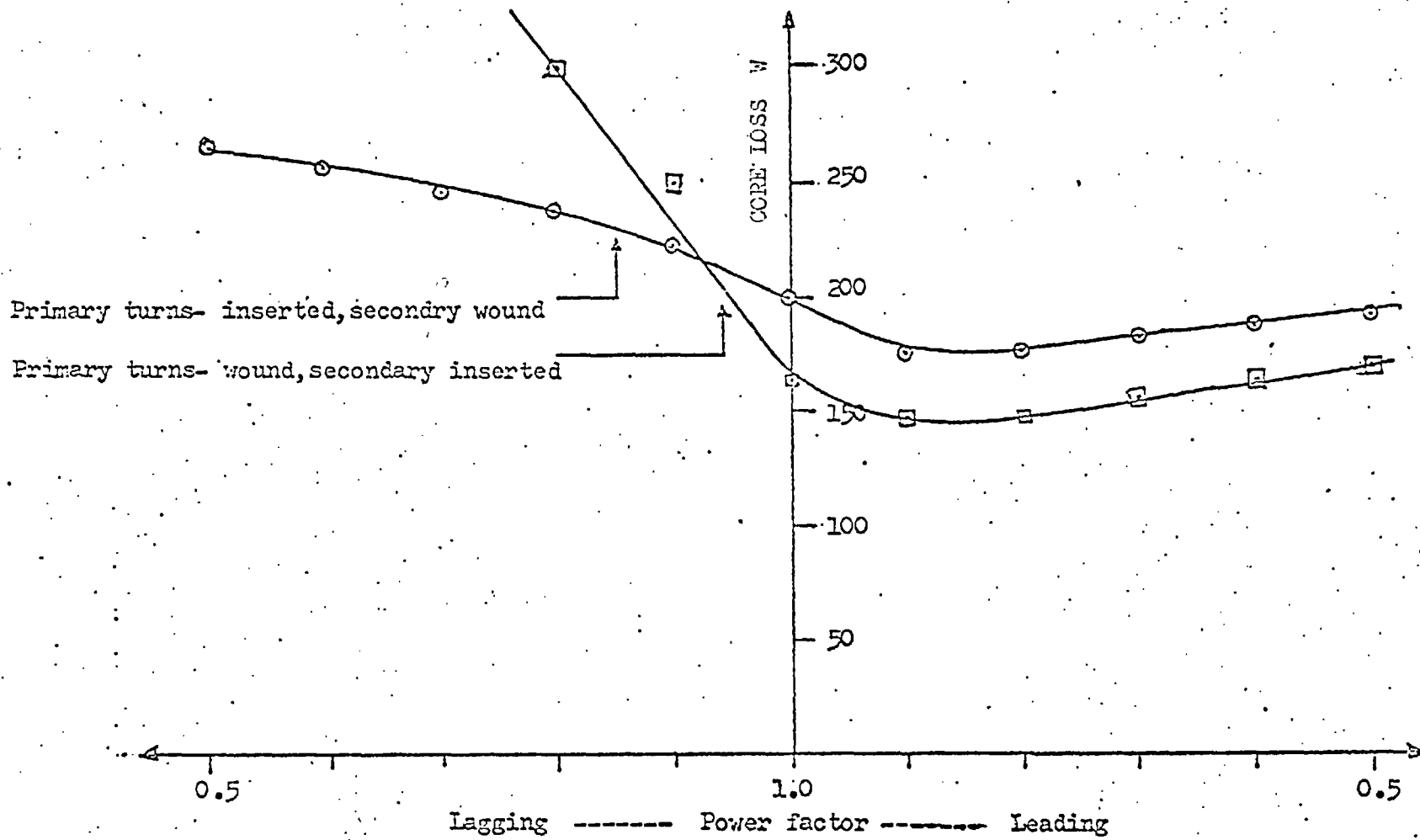


FIG. 3.10

Measurements of core loss by the current transformer differential method with interchanged connections.

Connections	P.F.	Core loss per phase (watts)			Total core loss Watts
		Red	Yellow	Blue	
C.T. Ratio 1:1 Primary inserted Secondary wound	Unity	115	-205	290	200
	.8 Lead	85	-200	300	185
	.8 Lag	125	-190	300	235
C.T. Ratio 1:1 Primary wound Secondary inserted	Unity	75	-210	300	165
	.8 Lead	30	-205	310	135
	.8 Lag	90	-175	370	285
C.T. Ratio 5:1 Primary wound Secondary wound	Unity	62.5	-203	312.5	172
	.8 Lead	62.5	-219	312.5	156
	.8 Lag	94	-194	300	200

TABLE 3.1

Comparison of core loss measurements made with type AI current transformers but interchanging the connections and current ratio.

In view of the above, this method of separation of excitation current is not very accurate even when best accuracy class of current transformers is employed. However, there are further suggestions on which work could not be done on the first two due to non-availability of the required current transformers and on the third due to lack of time. They are given in the following sections.

3.4.2.8 Use of compensated current transformers

Much work has been done at the National Research Council of Canada to develop a compensated current comparator, which is now commercially available^{*} for the precise measurement of current transformer errors^{3.14}. The current compensator, basically a three-winding unity ratio transformer with the energy transfer properties of a current transformer^{3.15}, can thus be used in this work with slight operational modifications. If its outer core be excited through the compensation winding by a separate source, the unit can work as an ideal current transformer of unity ratio having no ratio or phase error. The secondary ampere turns will be an exact reflection of the primary ampere turns. A pair of such transformers connected differentially will deliver a differential current which will correspond to the excitation current of the test transformer in magnitude and phase.

3.4.2.9 Use of current sensors

Current sensing devices based on Hall effect are now commercially available^{**}. Like current transformers these

* Available in U.K. through Lyons Instruments Ltd., Herts., England.

** Available in U.S.A. from F.W. Bell Inc., 4949 Freeway Drive, East Columbus, Ohio.

devices have the circuit isolation facility and thus can be used like current transformers in separation of excitation current. Since devices based on Hall effect take their supply from a separate source and give an output signal proportional to the magnetic field produced by the current passing through the conductor, around which the device is placed, if the supply to the Hall crystal is kept constant, there will be practically no ratio error. The phase angle error can be eliminated by well designed circuitry. The other advantage that this device has over the current transformer is that in the case of insertion of the device in any one phase, the other two phases of the three-phase transformer under test will not experience any unbalancing effect. The differential current taken through a pair of such sensors may have far less error than introduced by the current transformers, and this may be a true representation of the excitation current of the transformer under test.

3.4.2.10 Use of a single current transformer

If a single current transformer is used as in the detection of zero-phase sequence currents, i.e. a ring core wound with a secondary winding and with "go" and "return" primary bar conductors threaded symmetrically through its window, then the same current flowing in both primary conductors produces no net m.m.f. in the core. However, if a leakage current flows in either conductor, a m.m.f. appears in the core and a p.d. is produced across the terminals of the secondary winding with magnitude depending on the resultant m.m.f. which in turn depends on the difference of the currents in the go and return primary conductors. If a similar

arrangement is provided with both primaries wound around the core of a current transformer such that the input current of the test transformer magnetizes the core in one direction and the output current in the other, the net magnetizing ampere-turns will represent their ampere-turn difference. In this way the errors introduced will be those of a single current transformer. Secondly, it will be much easier to estimate the impedance being offered by the burden and thus to predict the errors. However, there may be an additional factor due to mutual inductance between the inserted windings and its effects on the errors would have to be investigated.

3.4.3 Series resistance differential method

3.4.3.1 The method

Ohm's Law in its original form states that the potential drop across a solid conductor, through which a current is flowing without affecting the temperature of the conductor is proportional to the current. Thus if two equal resistors are employed and equal currents are passed through them, the potential drop across each resistor will be the same. If, however, the magnitude of either of currents is changed, a proportional change will occur in the potential drop across that resistor. This is the basis of the present method to obtain a potential drop signal proportional to the excitation current of the test transformer.

Two three-phase banks of non-inductive resistors calibrated and adjusted to 0.549Ω by means of a Kelvin Bridge were inserted in each phase of the input and output sides of the test transformer.

Since three-wattmeter method was to be employed to measure the core loss, the primary and secondary of the test transformer were connected in star-star with isolated neutrals. The potential drops appearing across each resistor R_A and R_B of the respective phase were subtracted vectorially through isolating transformers T_1 and T_2 , having primaries connected across the potential drop signals and secondaries connected differentially as shown in Fig. 3.11. The isolating transformers were used in 1:5 ratio to get a substantial output signal when the core loss was measured by Hall effect wattmeter and 1:1 ratio when measured by VAW meter due to its capability to process lower voltage signals.

3.4.3.2 Effects of R_A and R_B on the impedance of the transformer

Since the impressed voltage V_1 on the input side of the test transformer was considered from terminal B, the resistance R_A will not become a part of the winding resistance R_1 , but will become the part of line impedance feeding the transformer. Similarly, the resistance R_B will become the part of the load impedance. The resistance R_A and R_B will therefore have no effects on the characteristics of the transformer. Fig. 3.12 shows the waveform of the signal extracted. Comparison with the waveform of the no-load current shows a precise agreement which was not achieved in the previous method. The phase relation of the signal when checked with the induced voltage was found to be the same as no-load current has with the induced voltage. The harmonic analysis of this signal was made and compared with that of no-load current. There appears to be no difference in the percentage content of the higher harmonics.

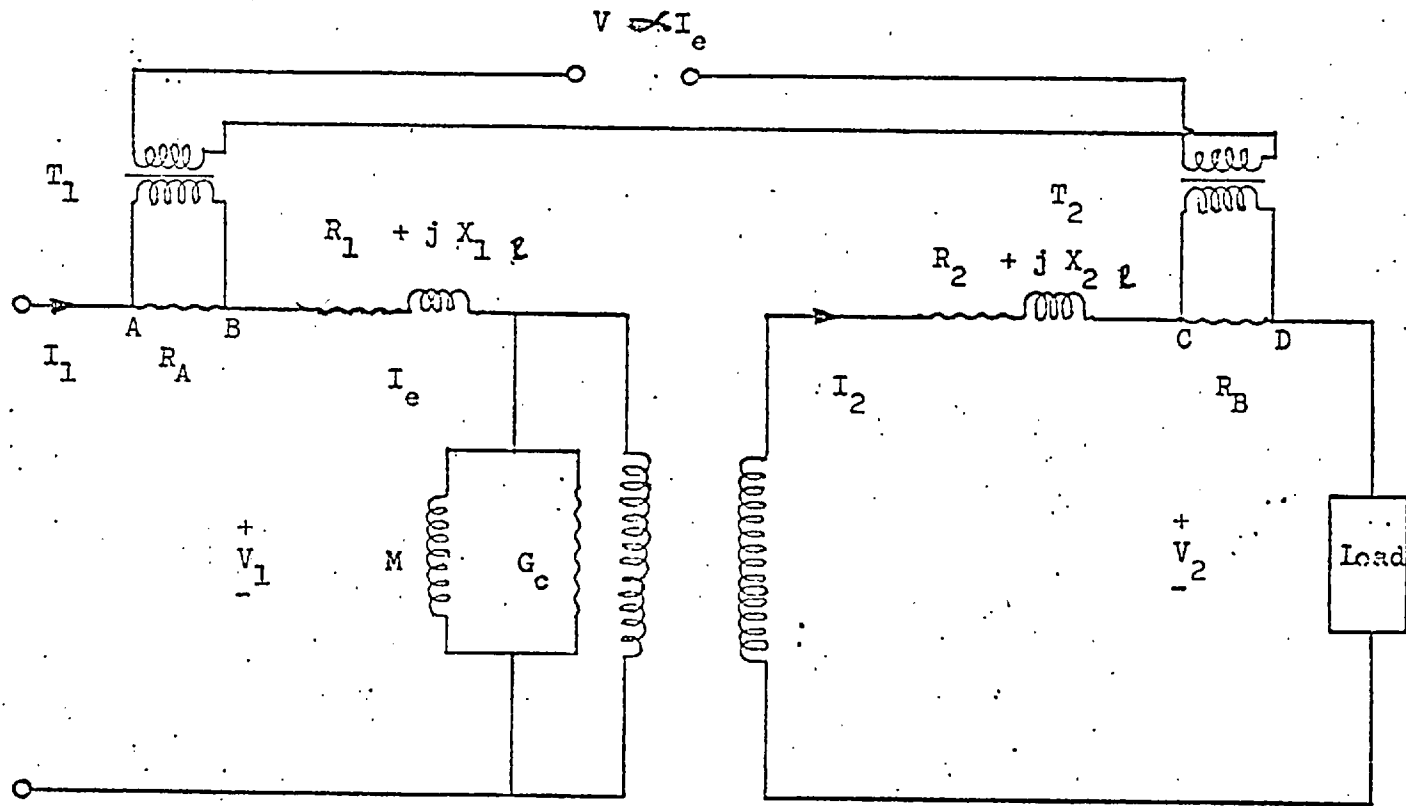
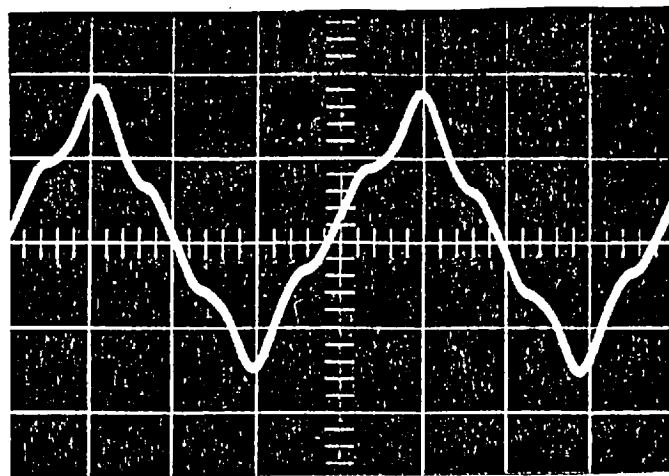
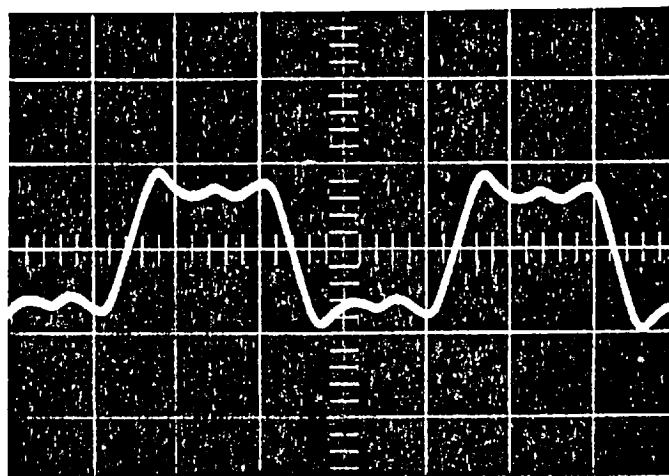


FIG. 3.11

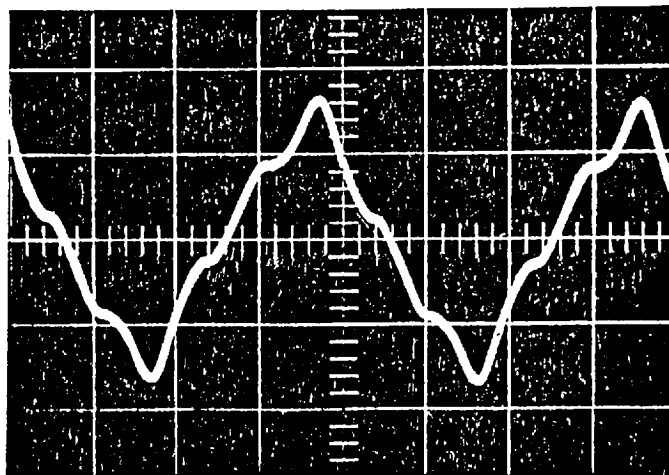
Arrangement for extracting a signal proportional to the excitation current by the differential of potential drop across series resistance.



(a)



(b)



(c)

FIG. 3.12

Oscillograms of the excitation current extracted by series resistance differential method. Waveforms correspond to phases as in Fig. 3.5.

3.4.3.3 Effects of ratio and phase angle error of an isolating transformer

In a current transformer the primary current, and hence the voltage generated across the primary terminals, varies over a wide range. This affects not only the secondary current but also the ratio and phase angle error. A voltage transformer, on the other hand, although not operating at constant voltage maintains a flux density and hence excitation current that is independent of the secondary burden. It follows that the change of ratio, i.e. input voltage to output voltage, is dependent only on the effects of resistance and leakage reactance of the transformer. Since these two factors are easily controllable at the manufacturing stage, the variation of ratio or phase error is slight. The dependence of these errors on secondary burden is very linear and thus if the isolating transformers are operated at a secondary burden smaller than rated, the error will be small.

Since the isolating transformers used to extract the voltage signal proportional to the excitation current were operated at very much lower burdens than their rating, the errors are assumed to be negligible and also constant over the range for which they were operated.

3.4.3.4 Flexibility of the method

This method, unlike the direct differential method, has no serious limitation regarding the voltage ratio of the transformer or the method of connection (in the case of a three-phase unit). The series resistance ratio in the input and output circuit can be

made proportional to the turns ratio of primary to secondary of the transformer under test and the series resistance ratio can even be combined with the isolating transformer ratio to give an overall unity ratio to the final output signals. This method of adjustment of series resistances ratio was used in the measurement of core loss of a single-phase "micro" transformer in Chapter 7, where the input to output voltage ratio was 8:1.

The connections for a three-phase unit can either be star-star or delta-delta, giving signals proportional to phase or line currents respectively and the core loss thus can be measured. If the transformer has other connections such as star-delta or delta-star, the series resistors on the star-connected side of the transformer can be adjusted such that the potential drop signals become proportional to the line currents and before making the vectorial subtraction one set of signals has to be shifted by an angle of 30° to become in phase with the other side. The only precaution to be taken in the selection of the resistors is that they must be non-inductive. As power transformers have reasonably large input and output currents, any linear resistor (strip type as used in instrument shunts) with practically no inductance can be used to give a measureable potential drop signal.

CHAPTER FOUR

POSSIBLE METHODS OF MEASUREMENT OF CORE LOSS ON LOAD;
THEIR COMPARISON, CHOICE AND LIMITATION

4.1 CORE LOSS

The power losses constituting the hysteresis and eddy current loss due to alternating flux in a ferromagnetic core are commonly considered together and are referred to as core loss or iron loss of the device under consideration. These losses have been expressed analytically by a number of equations; the most representative ones are:

$$\text{Hysteresis loss } = P_h = \mathcal{V} [K_h f (B_{\max})^n] \quad (4.1)$$

$$\text{Eddy Current loss } = P_{ec} = \mathcal{V} [K_{ec} \tau^2 f^2 (B_{\max})^2] \quad (4.2)$$

here, \mathcal{V} = volume of the core;

K_h = material constant, quality dependent;

K_{ec} = material constant, resistivity dependent;

f = frequency of alternating flux;

B_{\max} = peak flux density;

τ = thickness of lamination;

n = exponent always having a value ≈ 2.0 , although the historical value of 1.6 given by Steinmetz^{4.1} is often cited as representative (may only hold over a limited range of B_{\max}).

The total power loss is thus the sum of these two losses and is given by:

$$\text{core loss} = P_c = P_h + P_{ec} \quad (4.3)$$

The equations stated above are based on a number of assumptions which in practice may not be fulfilled and there could

be a wide difference between the numerically computed loss and the experimentally measured loss. However, these equations give a real understanding of the relationship between the loss and variables.

4.2 THE CORE LOSS CURRENT

Like the two components of power loss in the core, the core loss current is also divisible into two components, viz. hysteresis current and eddy current. Both of these currents flow in the circuit to meet the power loss due to hysteresis and eddy current effects respectively produced in a ferromagnetic core on account of the periodically changing flux between the two limits of induction. If the wave form of the excitation current is analysed, it appears that the hysteresis current waveform leads the flux waveform and thus magnetizing current waveform by 90° and is in phase with the induced voltage. The eddy currents circulating in the laminations have the direction such to oppose any change in the flux and thus to counter externally applied magnetomotive force tending to change the flux. The counter e.m.f. in the circuit and hence the induction in the core must remain unchanged and to keep this, a component of the m.m.f. must be supplied to neutralise the effect of eddy currents. This component of the exciting current is in phase with the induced voltage and this is directly additive to the hysteresis current. It supplies the power absorbed by the eddy current loss in the core. In circuit terms this means that each eddy current path constitutes a short circuited one turn winding which is perfectly coupled to the primary.

4.5 EQUIVALENT CIRCUIT WITH EDDY CURRENT AND HYSTERESIS LOSS

A transformer excited through one of its windings with the other winding open circuited can be represented by the equivalent circuit shown in Fig. 4.1.

Here, G_h and G_{ec} are the two fictitious shunt conductances representing hysteresis and eddy current effects, I_h and I_{ec} are the currents through these conductances, I_m is the reactive component of the excitation current which produces flux but does not supply any power loss associated with the magnetic circuit, E_1 and V_1 are the induced and impressed voltages in the excited winding.

In terms of power loss, the above can be expressed as:

Hysteresis loss:

$$P_h = E_1^2 G_h = E_1 I_h \quad (4.4)$$

$$= K_h \cup f (B_{\max})^n \quad (4.5)$$

$$\text{or } I_h = \frac{K_h \cup f (B_{\max})^n}{E_1} = \frac{K_h \cup (\phi_{\max})^n}{4.44 N \phi_{\max} A^n} \quad (4.6)$$

Eddy current loss:

$$P_{ec} = E_1^2 G_{ec} = E_1 I_{ec} \quad (4.7)$$

$$= K_{ec} \cup \tau^2 f^2 (B_{\max})^2 \quad (4.8)$$

$$I_{ec} = \frac{K_{ec} \cup \tau^2 f^2 (\phi_{\max})^2}{4.44 N \phi_{\max} A^2} \quad (4.9)$$

(A = cross-sectional area of core in equations (4.6) and (4.9).)

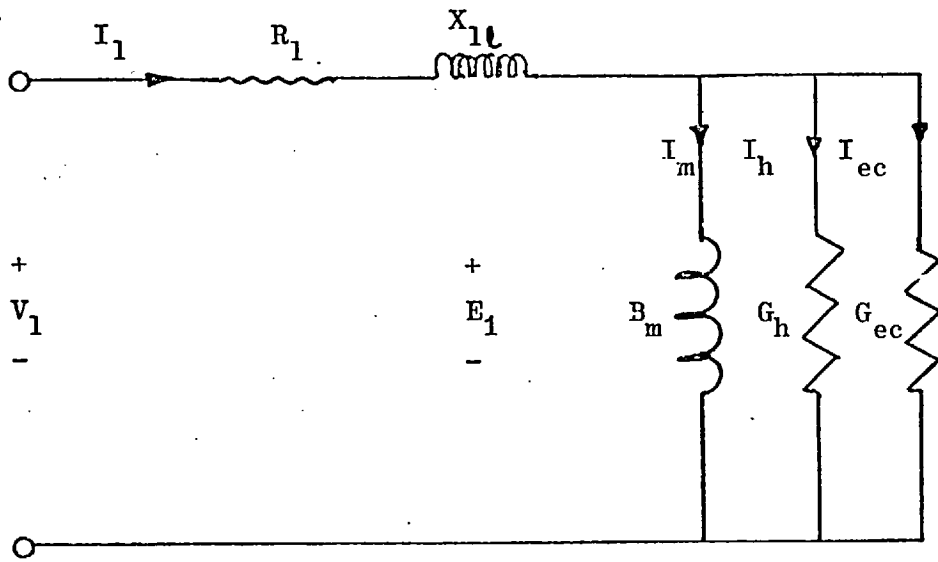


FIG. 4.1 Equivalent circuit of a transformer with open circuited secondary showing hysteresis and eddy currents.

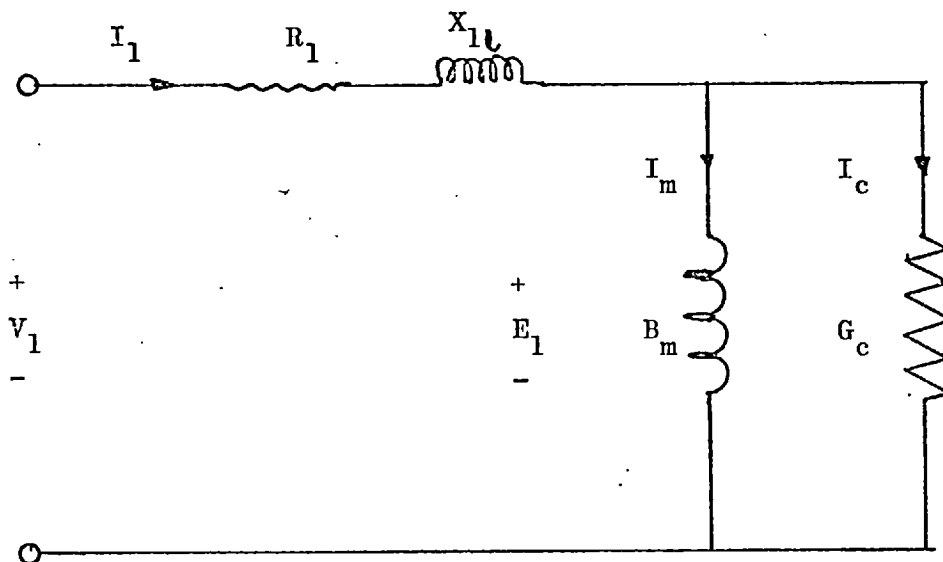


FIG. 4.2 Equivalent circuit of a transformer with open circuited secondary showing core loss current.

Since the conductances G_h and G_{ec} are in parallel, the combination of these two can be represented by a single conductance G_c representing the core loss conductance such that:

$$G_c = G_h + G_{ec} \quad (4.10)$$

Accordingly, a simple equivalent circuit can be drawn as shown in Fig. 4.2, where I_c is the core loss current:

$$I_c = I_h + I_{ec} \quad (4.11)$$

$$= G_c E_1 \quad (4.12)$$

The core loss P_c can thus be given by:

$$P_c = G_c E_1^2 \quad (4.13)$$

$$= I_c E_1 = (I_h + I_{ec}) E_1 \quad (4.14)$$

$$= P_h + P_{ec}$$

4.4 COMPUTATION OF CORE LOSS

The published literature (see 1.3) reveals that most of the work has been done for the measurement of core loss of a single lamination or a batch of laminations, the most popular one being the Epstein Square core loss test. This is because it is possible to make a number of assumptions in such a test regarding the magnetic homogeneities of the laminations, the uniformity of the flux density and purity of its wave shape, the symmetry of the hysteresis loop and elimination of minor loops, all factors that influence the hysteresis loss measurement. Similarly, factors influencing the eddy current loss can also be controlled. These

are mainly, the electrical homogeneity of the laminations, constant thickness of the laminations, their perfect insulation and the maintenance of the flux direction parallel to the plane of the laminations. The results thus obtained remain very nearly within the range of numerical computation.

Since these tests are performed with open circuited secondaries, the excitation current is wholly the current that maintains the magnetization in the core and thus the core loss can easily be measured by a wattmeter. The problem with a loaded secondary becomes difficult as the division of current into its load and excitation components requires a thorough investigation of the method to be used as discussed in 3.3.

Once the excitation current has been extracted from the primary and secondary currents of the transformer, the product of its in-phase component with the induced voltage will represent the average power loss in the core:

$$P_c = E_1 I_e \cos \phi \quad (4.15)$$

here, ϕ is the phase angle between E_1 and I_e .

The induced voltage can be picked up across the open circuited terminal of the secondary or any search coil wound around the core.

Electrodynamic and induction wattmeters are fundamentally designed on the basis that their torque is proportional to $VI \cos \phi$ ^{4.2}. The electronic wattmeter^{4.3} and multipliers based on Hall effect^{4.4} have the same capabilities that their output contains a signal proportional to the product of the two input signals and the cosine of the phase angle between them.

4.5 INDEPENDENCE OF POWER ON THE HARMONICS IN THE CURRENTS AND VOLTAGES

The instantaneous power absorbed by a circuit element through which an instantaneous fall of potential $v(t)$ occurs in the direction of the current $i(t)$ is:

$$p(t) = v(t) i(t) \quad (4.16)$$

Over any time Δt , the average power is:

$$P_{\text{avg}} = \frac{1}{\Delta t} \int_0^{\Delta t} v(t) i(t) dt \quad (4.17)$$

If both the current and voltage are sinusoidal functions of time with the same period, the instantaneous power is the sum of a constant component and a sinusoidal component of double frequency. The double frequency component represents an oscillation of power, the average of which is zero. The constant component thus represents the average power and its value is given by:

$$P_{\text{avg}} = V I \cos \phi$$

Here, V and I are the effective (r.m.s.) values of sinusoidal varying voltage and current, and ϕ is the phase angle between them. If both the current and voltage are functions of time with the same period but non-sinusoidal, they can then be expressed by Fourier Series as under:

$$v(t) = V_{\text{dc}} + \sqrt{2} V_1 \cos(\omega t + \alpha_1) + \sqrt{2} V_2 \cos(2\omega t + \alpha_2) + \dots \quad (4.18)$$

$$i(t) = I_{\text{dc}} + \sqrt{2} I_1 \cos(\omega t + \beta_1) + \sqrt{2} I_2 \cos(2\omega t + \beta_2) + \dots \quad (4.19)$$

here, V_{dc} and I_{dc} are the direct components,
 $V_1, V_2, \dots, I_1, I_2$ are the effective values of the harmonic components.

Equations (4.18) and (4.19) can be expressed in convenient form as:

$$v(t) = V_{dc} + \sum_k \sqrt{2} V_k \cos(k\omega t + \alpha_k) \quad (4.20)$$

$$i(t) = I_{dc} + \sum_n \sqrt{2} I_n \cos(n\omega t + \beta_n) \quad (4.21)$$

where k or n is the order of harmonics in the voltage and current, respectively. The instantaneous power

$$\begin{aligned} &= p(t) = v(t) i(t) \\ &= V_{dc} I_{dc} + V_{dc} \sum_n \sqrt{2} I_n \cos(n\omega t + \beta_n) \\ &\quad + I_{dc} \sum_k (\sqrt{2} V_k \cos(k\omega t + \alpha_k)) \\ &\quad + \left[\sum_k \sqrt{2} V_k \cos(k\omega t + \alpha_k) \right] \left[\sum_n \sqrt{2} I_n \cos(n\omega t + \beta_n) \right] \end{aligned} \quad (4.22)$$

When the last term of equation (4.22) is expanded, a typical term obtained would be:

$$2 V_k I_n \cos(k\omega t + \alpha_k) \cos(n\omega t + \beta_n) \quad (4.23)$$

From the trigonometric identity $\cos x \cos y = \frac{1}{2} [\cos(x+y) + \cos(x-y)]$ equation (4.23) will be simplified as:

$$\begin{aligned} &V_k I_n \cos [(k+n)\omega t + (\alpha_k + \beta_n)] \\ &+ V_k I_n \cos [(k-n)\omega t + (\alpha_k - \beta_n)] \end{aligned} \quad (4.24)$$

A typical term as above can be expressed as the sum of two cosine components whose frequencies are the sum and difference of the frequencies of the harmonic components in the voltage and current.

The last term of equation (4.22) from which this typical term has been evaluated is the summation of all such terms. The instantaneous power thus contains such harmonic components whose frequencies are the sums and differences of the frequencies of all the harmonic components in the voltage and current.

The average power, P_{avg} , is the average value of the instantaneous power taken over a complete cycle. In equation (4.22) the first term is constant and therefore its average value is $V_{dc}I_{dc}$. The second and third terms represent harmonic components whose frequencies are integral multiples of the fundamental frequency. These terms represent harmonic oscillations in the power, and the average value of each such component for an integral number of cycles is zero. Equation (4.22) shows that when $k \neq n$, the power resulting from the product of a harmonic voltage of one frequency and the harmonic current of another frequency is the sum of two alternating components with zero average value.

When $k = n$, the last term of equation (4.24) becomes:

$$V_n I_n \cos(\alpha_n - \beta_n) = V_n I_n \cos \theta_n \quad (4.25)$$

where $\theta_n = \alpha_n - \beta_n$ and is the phase angle between the n^{th} harmonic component of the voltage and current.

The average value of the last term in equation (4.22) is thus zero for harmonic components of voltage and current of different frequency but is $\sum_n V_n I_n \cos \theta_n$ for all the harmonic

components of voltage and current of the same frequency, consequently the average power is given by:

$$P_{\text{avg}} = V_{\text{dc}} I_{\text{dc}} + \sum_n V_n I_n \cos \theta_n \quad (4.26)$$

4.6 METHODS USED IN CORE LOSS MEASUREMENT

As discussed in 4.4, once the excitation current or a signal proportional to the excitation current of the transformer under test is extracted, the measurement of instantaneous power loss in the core can be done simply by the vectorial multiplication of this signal with a signal proportional to the induced voltage. This multiplication can be done by a number of devices. The devices used in the present work have been discussed in this section.

The excitation current was extracted by the methods discussed in 3.4 and the induced voltage was taken from the open circuited terminals of the tertiary winding which has a unity ratio with the primary and secondary windings. The induced voltage signal was also available from the shadow winding of the transformer tested, the details of which are given in 6.1.3.

Apart from the core loss measurement by indicating instruments, various other ways of demonstrating the instantaneous core loss are also available, giving a dynamic hysteresis loop and the instantaneous power curve. These methods were also used in this work, as discussed in 4.6.4.

4.6.1 Measurement with dynamometer wattmeter

When the excitation current has been extracted using the direct differential method or by means of current transformers, the

measurement of core loss can be made by a dynamometer wattmeter as for any other electric circuit or as in the open circuit core loss measurement test. The wattmeter current coil carries the differential current and the induced voltage is applied to the potential coil. The wattmeter used must be of low power factor type or with a relatively low potential coil resistance^{4.5,4.6} to allow sufficient current in this circuit to produce a good working torque as the current and voltage vectors lie almost in quadrature when the core is magnetized to a high flux density.

The wattmeter used was a Weston Model S.67 Form 2 which has a compensation circuit to eliminate the indication of power consumption of the potential coil circuit from the instrument reading.

The other meter used was a Cambridge Type 44371 A.C. test set in which a number of settings of input range switches for current and voltage can give a large ratio of W/VA and thus can be used at low power factor without loss of accuracy^{4.7}.

This method can only be used when the excitation current is derived either by direct differential method or through current transformers. The former is only possible for a unity ratio transformer and the latter is not an accurate method as shown in 6.3.3. Due to these limitations, other methods were investigated as shown in the following sections.

4.6.2 Measurement with VAW meter Model 102

The VAW meter is an electronic wattmeter^{4.8} having two main amplifying channels. One channel takes the voltage signal proportional to the circuit voltage and the other a voltage signal proportional to

the circuit current. The voltage channel's gain is adjusted in steps from 1.5 to 600 V by the "Voltage Range Switch", while plug-in type shunts are provided for current channel, each giving a potential drop of 0.045 V at the shunt rating. For measurement of voltage or current, the output of the respective channel is rectified after due amplification and supplied to a direct current meter to give a direct indication of the quantity being measured. For power measurement, after amplification both signals are suitably combined and applied to a multiplier which works on the square law principle. The response to the output of the multiplier on a direct current meter (D'Arsonval movement meter) will be proportional to the product of the input signals and the cosine of their relative phase displacement angle. The output signal, however, also represents the instantaneous power flowing in the circuit which contains both d.c. and oscillating terms. The average of this latter term if taken over a complete cycle is zero.

The VAW meter can be used to multiply two signals A and B of the same frequency if fed separately to its two channels and the response as stated above will be $AB \cos \phi$, where ϕ is the phase displacement angle between A and B. On the basis of the above, the VAW meter was considered for use to measure the core loss of the transformer being tested as below:

A signal proportional to the excitation current was taken by the series resistance differential method given in 3.4.3.1 and fed to the voltage channel of the meter. Another signal from a "Zenith" three-phase, phase shift unit with secondaries fed to a star connected resistive load allowing a current of 0.5A to flow in the current channel of the meter with 0.6 A shunt in the circuit.

This signal was shifted into phase with the induced voltage of each phase of the transformer under test, the differential current signal of which was fed to the voltage channel. The direct current meter reading was thus the product of two signals, one proportional to the excitation current of the transformer and the other in phase with the induced voltage, and the cosine of the phase angle between them. The VAW meter can work down to a power factor of 0.1 without any loss of accuracy and this was considered a better alternative to the dynamometer wattmeter for the measurement of core loss.

The VAW meter output thus does not directly indicate the core loss but this can be computed if some kind of calibration is made. Since the main interest of the work was to study dependence of core loss on the load phase angle rather than to obtain numerical values of the core power loss, the actual readings were plotted as shown in Fig. 6.11 and compared with other results on dimensionless basis as shown in Figs. 6.13 and 6.14. No calibration curves were made to compute actual core loss. The phase alignment of the current vector taken from the phase shift unit with respect to the induced voltage was effected by feeding one signal to the X-plates of an oscilloscope with the internal time base switched off and the other to Y-plates. The straight line pattern on the screen indicates the alignment of both signals.

4.6.3 Measurement with a Hall effect wattmeter

Since there were certain drawbacks with the VAW meter measurements, e.g.

1. No direct indication of core loss can be given without calibration curves.

2. There are only two meters of this kind in the Department and, as discussed in 2.5, the most accurate method of core loss measurement for three-phase, three-limb transformers is to use the 3-wattmeter method. One VAW meter had therefore to be switched from one phase to the other. By doing so, the ohmic loss of the circuit components were also included in the phase under consideration, thus introducing an unbalancing factor into the system.

3. The current vector taken from the phase shift unit had to be adjusted each time to align with the reference vector and, although made through an oscilloscope, a small error in phase alignment can affect the indication of VAW meter significantly.

It was considered worthwhile to build a meter in which the above factors can be eliminated and the signal could be fed in directly. Hall effect multipliers were chosen for this purpose and a three-phase meter based on these multipliers was made. Details of its construction are given in Chapter 5. A signal proportional to the excitation current was passed through the Hall plates and a magnetic field was produced by a very small current supplied by the induced voltage circuit. The output signal was proportional to the product of these signals and the cosine of their phase angle.

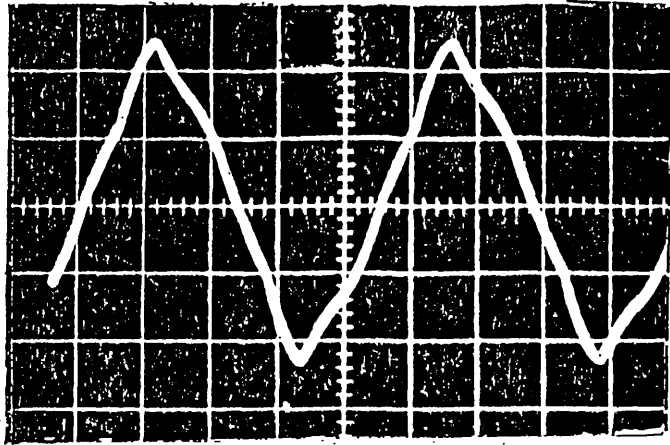
4.6.4 Derivation of core loss from the instantaneous power loss

Since the output signals of both the VAW meter and the Hall effect wattmeter represent the instantaneous power containing the d.c. and oscillating terms, the area under the positive and negative half cycles respectively should represent the total energy

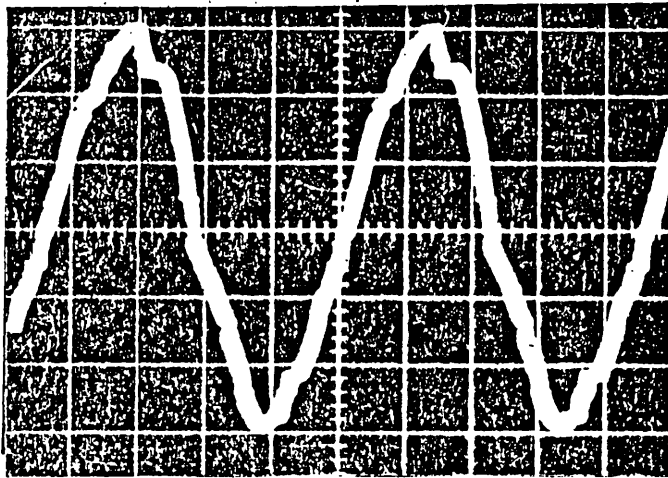
supplied to the circuit and returned by the circuit over a period of one cycle. The difference of these areas will thus represent the energy consumed by the magnetic circuit. Ohmic loss due to winding resistance has already been eliminated from the power curve by using the induced voltage rather than the applied voltage as reference. A set of such curves was photographed for the three-phase transformer as shown in Fig. 4.3 for the summated output of the Hall effect wattmeter at different load power factors. These curves do show differences in the positive and negative half cycles but have not been evaluated to compute the core loss. The areas under these curves can be measured by planimeter and this was done in the case of the core loss measurement in the single-phase micro-transformer detailed in 7.6.4, where the instantaneous power signal was taken from the VAW meter. The comparison of these results with those of the direct indication by VAW meter has been given in Table 7.2.

4.6.5 Core loss display through dynamic hysteresis loss loop

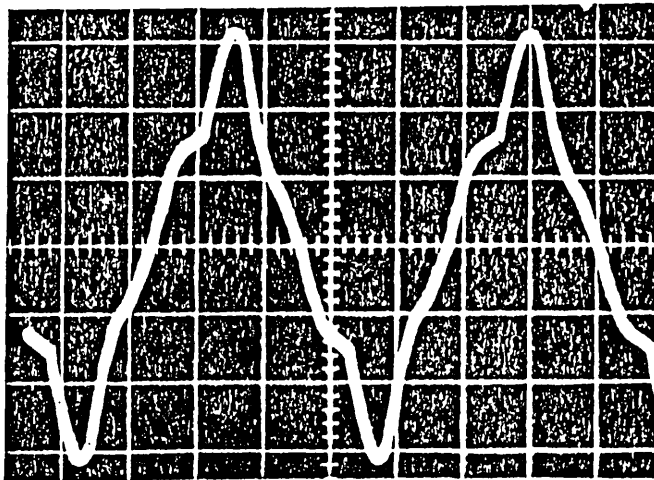
Since the area of the dynamic (or a.c.) hysteresis loop can be associated with the total core loss, i.e. eddy current plus hysteresis, such loops if plotted with excitation current as abscissa and flux linkages as ordinates, have areas proportional to, and represent the total energy loss per cycle in the transformer core. Dynamic loops obtained on the above basis for different load power factors represent the energy loss per cycle at that particular load power factor. If core loss depends on load angle, the area of the loops will not be constant but will change with the power factor of the load. Since core loss measurement had shown its dependence on load angle, an attempt was made to display these loops on oscilloscope



(a)



(b)



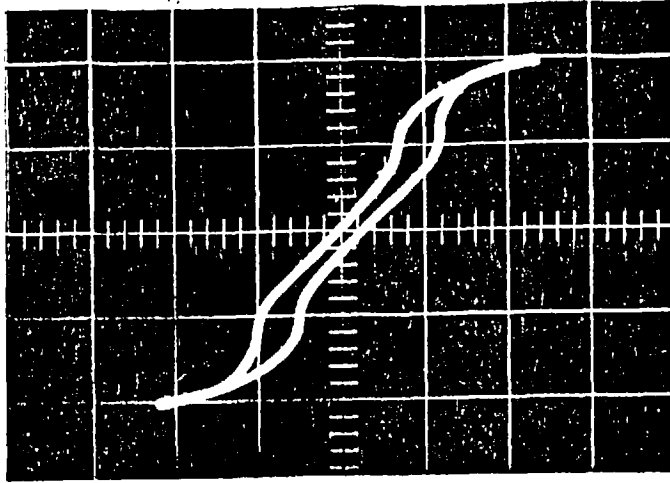
(c)

FIG. 4.3

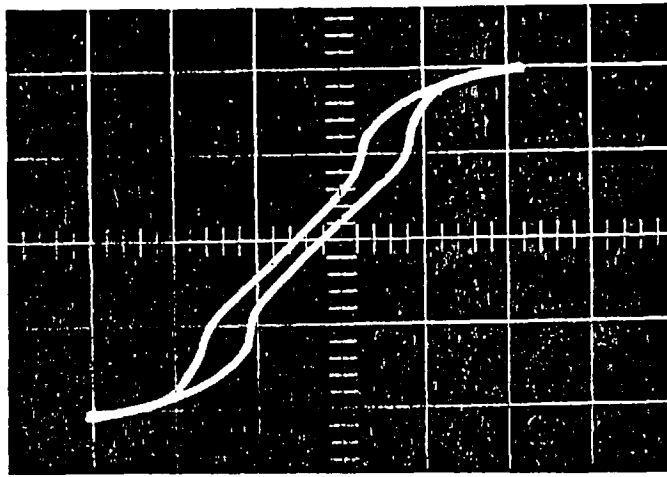
Instantaneous power curves for three-phase transformer representing summated core loss of all three phases.

Diagrams (a), (b) and (c) correspond to P.F.s unity, 0.64 lagging and 0.56 leading respectively.

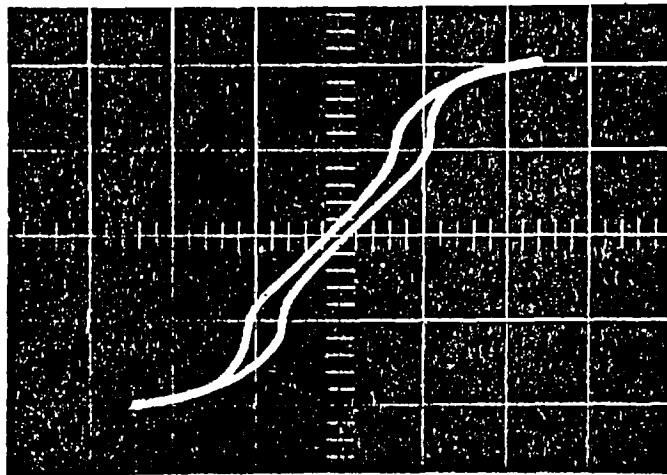
by feeding the X-plates with a signal proportional to the excitation current extracted by method given in 3.4.3 and Y-plates with a flux linkage signal derived from a simple passive element (resistance-capacitance) screened (co-axial) integrator of known efficacy. The loops were displayed at different load angles for the three-phase transformer, showing a change in the loop area for each phase with varying load angle (see Figs. 4.4, 4.5 and 4.6). However, it is difficult to associate these loops with increase or decrease in core loss, since as shown in 2.6 core loss in each phase is not positive and the total loss is the algebraic sum of the per phase losses. When, however, this experiment performed for the single-phase micro-transformer, the change in the loop area was directly relateable to the load angle. The area increases with the capacitive and decreases with inductive load as for the results obtained by other measurement methods. The change is quite significant and is a very good means of displaying the loss and to show the dependence on load angle. These loops are shown in Fig. 7.12.



(a)



(b)

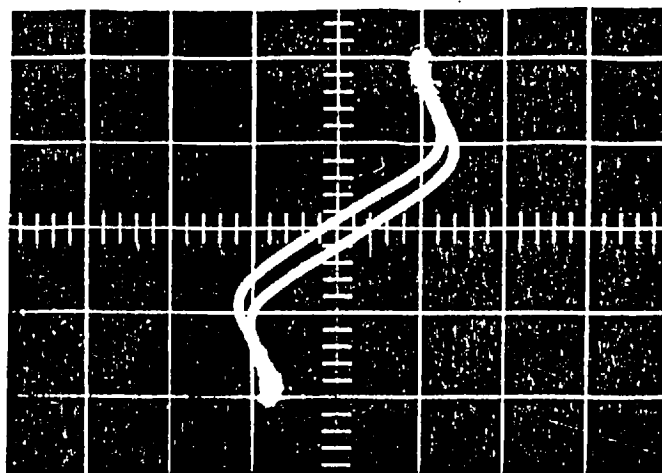


(c)

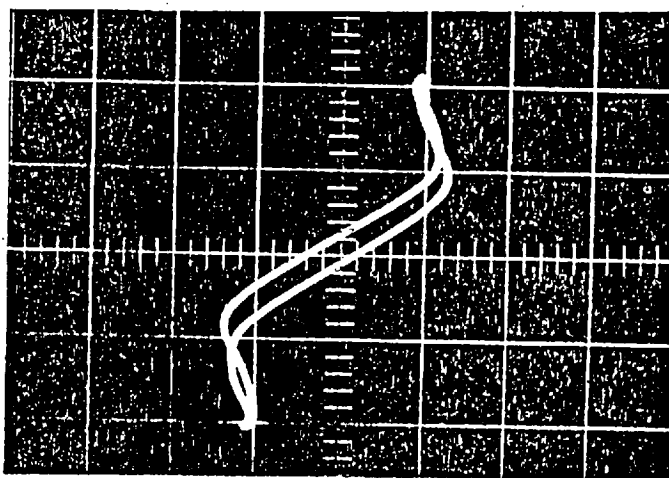
FIG. 4.4

Dynamic hysteresis loop representing core loss of red phase in a three-phase transformer.

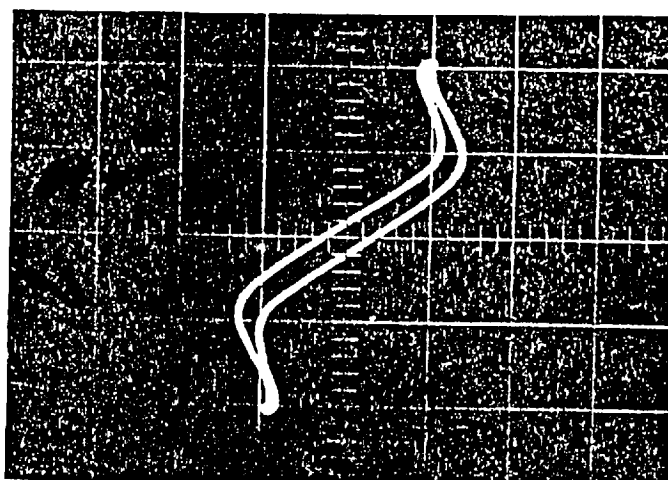
Diagrams (a), (b) and (c) represent the P.F.s as in Fig. 4.3.



(a)



(b)

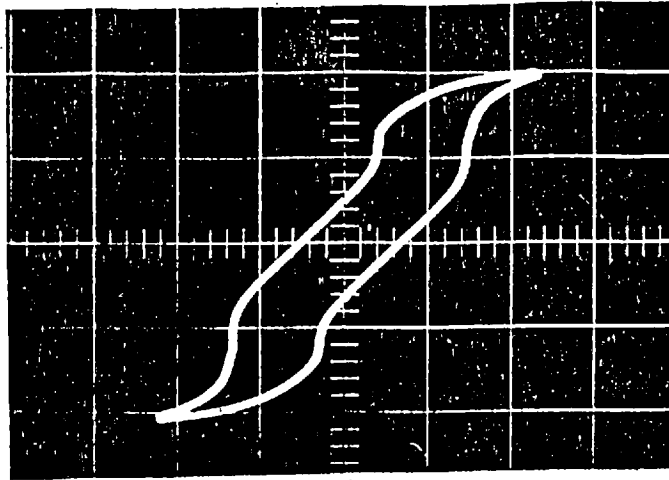


(c)

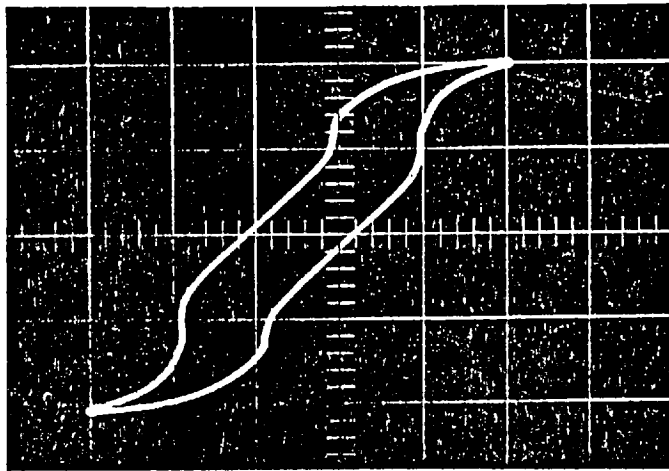
FIG. 4.5

Dynamic hysteresis loop representing core loss of yellow phase in a three-phase transformer.

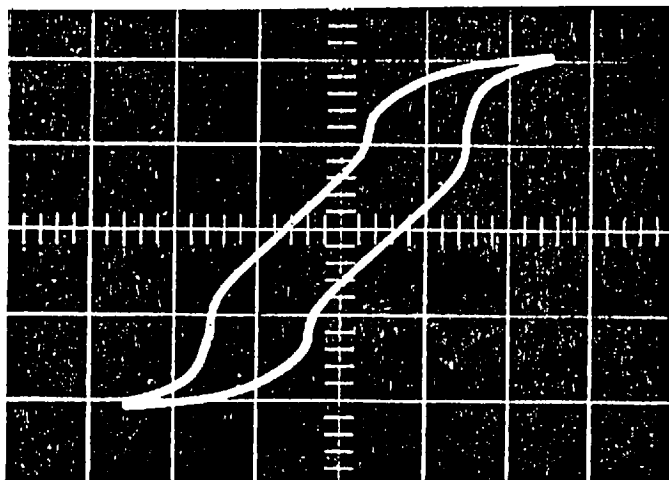
Diagrams (a), (b) and (c) correspond to the P.F.s as in Fig. 4.3.



(a)



(b)



(c)

FIG. 4.6

Dynamic hysteresis loop representing core loss of blue phase in a three-phase transformer.

Diagrams (a), (b) and (c) correspond to P.F.s as in Fig. 4.3.

CHAPTER FIVETHREE-PHASE ELECTRONIC WATTMETER USING HALL
EFFECT MULTIPLIERS5.0 INTRODUCTION

The Hall effect^{5.1}, since its discovery a century ago, has been used in a number of ways in the field of measurements. Most work has been done in the measurement of power flow in an electromagnetic field where conventional measuring instruments cannot be applied directly. Input limitations often require the conversion of the measured quantities into analogous ones, i.e. current into a proportional voltage. In certain cases, the power to be measured is so small that a large percentage error is introduced during this conversion process.

Probes based on this effect have shown their superiority in the investigation of magnetic circuit behaviour in machines where search coils could not be employed due to space limitations and to their dependence on flux density and frequency^{5.2}. The most significant use of these probes is to investigate the flux pattern in d.c. machines where search coils only respond to the time varying component of flux.

Hall effect metering has been developed considerably in the recent past, following the commercial availability of cheaper semi-conducting materials which exhibit a greater effect relative to metallic conductors.

5.1 HALL EFFECT

If a transverse magnetic field is applied to a conductor carrying a current in the longitudinal direction, an e.m.f. is set up in the conductor at right angles to both the magnetic field and the conductor longitudinal axis. The effect is more pronounced in semi-conductors than in metallic conductors. Fig. 5.1 shows a crystal of semi-conductor placed in a magnetic field. Assuming a Cartesian co-ordinate system, if the field is in the Z-direction and the current through the crystal is in the Y-direction, the generated e.m.f. due to Hall effect will be in the X-direction.

5.1.1 Explanation of the Hall e.m.f.

When a current carrying conductor is placed in the magnetic field, a force is experienced by the conductor, the direction of which is determined by the left hand rule. This force is in fact the sum of the forces on the individual current carrying charges and each charge under the influence of this force tends to move in the direction of force, i.e. at right angles to both the magnetic field and the axis of the conductor. This deflection of charges from their original paths creates a non-uniform charge density and thus a voltage gradient is set up within the conductor.

5.1.2 Magnitude of the Hall e.m.f.

The magnitude of e.m.f. due to Hall effect can be given at any instant by:

$$V = R_H \frac{BI}{t} \text{ volts}$$

where, R_H = Hall coefficient, $\text{Vm}^2\text{A}^{-1}\text{T}^{-1}$,
 B = Magnetic field density, T,

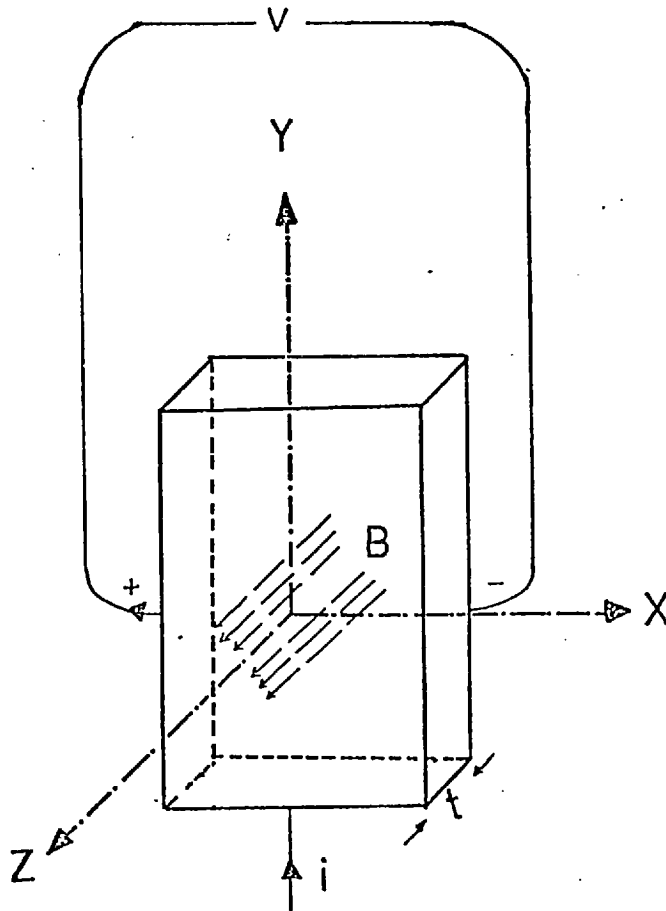


FIG. 5.1

Semi-conductor element and Cartesian co-ordinate system. The polarity of Hall e.m.f. for mobile negative carriers is shown by positive and negative signs.

I = Longitudinal current in Hall plate, A,

t = Thickness of Hall plate in Z-direction, m.

The magnitude of the generated e.m.f. is dependent on R_H and t for specified conditions of operation, i.e. flux density and plate current. The thickness of the plate can only be reduced to a certain degree due to mechanical limitations. The Hall coefficient is a function of carrier concentration and mobility in the semiconductor; these two factors are, to a certain extent, controllable in the manufacture of the semi-conductor.

5.2 THE WATTMETER

As discussed in 3.4.3, a signal proportional to the excitation current of the transformer of which the core loss measurement is to be made can be extracted by ohmic voltage drop method. If this signal is fed to the Hall crystal and a field is produced by the current supplied by the induced voltage circuit, the generated e.m.f. signal will thus be proportional to the product of their in phase components, which in fact is proportional to the instantaneous power delivered by the circuit to the core to meet its energy loss.

5.2.1 The Advantages

The main advantages over dynamometer wattmeter are:

1. It is practically independent of frequency over a considerable range.
2. It has no moving mechanism for the process of multiplication.

3. It can be made compact in size.
4. The introduction of errors for low power factor operation is far less than with a dynamometer wattmeter.

5.2.1 The Limitations

The fundamental limitation of this wattmeter is its very small output which is in the range of mV. To measure this signal even on a highly sensitive D'Arsonval movement meter, which is probably the most common analog form of electrical measurement, some sort of amplification of the signal is necessary. Digital instruments can be used to process the signal directly due to their own built-in amplifier circuits. The selection of a proper digital instrument, however, requires a thorough knowledge of the circuitry employed by the manufacturer. For a.c. measurement an a.c. to d.c. converter is always inserted between the a.c. signal and the digital voltmeter which measures the d.c. voltage^{5.3}. Depending on the method of conversion used, the display is derived from a mean sensing, a peak sensing or a true r.m.s. conversion. The latter can only be done by a thermocouple device. Thus much care is required in selecting the correct instrument for the type of signal to be processed. The output is usually calibrated in r.m.s. and a waveform with form factor other than a pure sine wave, i.e. 1.11, will result in erroneous measurement if the conversion is done on the basis of average of positive or negative half cycle. In the case of a peak responding instrument, the effect of a distorted waveform on the error in the output is much greater.

It is , however, convenient to take the signal to a moving coil instrument after due amplification. The instrument will respond to the mean value of the signal which is very much independent of the harmonics so long as the content of the harmonics is not so great as to produce such a distortion as to enable the waveform to cut the axis more than once in each half cycle^{5.4}.

For better accuracy, to measure the power of a low level signal, the optical type of galvanometer based on moving coil principle can be used.

5.3 CRITERIA OF CIRCUIT DESIGN

The important consideration in the design of a circuit for any measuring instrument is the fact that its insertion in the circuit should disturb the circuit conditions to a minimum.

Fig. 5.2 shows the basic circuit for the Hall effect single-phase wattmeter. The major component which will consume power other than the load, are R_A , R_B and R_S . For a good design R_S and R_B should be minimum, with R_A a maximum valued resistor when the meter is to be used for the measurement of power in an ordinary circuit. Since the meter is to be designed to measure the power, but in an unconventional manner, each circuit component needs a thorough investigation before assigning any value.

R_S , if given a very small value, will give a very small p.d. signal which will require an amplification stage before its subtraction through isolating transformers. Since this resistor is connected in series with the input and load feeders, although it

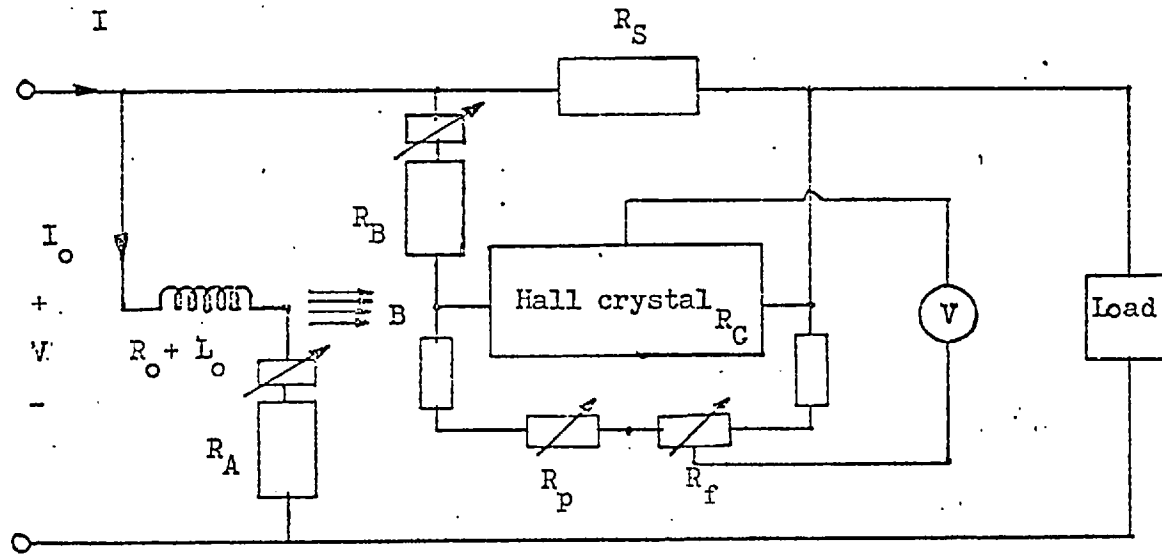


FIG. 5.2 Circuit for a single-phase Hall effect wattmeter.

$$R_A = 2 \text{ K}\Omega + 250\Omega \text{ (variable)}$$

$$R_B = 680\Omega + 25\Omega \text{ (variable)}$$

R_S = Series resistance in the load circuit, value depends on the load circuit current and wattmeter circuitry.

Values of other components given in the text.

will consume power, this will not be indicated in the wattmeter measurement like an ordinary circuit due to its present position in the circuit where it becomes either the part of the line impedance or part of the load.

Resistor R_B has a position such that the power dissipated by it is measured by the meter together with the load power. The power measured by the meter must therefore be corrected by subtracting the power consumed by this resistor from the measured value. The value of this resistor is defined by the circuit design. However, this resistor should be of such a value to allow sufficient current through Hall crystal to give a large ratio of V_H/watts .

Resistance R_A is decided on the basis of the required magnetic field in which the crystal is to be placed and the current rating of the magnetising coil. It should, however, be as high as possible compared to the reactance of the coil.

On the basis of the above, the following values were assigned to these components:

$$R_A = 2 \text{ K}\Omega + 250\Omega \text{ (variable resistor),}$$

$$R_B = 680 \Omega + 25\Omega \text{ (variable resistor),}$$

$$R_S = .549 \Omega.$$

The values of the other components are shown in 5.3.4 (manufacturer's data). The variable resistors were inserted in the circuits of R_A and R_B to adjust the total resistances of each circuit such that the same current should pass through the magnetising circuit or plate circuit when equal voltages are impressed on these circuits, respectively, for any channel in the case of the three-phase wattmeter.

5.3.1 Frequency dependence of series resistor R_S

The series resistance R_S should have no inductance so that the p.d. signal to be picked up across this resistor should give a direct measure of the current passing through it, independent of the frequency. The resistors used in this work are doubly-wound in opposition so that the magnetic field produced by one turn is nullified by another.

5.3.2 Frequency dependence of the magnetizing coil circuit

The impedance $(R_A + R_o + \omega L_o)$ of the magnetizing coil circuit is frequency dependent. On the low range of frequency when the effect of the stray capacitance is negligible, the percentage increase in the impedance over zero frequency can be given by:

$$\begin{aligned}
 & \text{Let the impedance at zero frequency} = Z_1 = R_A + R_o. \\
 & \text{Let the impedance at } \omega \text{ frequency} = Z_2 = \sqrt{(R_A + R_o)^2 + (\omega L_o)^2}. \\
 & \text{percentage increase in impedance} = \left(\frac{Z_2 - Z_1}{Z_1} \right) \times 100\% \\
 & = \left[\frac{\sqrt{(R_A + R_o)^2 + (\omega L_o)^2} - (R_A + R_o)}{(R_A + R_o)} \right] \times 100\% \\
 & = \left[\frac{\left\{ (R_A + R_o) \sqrt{1 + \left(\frac{\omega L_o}{R_A + R_o} \right)^2} \right\} - (R_A + R_o)}{(R_A + R_o)} \right] \times 100\% \\
 & = \left[\left\{ 1 + \left(\frac{\omega L_o}{R_A + R_o} \right)^2 \right\}^{\frac{1}{2}} - 1 \right] \times 100\% \\
 & \approx 50 \left(\frac{\omega L_o}{R_A + R_o} \right)^2 \% \quad \text{if} \quad \left(\frac{\omega L_o}{R_A + R_o} \right) \ll 1.
 \end{aligned}$$

The ratio of $\omega L_o / R_A$ is thus the deciding factor for the range of frequency over which the meter can be used (R_o being $\ll R_A$). This ratio is also very important to reduce the phase shift error, as

explained in 5.3.3. The percentage increase in the impedance of present circuit at 50 Hz is almost negligible.

5.3.3 Phase shift error

A small phase shift in the magnetizing circuit current and the magnetic field produced by it is inevitable due to the inductance of the magnetizing coil. The simplest way to eliminate this error is to shift the phase of the current through the crystal by the same angle. This can be done by providing the plate current circuit with an inductance of similar impedance characteristics to that of the magnetizing coil circuit, i.e. the resistance to inductance ratio of both the circuits should be the same:

$$\frac{R_A + R_o}{L_o} = \frac{R_B + R_C}{L_B}$$

where, L_B is the inductance inserted in the plate current circuit.

In the multipliers used, an additional coil of the same characteristics as that of the magnetizing coil is provided by the manufacturer. Initially this coil was used in the plate circuit, but later on eliminated for the following reasons:

1. The resistances R_A and R_B are not of the same value, being decided by other parameters, whereas $R_o \approx R_C$ and $L_o = L_B$. The phase shift in each circuit was different and thus additional errors were introduced, as

$$\frac{R_A + R_o}{L_o} \neq \frac{R_B + R_C}{L_B}$$

2. The ratio of R_A/L_o being very small did not introduce significant shift in the magnetizing coil circuit current which

was checked individually and found to be around 0.25° at 50 Hz in each multiplier.

5.3.4 Manufacturer's data for the multipliers

The manufacturer's data of the multipliers type HMCI used in the construction of the wattmeter are as under:

Plate current	=	300 mA	r.m.s. maximum
Coil current	=	200 mA	r.m.s. maximum
Coil inductance (L_o)	=	22 mH	nominal
Coil resistance (R_o)	=	9 Ω	nominal
Plate input resistance (R_c)	=	2-8 Ω	
Plate output resistance	=	5-15 Ω	
Sensitivity	=	.0044-.0066 mV mA ⁻¹ (AT) ⁻¹	
Misalignment voltage	<	3.0 mV	for 200 mA plate current.

5.4 SOURCES OF ERROR IN MULTIPLIER OUTPUT AND THEIR ELIMINATION

5.4.1 Introduction

The inputs to Hall effect multiplier are the current and a magnetic field. If the plate current I_c is varied according to signal X and the magnetic flux density to signal Y, the output signal V_H in the case of a perfect multiplier assuming no phase displacement between the sources of these signals would be:

$$V_H = KXY \text{ volts}$$

here, K is the constant, dependent upon Hall coefficient and the thickness of the plate.

In practice, the output signal contains the above plus a number of other signals, introduced by certain factors, which requires a thorough understanding for their elimination from the output. These factors can be divided into three main categories according to their nature:

1. Coupling between input and output,
2. Non-linear processes within the semi-conductor,
3. Operational conditions.

5.4.2 Errors due to coupling

The introduction of these errors in the output is essentially due to the magnetic coupling as follows:

1. Between the magnetizing field and output,
2. Hall effect due to the magnetic field produced by the input current which is also perpendicular to the plane of the crystal, thus it could be either additive or subtractive to the main magnetic field, depending upon the direction of current flow.
3. Mutual inductance between input and output loops.

The above errors generally depend upon the physical arrangement of the multiplier and can be minimised by the proper selection of crystal's geometrical parameters, positioning of the magnetizing coil with respect to the plate and the arrangement of the input and output leads to have minimum mutual coupling between these loops. This error minimisation is, however, achieved at the expense of the conversion efficiency.

The multipliers used in this work are factory assembled and housed in sealed containers with pins brought out. There is therefore no possibility of checking any of the above factors. One must select the appropriate grade of multipliers from the manufacturer's data sheet and accept his accuracy data.

5.4.3 Error due to non-linearity

These errors are inherent in the semi-conductor crystal and the most common of these, which can become a large percentage of the output signal if no precautions are taken for their elimination, are discussed in this section.

5.4.3.1 Imbalance error

The fundamental requirement for the output contacts is that they should be placed on a common equipotential for current flowing in the input circuit in the absence of magnetic field, so that there is no output when the field is zero. In practice, however, this is not possible and there is always a residual imbalance, although much care may be taken in soldering the contacts on the semi-conductor. The usual way to eliminate this error is to feed a part of the input into the output circuit in opposition to the unbalanced voltage present there. The manufacturer's data given in 5.3.4 quotes a misalignment voltage ± 3 mV at a plate current of 200 mA and recommended a circuit to balance out this misalignment as shown in Fig. 5.3. This circuit was tried but a complete balance was not achieved. A small voltage was detected on a micro voltmeter when d.c. was passed through the plate in the absence of a magnetic field. A slight increase was recorded with the application of a.c.

The percentage reduction in the error depends on the accuracy of measurement required and since a variation in the output as little as 1% is of much importance in the present measurements, other circuits given by Barlow^{5.5} were tried but little improvement was achieved in the reduction of this error. Finally the circuit shown in Fig. 5.4 and devised by Kuhrt^{5.6} was used. In this circuit two potentiometers R_p and R_f were used instead of one. Additionally two resistors R_1 and R_2 were also employed. These resistors not originally used by Kuhrt were used in this circuit for the following reasons:

1. Reduction in the values of the potentiometers is possible and finer adjustment can be made as resistance/travel ratio is reduced.
2. A resistor larger than the plate input resistance is always present between the input and output terminals and the chance of any malfunctioning in case of accidental short circuit between these terminals is avoided.

5.4.3.2 Feedback error

This error is due to the generation of Hall voltage in the input circuit when the current is allowed to flow in the output circuit. This error can be minimised as a percentage of the desired output by increasing either source impedance, load impedance or both. Since it was not possible to increase source resistance due to its effect in limiting the plate current, the alternative was to increase the load resistance and this was done as detailed in 5.6. The reduction of this error can be done at the expense of the conversion

efficiency. Therefore, the load impedance cannot be increased without a check.

5.4.3.3 Magneto resistance error

The Hall plate can be considered as a bridge with four resistive arms which are balanced at zero flux density. If under the influence of a magnetic field, the proportional increase of resistance in one arm of the bridge is more than the others, the bridge becomes unbalanced causing additional error. The elimination of this error is possible through the same circuit which is employed for imbalance error by making the final adjustment in the output signal on the application of the magnetic field.

5.4.3.4 Rectifying contact error

The resistance between the input and the output could be non-ohmic due to rectifying contacts. This can introduce a significant error and can be eliminated only by balancing circuit. However, this error has not been reported in the low resistivity semi-conductors^{5.7} which have been used in HMC series multipliers. This effect is much pronounced in high resistivity semi-conductors such as germanium^{5.8}.

5.4.4 Errors due to operating conditions

There are certain errors which are associated with operating conditions and must be kept in view while using Hall effect multipliers:

1. Magnetic saturation error - this error is introduced when magnetic circuit is operated at high flux density and drives into saturation.
2. Temperature sensitivity of semi-conductor. Different semi-conductors have different sensitivity to temperature. Some materials are extrinsic at room temperature and therefore their conductivity does not vary greatly with temperature, on the other hand materials intrinsic at room temperature undergo a large change in conductivity with fluctuation in the temperature.

5.5 FINAL BALANCING CIRCUIT

On the basis of the foregoing discussion, the balancing circuit shown in Fig. 5.4 was adopted and the values of circuit components selected for each multiplier by balancing the output against null position of a d.c. micro-voltmeter in the absence of the magnetic field. The final adjustment was made by passing an a.c. current through the plate in the presence of a 50 Hz magnetic field. The output signal was monitored on an oscilloscope and getting an exact symmetry between positive and negative half cycle of the output signals. The component values are given in Table 5.1. The potentiometers were locked in the final adjusted position by "collect" type spindle locks.

The output signal from each multiplier was taken on a "Unilab" 1.0 mA F.S.D. moving coil instrument through its micro-amplifier type 002.601. The output response of each unit was checked providing a fixed field against varying plate current at U.P.F. and plotted accordingly in Fig. 5.5. Similarly, the output

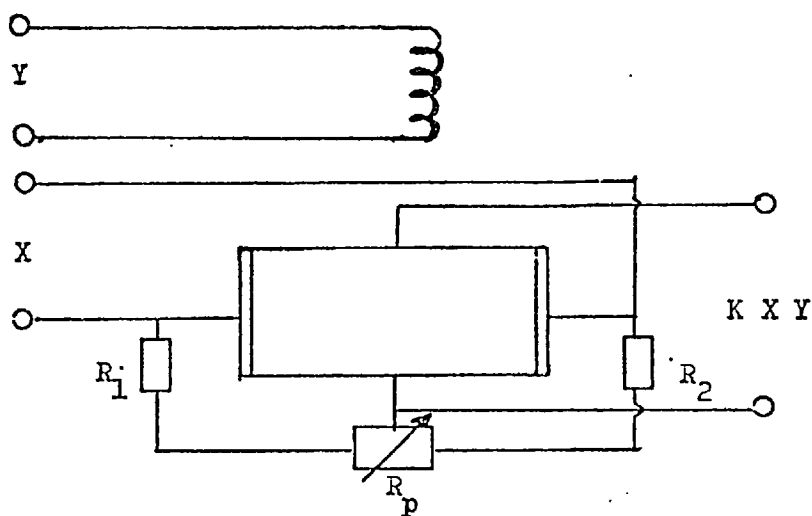


FIG. 5.3 Manufacturer's recommended balancing circuit.

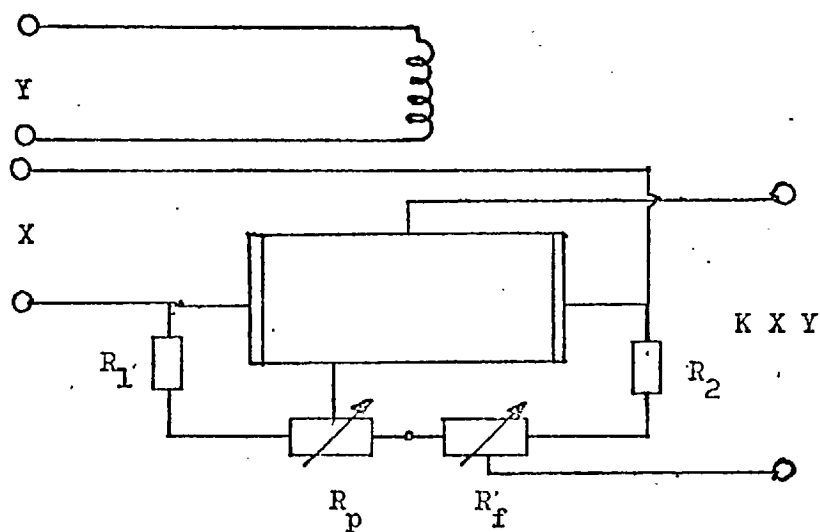


FIG. 5.4 Balancing circuit used.

Multiplier No.	R_1	R_2	R_p	R_f
<u>Recommended:</u> (for all multipliers)	470	470	250	-
<u>Used:</u>				
1	10	2000	2000	25
2	2200	100	250	25
3	1000	1500	500	50

All values in Ohms.

with fixed signals but varying phase angle was checked and plotted in Fig. 5.6. Excellent linearity is shown with little scatter of measured values. The output of each multiplier with the same input, however, differs slightly which is due to the difference in their conversion efficiencies.

5.6 THE SUMMATION OF SIGNALS

The circuit used for summation of output signals from three multipliers is based on the operational amplifier. The response of this circuit is remarkably good even in the addition of signals of different frequencies and phase displacements^{5.9}. The output signals which are available from the multipliers and are to be added have the following characteristics:

1. Are non-sinusoidal and displaced from each other by $\approx 120^\circ$.
2. Have no common potential.
3. Output signals have no isolation with the inputs (contacts soldered on the same plate, forming a four-arm bridge).
4. Have negligible source impedance.

In view of 2 and 3, the direct summation of signals is not possible as this will provide a path to circulate a current within the multipliers and thus additional complications. To overcome this problem of isolation and a common potential reference, a coupling circuit, known as "subtraction" circuit, was designed as shown in Fig. 5.7.

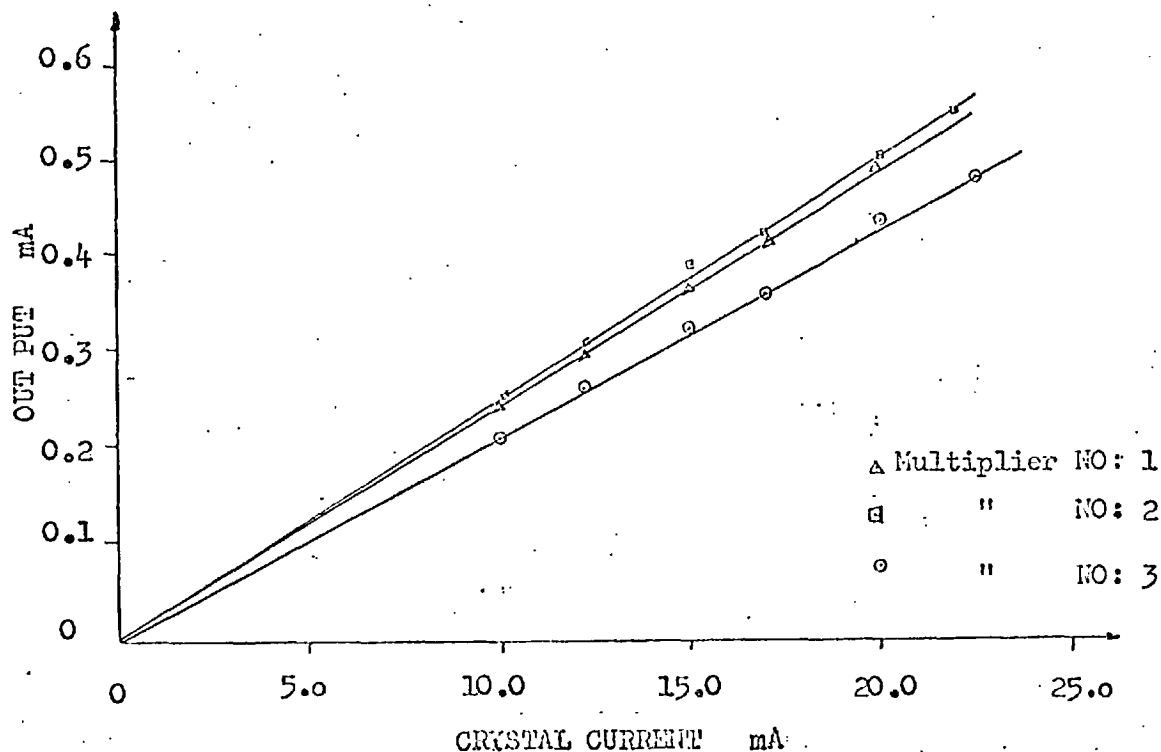


FIG. 5.5 Output of individual multiplier against varying plate current but fixed magnetic field and phase angle.

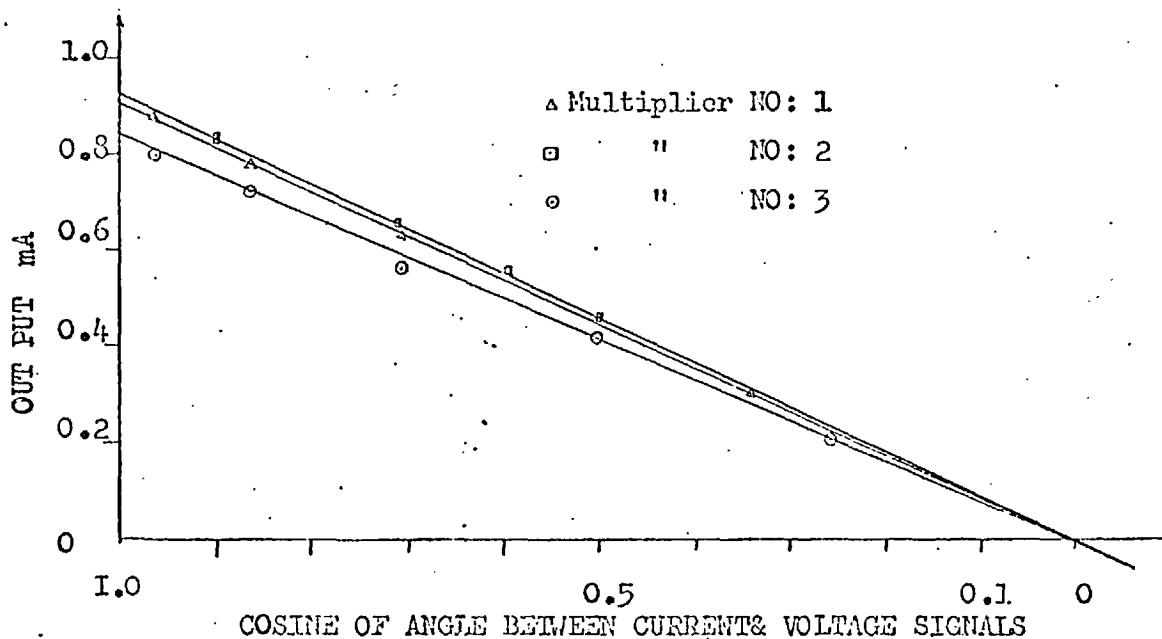


FIG. 5.6 Output of individual multiplier against varying phase angle but fixed magnetic field and plate current.

5.6.1 The subtraction circuit

An operational amplifier 741 was used in differential mode. The d.c. supply to the operational amplifier was from a ± 10 V d.c. source and the offset null was achieved by the feedback through a $10\text{ k}\Omega$ preset control with a 500Ω preset control in series for finer adjustments. One such subtraction circuit was provided on the output side of each multiplier, thus giving an output signal having potential with a common reference and also with considerable isolation as the input impedance is very high when compared to output impedance. Since it was possible to get an amplification from this circuit along with the above, the selection of R_F and R_A was made such that a gain factor ≈ 1.76 was achieved from the output circuit of multiplier one and two while a gain factor ≈ 1.85 was achieved in three. This was done to reduce the difference in the output of the multiplier due to their conversion efficiency. The final output signals from the subtraction circuit were therefore nearly equal for the same input signals. This is shown in Fig. 5.8.

5.6.2 The summation circuit

The operational amplifier circuit referred to in 5.6 for summation signals can now be employed without any problem as the requirement of isolation and of common point potentials have been achieved through the subtraction circuit. Due to the possibility of large amplification by the use of an op. amp. circuit, it was decided that the output of the summation circuit should be of such a magnitude that it could deflect the movement of a high resistance moving coil instrument, thus the true mean value of the Hall e.m.f. can be related directly to the power loss of the core. A moving

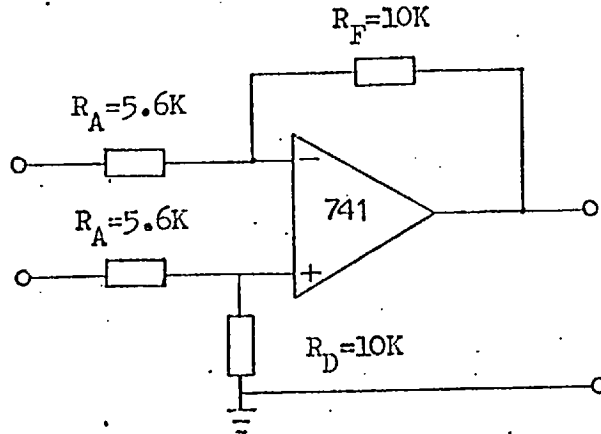


FIG. 5.7

Subtraction circuit.

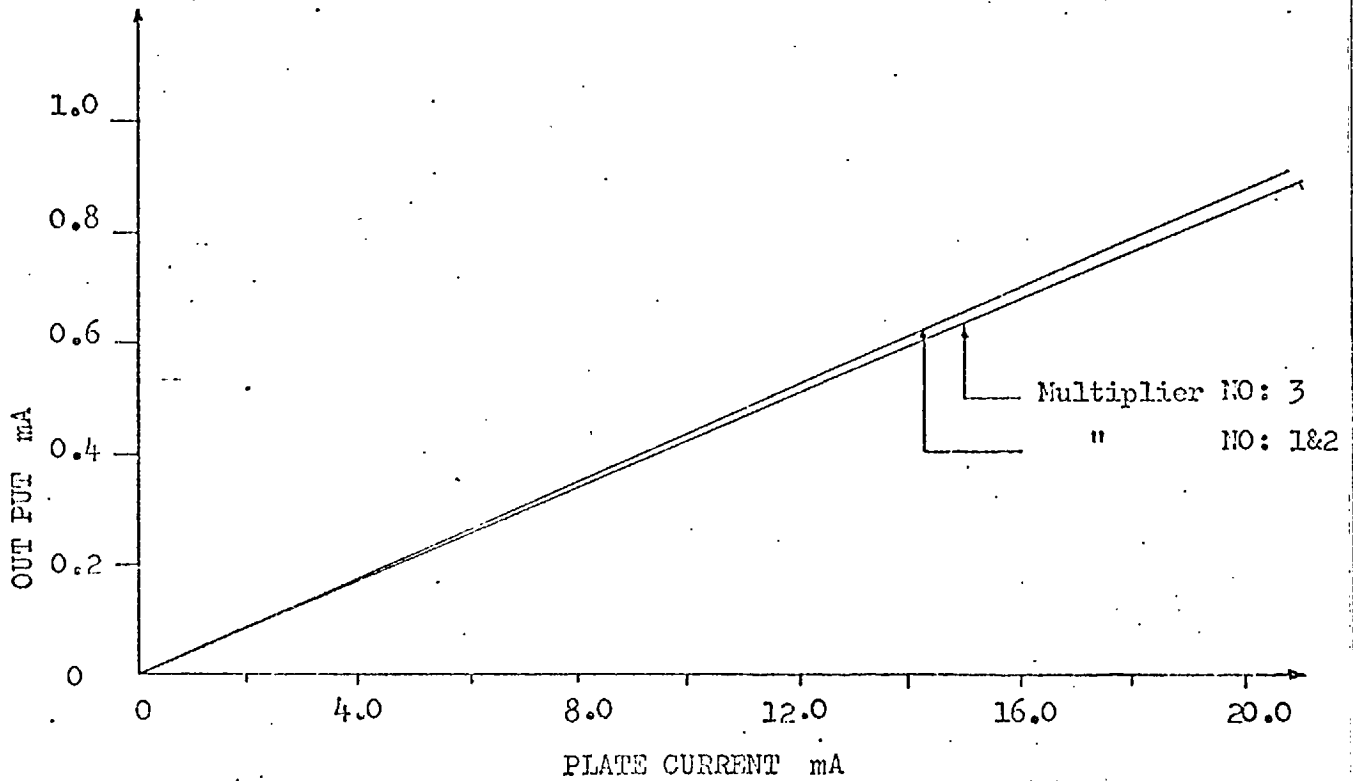


FIG. 5.8

Output of individual multiplier from subtraction circuit against varying plate current as in Fig: 5.5.

coil voltmeter with a coil resistance of 1200Ω and F.S.D. of 100 micro A was selected. By the addition of external resistances the meter was calibrated to give a full scale deflection of 0.3, 1.0, 3.0 and 10.0 V through a selector switch. A polarity reversing switch was also included in the circuit so that any indication below zero can be read on the scale without altering the connection.

The gain and bandwidth of a perfect op. amp. is infinite and ideally the output voltage is controlled by the ratio of R_F to R_A or $V_{out} = (-V_{in})\frac{R_F}{R_A}$. However, in a commercial op. amp. it is not possible to match the input transistors and therefore there is always some input voltage offset and input current offset. Similarly the differential input impedance between the input transistor bases is less than infinity and the output impedance of the amplifier is greater than zero. In view of this, at very large gain the op. amplifier in some circuits introduces some error. Since the aim was to get an output of such a magnitude which can deflect the movement of the above instrument, the output signals from the subtraction circuit were treated in two stages. In the first stage the addition was done with a gain factor of 23.8 and at the second stage a closed loop gain of x 10 was obtained. The total gain of this circuit is thus x 238. The circuit is shown in Fig. 5.9.

5.7 CALIBRATION OF WATTMETER

The output was measured by the moving coil instrument when the meter was measuring power in a pure resistive circuit. The plate current was drawn from a 0.55Ω resistance in each phase of the supply and fed to the Hall plates through isolating transformers of 1:5

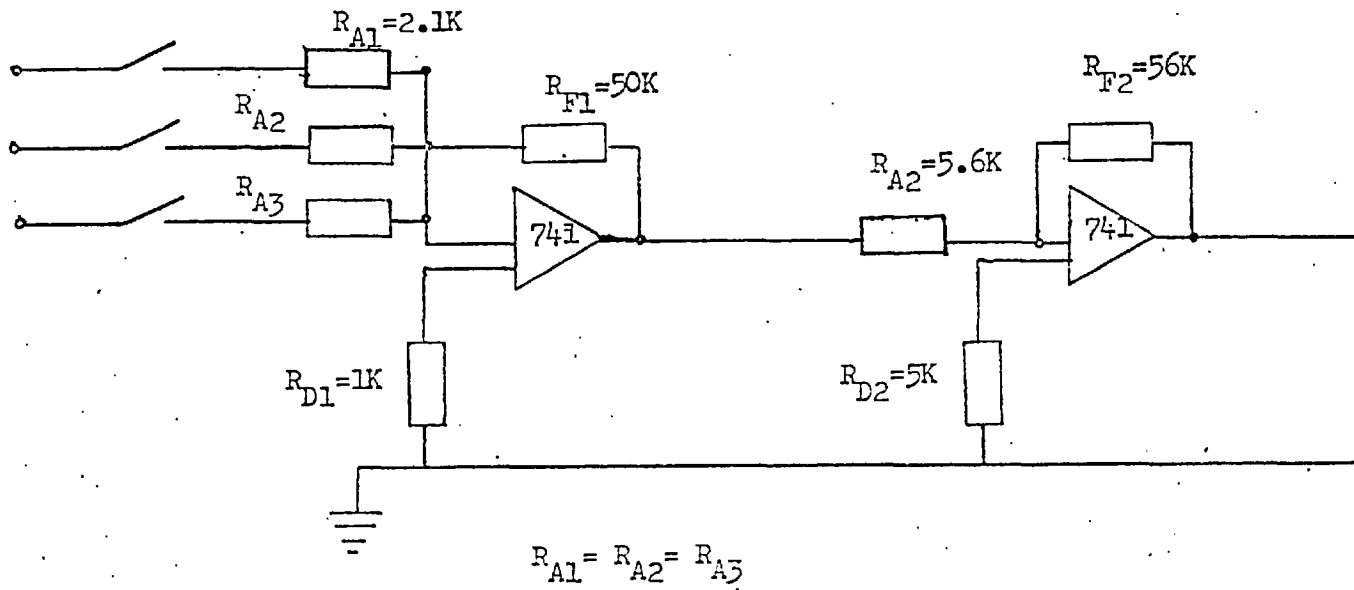


FIG. 5.9

Two-stage summation and amplification circuit for three-channel Hall effect wattmeter.

ratio. These isolating transformers are the same as used in the actual measurement of the on-load core loss and the same turn ratios were taken both for calibration and actual measurement. The wattmeter was calibrated at U.P.F. on 10 V scale and as the actual measurements are to be taken where P.F. is at very low range (being excitation current and induced voltage nearly in quadrature), the meter can be switched to the low range of the moving coil instrument for more accurate reading.

5.8 POWER CONSUMPTION OF WATTMETER

The power consumption of the meter is quite appreciable in comparison with the measured power due to the introduction of the large swamping resistors in the magnetic circuit. It is, however, comparable to the conventional dynamometer wattmeter.

The total power consumption for a three-phase circuit of 10 A and 110 V per phase delivering power at U.P.F. would be:

Hall plate current (using 1:5 isolating transformer and taking p.d. across $.55\Omega$ resistor)	≈ 35.5 mA
Watt loss per phase	≈ 0.9 W
Watt loss per phase in magnetic coil circuit	≈ 6.0 W
Total watt loss in three phases	≈ 20.7 W
Total power delivered to load	$= 3 [10 \times 110] = 3300$ W
Percentage of power consumed in the wattmeter of the total power delivered	$\approx 0.63\%$

The power dissipated in R_s on both primary and secondary side is a major factor, but this is not affecting the wattmeter reading. This power loss too can be reduced to a greater extent by using the isolating

transformers of large turn ratio and thus reducing the values of these resistances accordingly. Since small non-inductive resistances were not available in the laboratory, this power loss could not be reduced.

5.9 CORRECTION FOR POWER CONSUMED IN THE WATTMETER

The error introduced in the wattmeter reading is only due to the power consumed in the Hall plates circuits. Since this is less than 1 watt per phase for the conditions given in 5.8 and which are very near to the transformer to be tested, it was decided not to make any correction in the final reading of the wattmeter due to the above, and also:

1. The concern is more towards the relative losses at different load power factor rather than to the actual losses.
2. The introduction of the isolation transformers has introduced another source of error into the measurement, which though negligibly small is difficult to predict.

5.10 SENSITIVITY OF WATTMETER

The design data given by the manufacturer specify the sensitivity of the Type HMCl multipliers as $.0044-.0066 \text{ mV.mA}^{-1} (\text{AT})^{-1}$. The output obtained from each multiplier is shown in Table 5.2 on the basis of which the sensitivity of the meter is calibrated as 103.6 mV.mA^{-1} R.M.S. In terms of power measurement, the calibration with respect to true mean value of Hall e.m.f. indicated by moving coil meter is very nearly 1 mV.W^{-1} .

Multiplier number	Sensitivity * mV.mA ⁻¹ (AT) ⁻¹	Subtraction circuit		Summation and Amplifier Circuit circuit mV.mA ⁻¹	Summated output mV.mA ⁻¹
		Gain	Output mV.mA ⁻¹		
1.	.00486	1.76	.1411	34.27	**
2.	.00488	1.76	.1417	34.41	103.06
3.	.00464	1.85	.1416	34.38	

1. * Values established using d.c. quantities and a micro-digital voltmeter.

2. Circuits outputs expressed in r.m.s.

3. Gain of summation and amplifier circuit = $\frac{50}{2.1} \times \frac{56}{5.6} = 238.09$.

4. ** Indication on moving coil instrument ≈ 93 mV.

TABLE 5.2

Sensitivity of wattmeter.

Fig. 5.10 shows the calibration curve for circuit power against Hall e.m.f. (final output from wattmeter) taken on 1.0 V scale of moving coil meter. This calibration was made using isolating transformer of 1:25 ratio to limit the energy wasted in the resistive load.

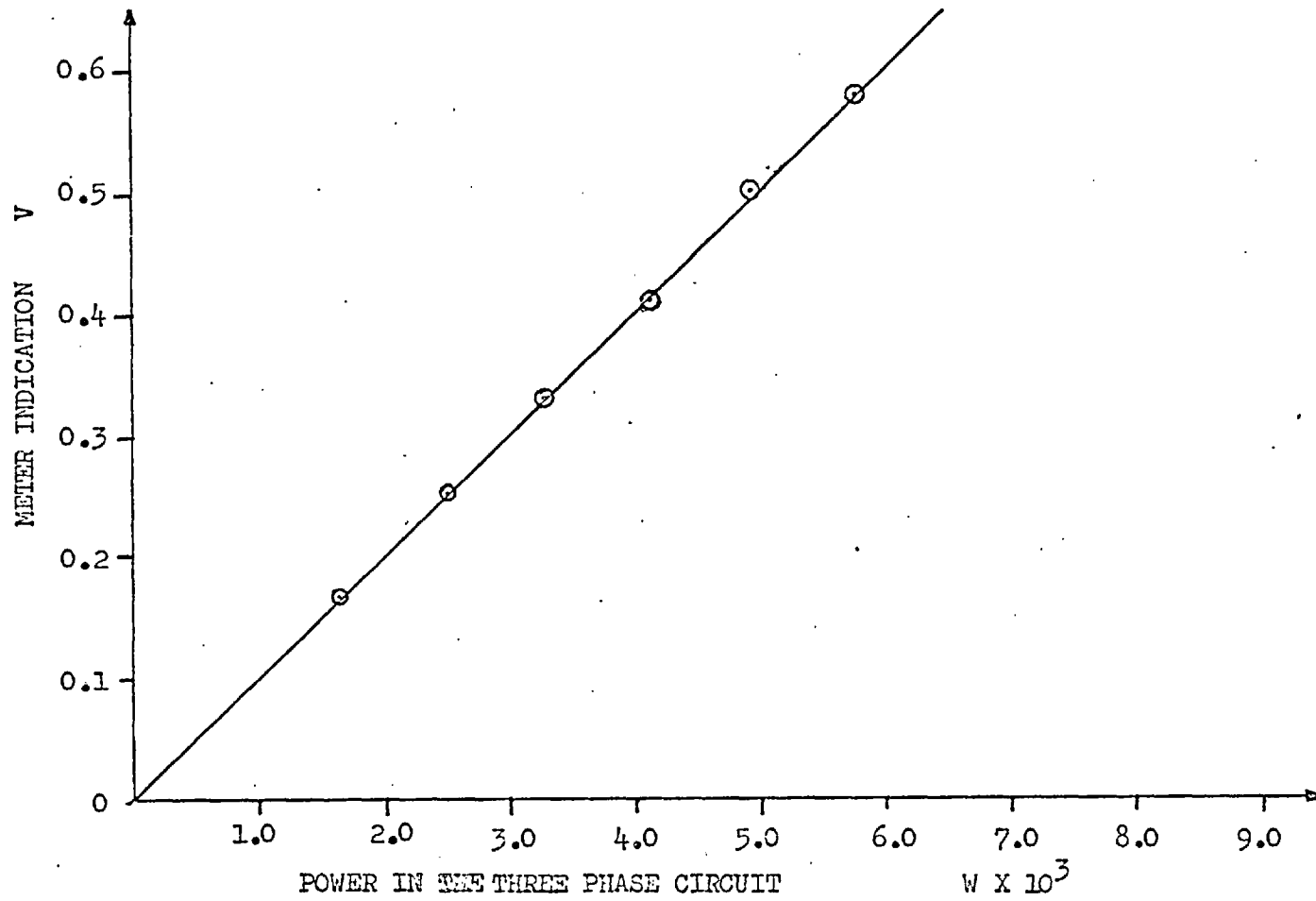


FIG. 5.10

Calibration curve of three-phase Hall effect wattmeter.

CHAPTER SIXEXPERIMENTAL ARRANGEMENTS AND TEST RESULTS6.1 THE TRANSFORMER AND ITS CHARACTERISTICS6.1.1 Core

The transformer on which the tests were performed was designed and constructed in the Department for a previous project to investigate the effects of over-fluxing.

The three-phase core was assembled from phosphate-coated laminations of coiled rolled grain orientated steel grade 51, the material used for CEGB generator transformers. These laminations were not annealed after slitting and cutting so as to exhibit more losses. Butt joints were provided between the legs and yokes. The laminations were held in position and under even pressure by wrapping "cellotape" around end joints and steel banding (insulated with "Permaglass XE6" buckles to prevent short circuits around the core flux) around legs and yokes to provide ample pressure on laminations to keep them in place. Finally the top and bottom yokes were held between wooden beams.

6.1.2 Search coils

Nineteen search coils, each having ten turns of 23/.0076 flexible cable, were wound around limbs and yokes and their ends brought out to a wooden terminal board fixed to the bottom yoke clamp. The arrangement is shown in Fig. 6.1.

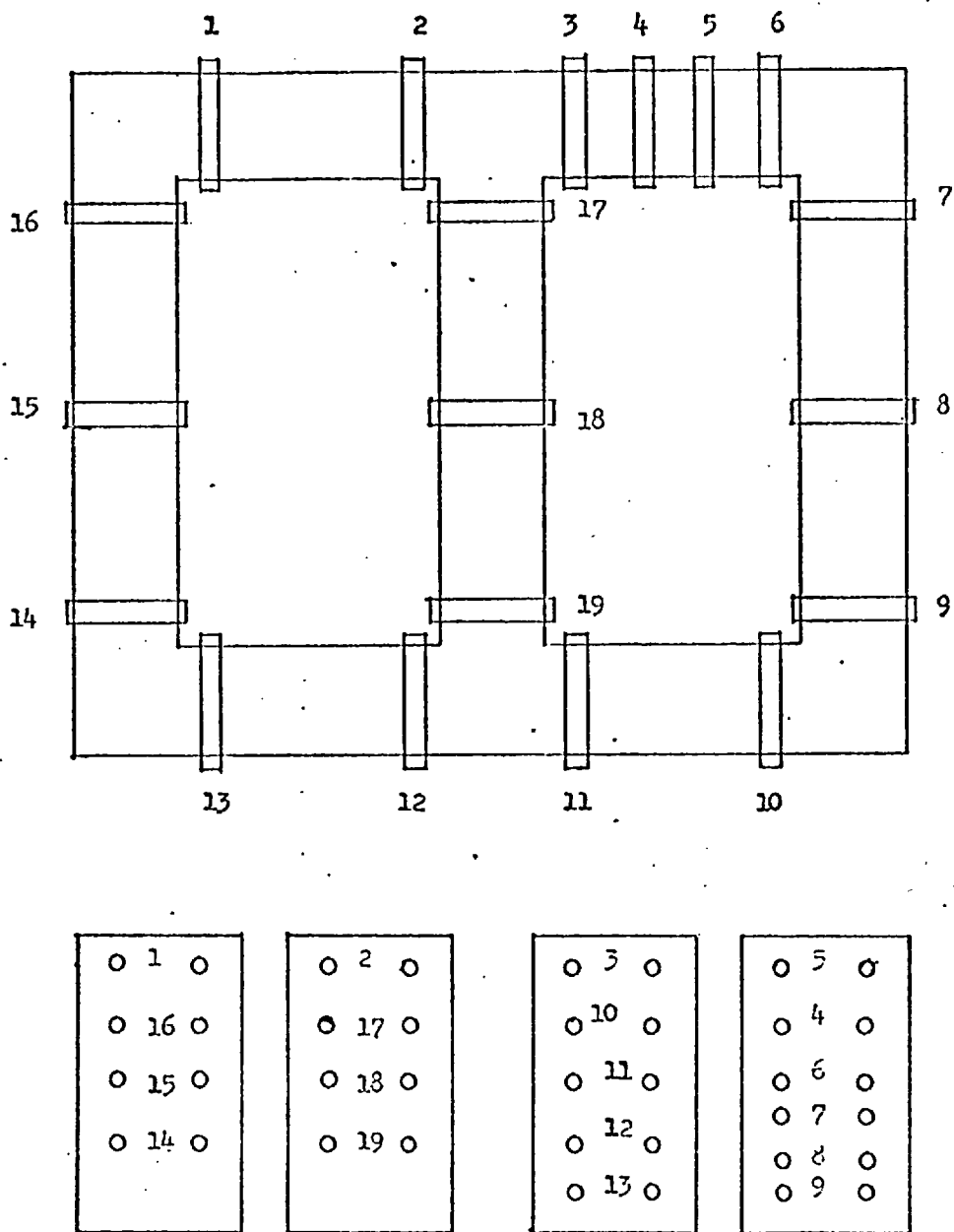


FIG. 6.1

Position of search coils and their terminal marking.

6.1.3 Main windings

The transformer was designed to have three windings per phase each of 55 turns of enamelled copper conductor with rectangular section 0.18 x 0.07 in. With each turn of each main winding, a shadow winding turn of 1 S.W.G. enamelled copper wire was wound. The coils were wound on synthetic resin bonded paper cylinders of $\frac{1}{8}$ " thickness and 4.5, 6.0 and 8.0 in. outer diameter. Ends of the windings were brought to a terminal board fixed to the top yoke clamp. A three character code was used to designate each terminal. Facing the terminalboard, the left hand side limb was designated as red phase, middle as yellow and right hand side limb as blue phase, respectively.

The terminals were marked as under:

<u>First character</u>	<u>Second character</u>	<u>Third character</u>
R - Red phase	1 - Inner winding	T - Top end of winding
Y - Yellow phase	2 - Middle winding	
B - Blue phase	3 - Outer winding	B - Bottom end of winding

The shadow windings were similarly designated, but their terminals are of small size to differentiate between the windings.

6.1.4 Rating

The transformer was nominally rated 5 kVA and designed to work at a flux density of 1.8 T to give 2 volts per turn or 110 V. per phase and nominal phase current is 15.2 A. The thermal rating of the main winding conductors is, however, much larger than their nominal current rating. The high flux density design was adopted in

view of the fact that CEGB generator transformers manufactured from the same core material to work in this flux density range gave rise to problems of core heating at leading load phase angles. However, although the working flux density was that of a generator transformer, the test transformer's per unit characteristics were not. The assembled transformer and the experimental arrangements are shown in Figs. 6.2 and 6.3.

6.2 PARAMETERS FOR CORE LOSS MEASUREMENTS

In practice, generator transformers are operated at a constant terminal voltage on the generator side and the matching system voltage is maintained by tap change facility on the high voltage winding^{6.1}. This condition is maintained even when the system is exciting the machine with MVar, a condition under which a high voltage per turn exists on the high voltage winding.

In view of the above it was decided to operate the transformer with fixed input voltage of 110 V (fixed induction) and a fixed output current of 10 A. The latter was not necessary but was used by reason of the thermal rating of the input winding.

6.3 EXPERIMENTAL ARRANGEMENTS

In an attempt to simulate experimental conditions similar to those of a generator transformer connecting a generator to a system, the input windings of the transformer were connected to a GEC 20 kVA d.c. motor driven alternator. The fields of the motor and of the alternator field exciter were controlled through two different motor generator sets using a Ward-Leonard system. The transformer output windings were connected to the 400 V 3-phase



FIG. 6.2

Assembled three-phase, three-limb transformer with terminals brought out.

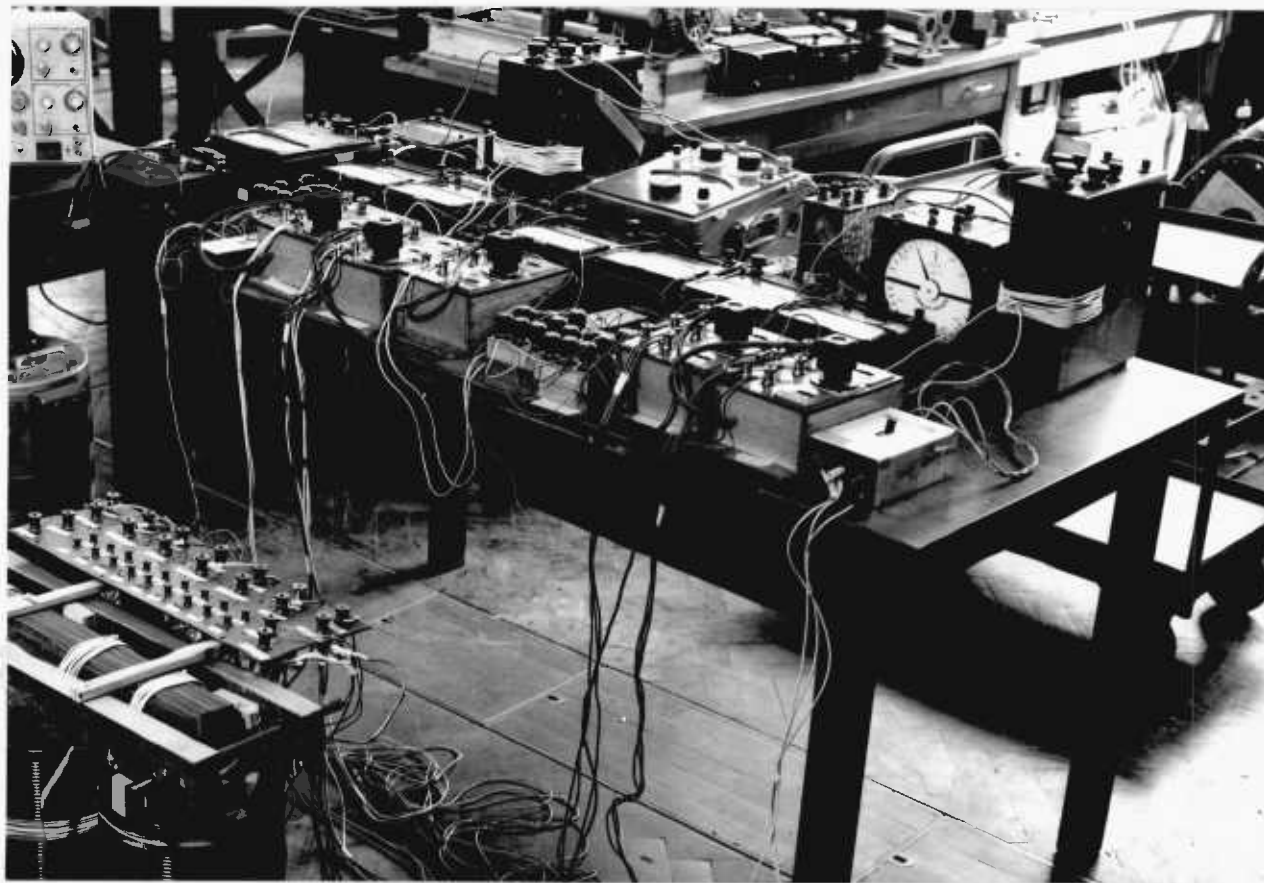


FIG. 6.3

Experimental arrangement for on-load core loss measurement.

laboratory mains through an induction regulator to step up the voltage and a synchronising switch. Although the control on voltage and phase angle was quite satisfactory, due to certain other machines operating on the same mains for experimental purposes or to drive ancillaries, the mains voltage fluctuation was so frequent that it was difficult to obtain consistent measurements. It was therefore decided to modify the arrangements and the secondary was connected to a three-phase static load consisting of adjustable resistors, capacitors and inductors in a mesh combination. The input side was connected to the mains through three single-phase autotransformers. Since the current rating of these was insufficient to meet the requirements, a three-phase two-winding transformer of 2:1 ratio was provided between the input side and autotransformers.

6.4 MEASUREMENT OF LOAD POWER FACTOR

The power factor of the load was measured either by a phase angle reading meter connected in the load circuit or by the measurement of the total load current and of the currents flowing in each branch of the load (depending upon the availability of the instrument). Since the capacitors and the inductors were connected through a change-over switch with the resistors in such a way that either of them could be "switched in" in parallel with the resistors the power factor can be calculated from the currents as:

$$\text{Power Factor} = \frac{1}{I} \left[I_R + \left\{ \frac{I^2 - (I_R^2 - I_L^2)}{2I_R} \right\} \right]$$

where, I = Total secondary current,
 I_R = Current flowing in the resistive branch,
 I_L = Current flowing in the reactive branch.

6.5 CORE LOSS TESTS AND TEST RESULTS

The following methods, described in detail in Chapter 4, were used to measure the core loss:

1. Open circuit (no-load) test method,
2. Direct differential current method,
3. Current transformer differential method,
4. Series resistance differential method.

6.5.1 Open circuit (no-load) test for the measurement of core loss

The open circuit test was performed according to B.S. 171 by exciting the primary from the alternator with the secondary open circuited. The supply voltage was measured by a "Ballantine" Model 321 electronic voltmeter indicating the average and true r.m.s. values of the input voltage waveforms. A low power factor wattmeter was used in compensated mode and the potential coil of the wattmeter was connected across the voltage induced in the shadow coil wound with the input winding so as to eliminate the ohmic loss due to excitation current from the measured loss. Three-wattmeter method was used to measure the core loss. The total core loss (algebraic sum of the three wattmeter readings) has been plotted against supply voltage as shown in Fig. 6.4.

6.5.2 Direct differential current method

The "finish" end terminals of each of the windings No. 2 & 3 of each phase were connected together and the common connections brought to a three-channel 50 A jack-socket, the output secondary

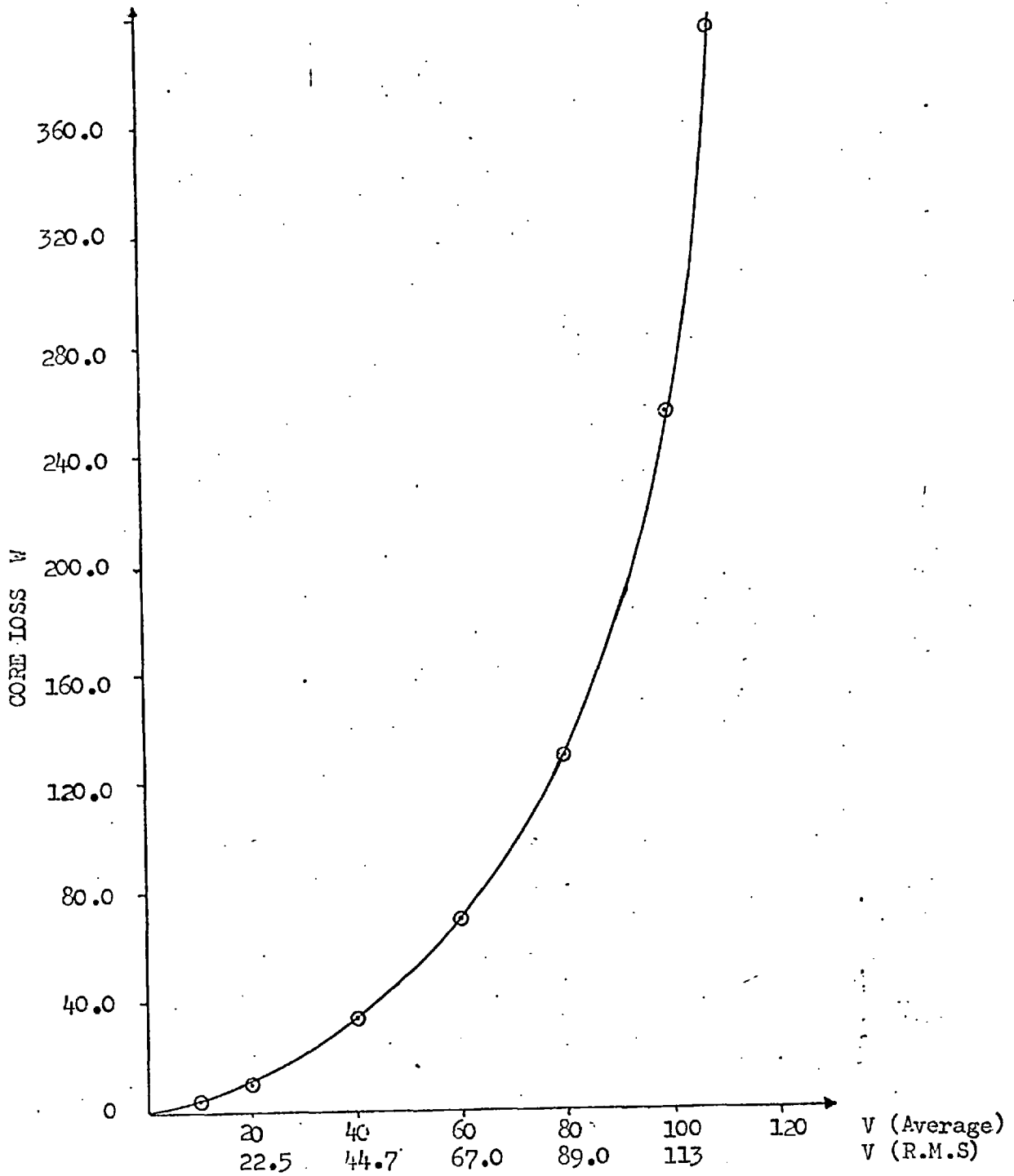


FIG. 6.4

No-load core loss measurement of three-phase transformer with open circuited secondaries.

terminals of which were connected together to make the neutral point of the system, thus making both windings Y-Y connected system. The 'start' end of the No. 2 windings were connected to the supply and those of No. 3 to the load. The differential current from the jack-socket was fed to the current coil of the wattmeter, the potential coil of which was connected across the induced voltage of the corresponding no. 1 winding. The core loss for each phase was measured by jacking the current coil of the wattmeter from one phase to another and switching the voltage to the potential coil correspondingly. The circuit diagram is shown in Fig. 6.5. Measurements were taken over a range of load power factor and total core loss values plotted against the power factor, as shown in Fig. 6.6.

6.5.3 Current transformer differential method

The transformer was connected in Y-Y with isolated neutral. The supply was connected to no. 2 winding. A current transformer type AL on which 12 turns were symmetrically wound to have unity input/output ratio with its winding marked M-100 was connected in series with the supply. The load was connected to no. 3 winding having a similar unity ratio C.T. in its circuit as the input side. The secondaries of these C.T.s were connected differentially so that the difference current, equal to the excitation current of the test transformer, could circulate in the current coil of the wattmeter connected in this circuit. The potential coil of the wattmeter was connected across the induced voltage of no. 1 winding. Since only one pair of C.T.s was available, this had to be switched from one phase to another through the three-channel jack socket box, the voltage circuit of the potential coil being switched appropriately.

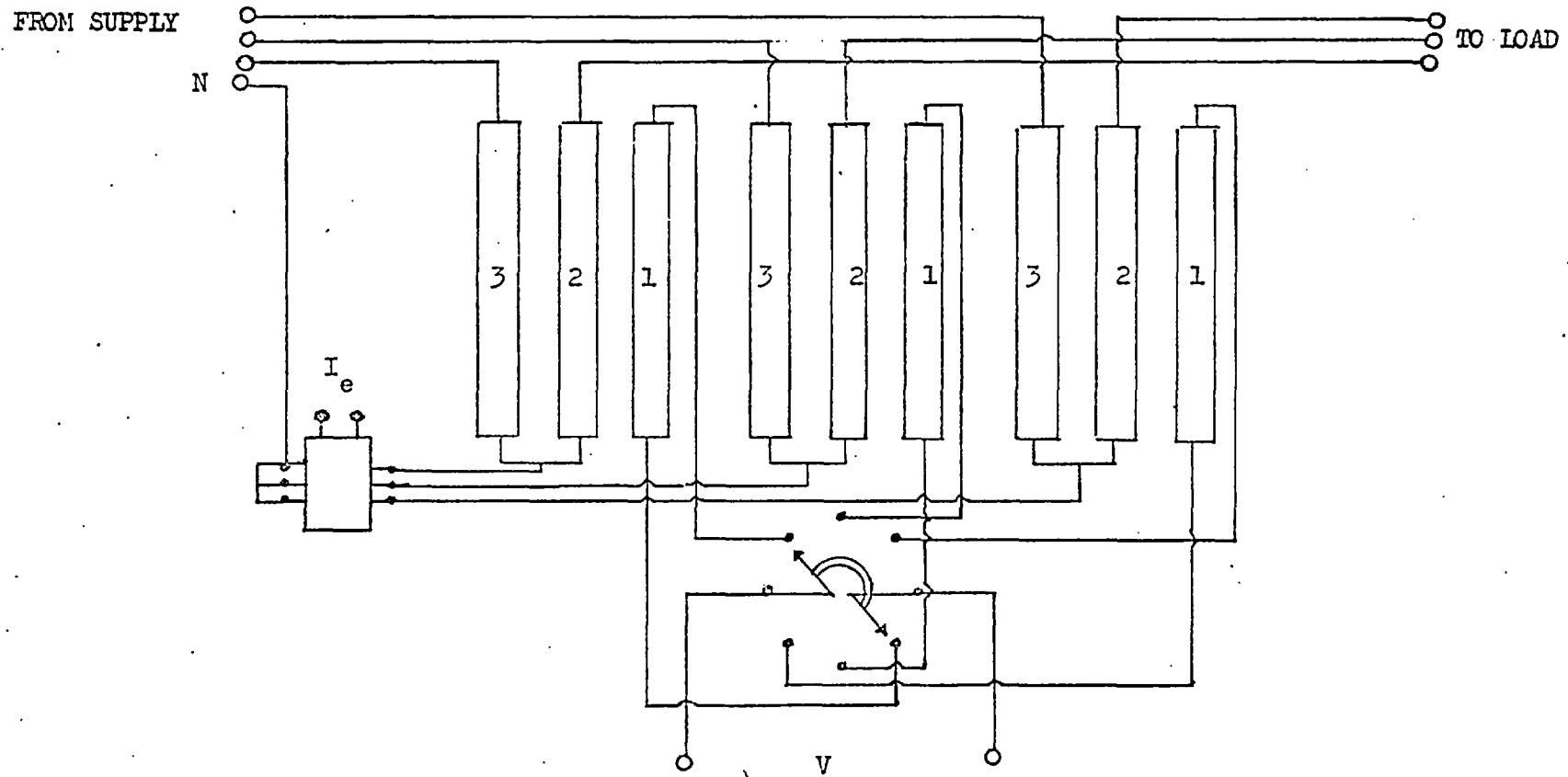


FIG. 6.5

Circuit for measurement of core loss by direct differential method.

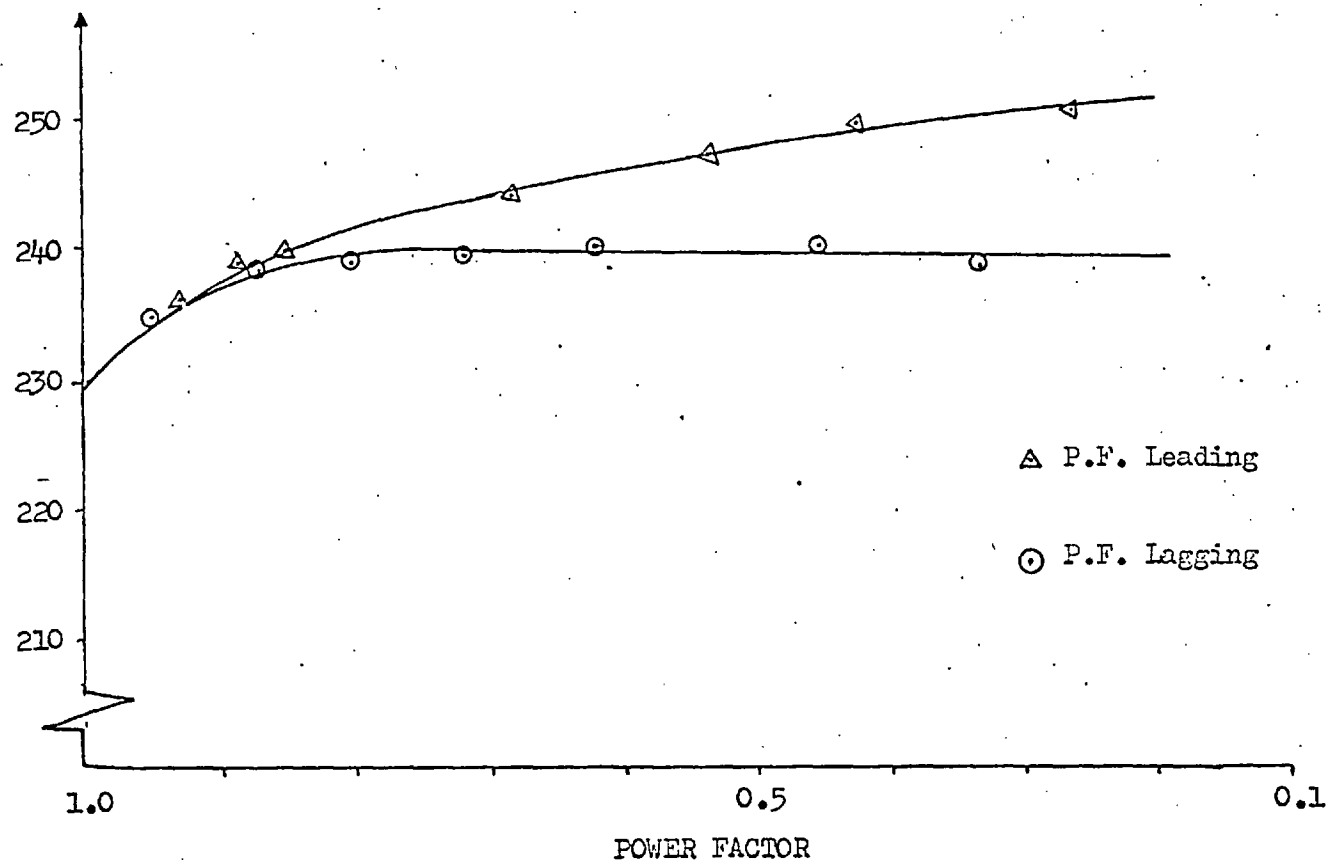


FIG. 6.6 Core loss measurement by direct differential method.

A similar test was performed with type CM C.T.s, wound with 8 turns to make unity ratio with their 40 A winding. The circuit diagram is shown in Fig. 6.7, core loss measurements taken over a range of load power factor and plotted against the same for both type of C.T.s are shown in Figs. 6.8 and 6.9.

As discussed earlier (section 3.4.2) the losses measured by this method, due to the inherent and operational errors of C.T.s, neither represent the correct magnitude nor their dependence on the load power factor.

6.5.4 Series resistance differential method

The transformer was connected in Y-Y with isolated neutrals. Three-phase non-inductive calibrated resistors were connected in series with the input and with the load feeders of the transformer. The p.d. signal from each resistor was fed to an isolating transformer of 25 VA rating with 0-24-120-240 tappings on each winding. The secondary of the input feeder isolating transformer was connected differentially to the secondary of the load feeder isolating transformer such that the output signal was proportional to and in phase with the excitation current of the test transformer. The circuit diagram is shown in Fig. 6.10. Two methods were employed to process this signal and relate the results to the core loss of the transformer under test.

1. By VAW meter:

As discussed in 4.6.2, the differential signal was multiplied with a fixed current signal taken from a separate source and

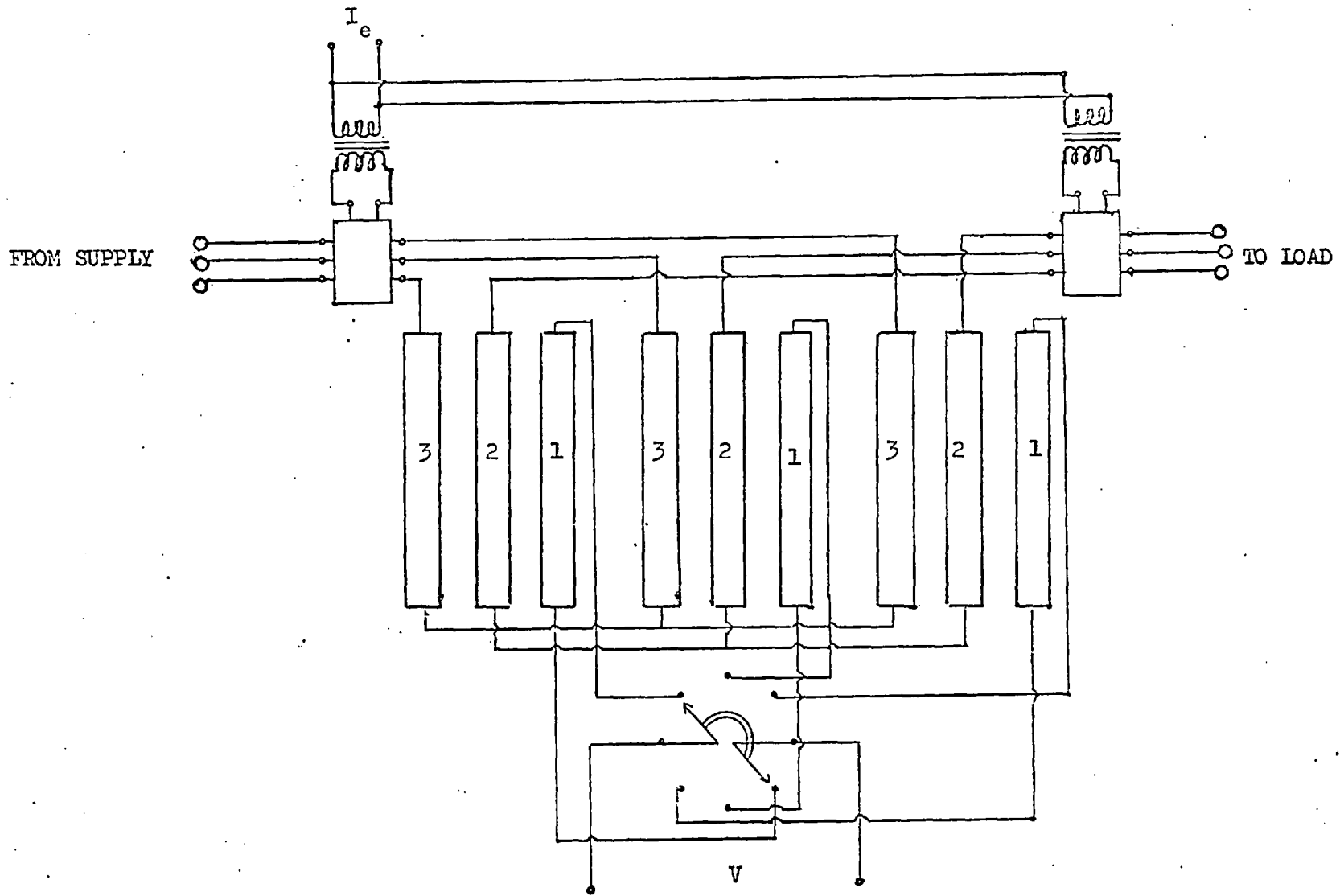


FIG. 6.7

Circuit for measurement of core loss by current transformer differential method.

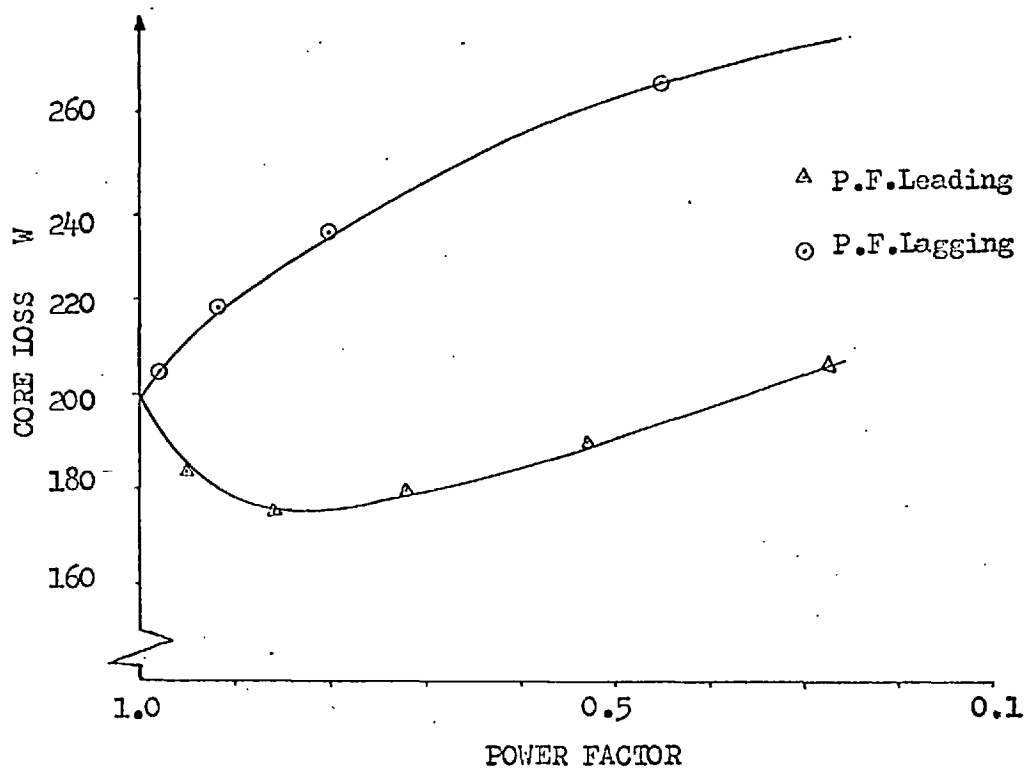


FIG. 6.8 Core loss measurement by C.T. differential method - C.T. type AL.

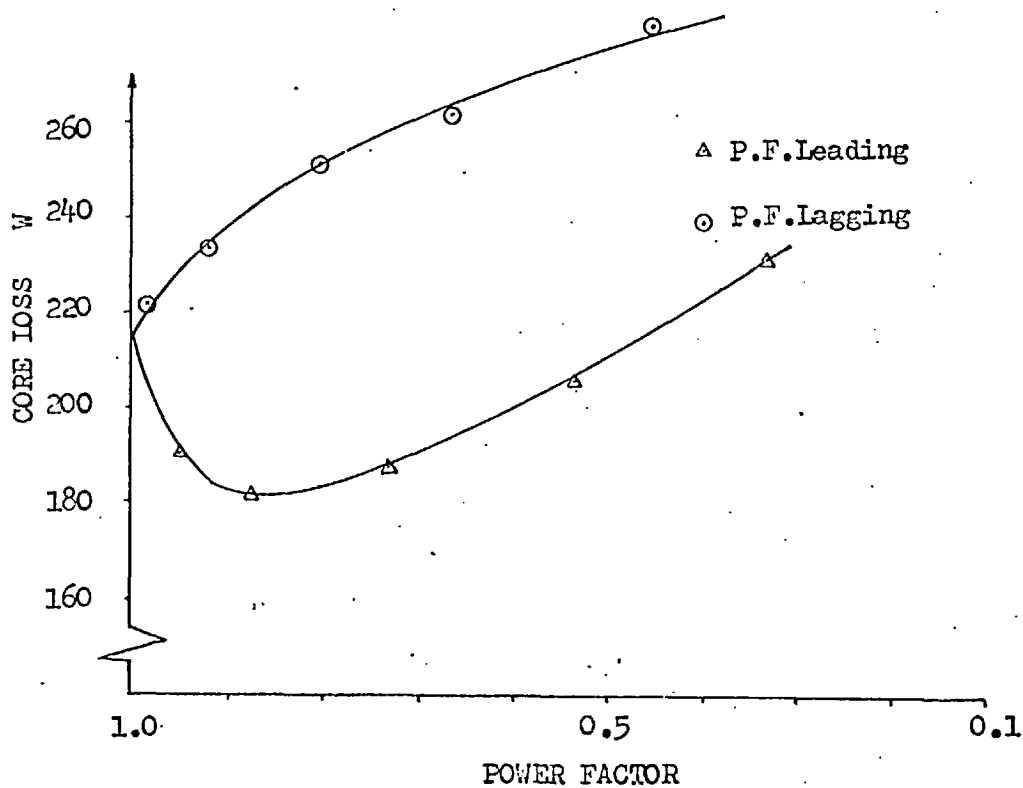


FIG. 6.9 Core loss measurement by C.T. differential method - C.T. type CM.

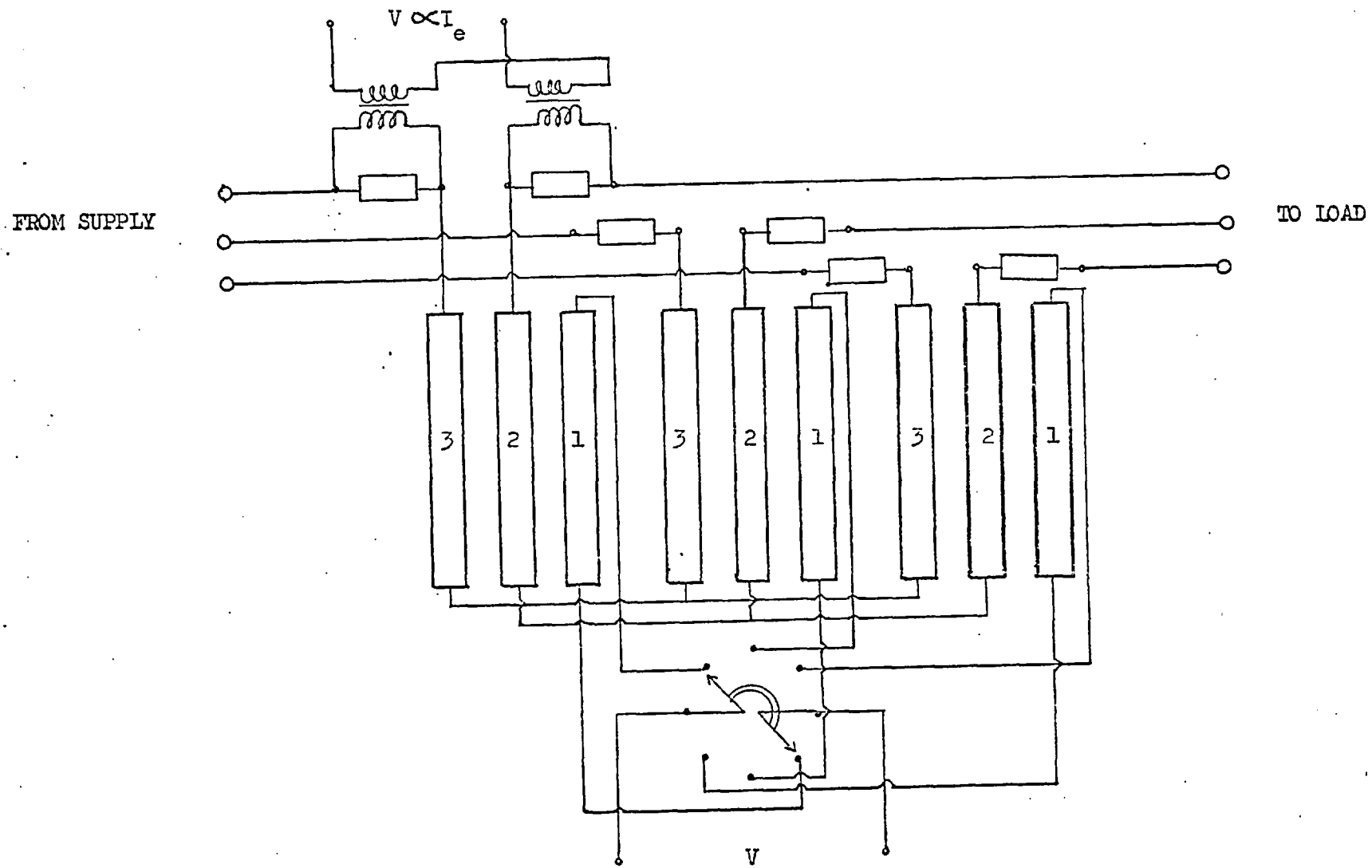


FIG. 6.10

Circuit for measurement of core loss by resistance p.d. differential method.

shifted in phase with the induced voltage. The multiplication was effected by the multiplying circuit of VAW meter after processing the signals through its voltage and current channels. The core loss signal was measured over the range of load power factor. Since the meter was not calibrated to give readings in watts, the meter readings were plotted against load power factor as shown in Fig. 6.11.

2. By Hall effect wattmeter:

The differential signals were fed to the plates of the Hall crystals which were in the magnetic field produced by the current flowing due to the induced voltage of no. 1 winding of the corresponding phase. The output signal from each multiplier was proportional to the power loss associated with each limb of the transformer. The final output signal was the summation of all three phases. As the meter was calibrated as described in Chapter 5, the output was directly relateable to the core loss. Measurements were made over the range of load power factor and plotted against the same as shown in Fig. 6.12. Dimensionless plots on the basis of unity power factor for measurements made by all the methods described in this chapter were plotted for leading and lagging power factors for comparison purposes and have been shown in Figs. 6.13 and 6.14 respectively.

A statistical comparison between the results of VAW and Hall effect meters taken from the dimensionless plots has been shown in Table 6.1.

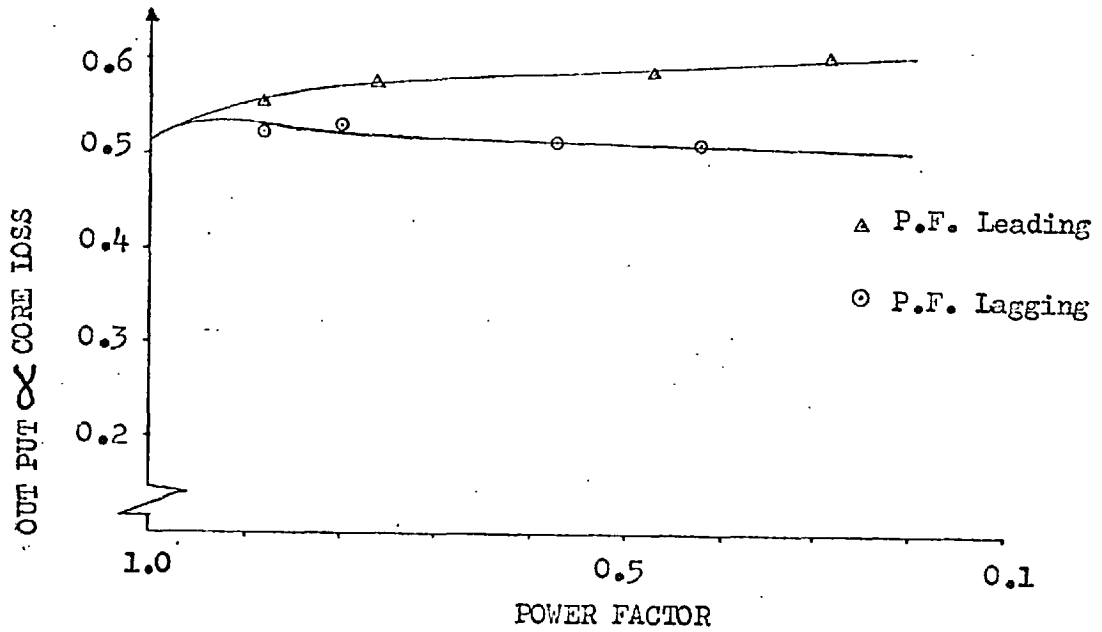


FIG. 6.11 Core loss measurement by resistance p.d. differential method, using VAW meter.

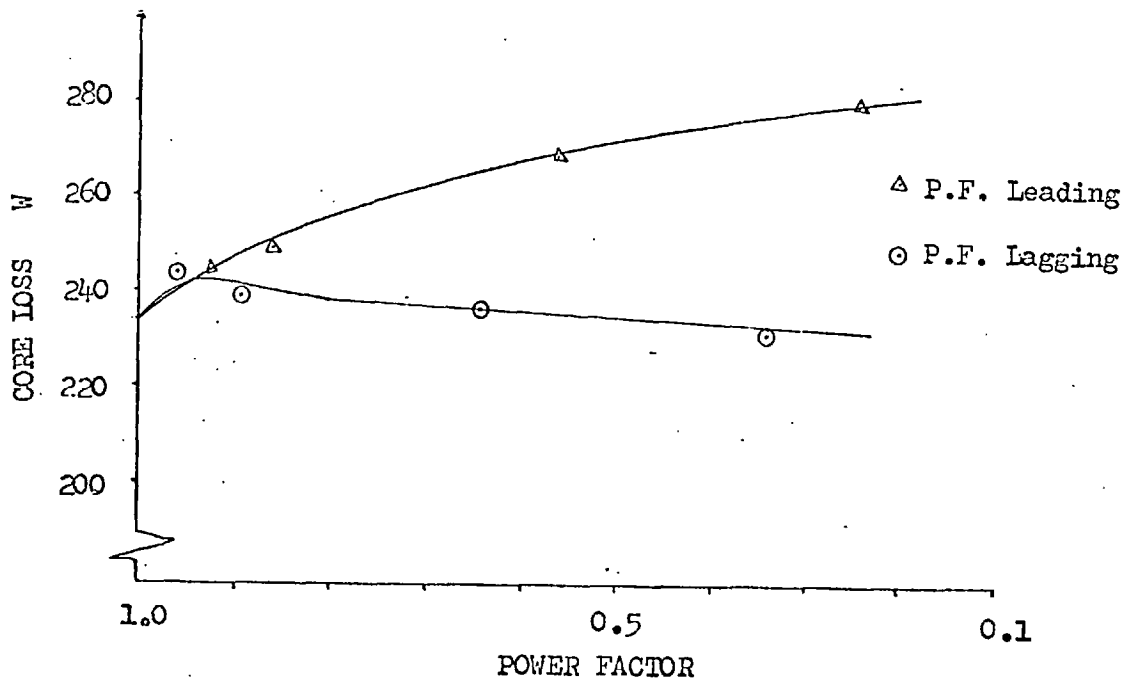


FIG. 6.12 Core loss measurement by resistance p.d. differential method, using Hall effect wattmeter.

A, B, C and D correspond to the measurements made by:

- A - Hall effect meter by resistance drop method.
- B - VAW meter by resistance drop method.
- C - Dynamometer wattmeter by direct differential method.
- D - Dynamometer wattmeter by C.T. differential method.

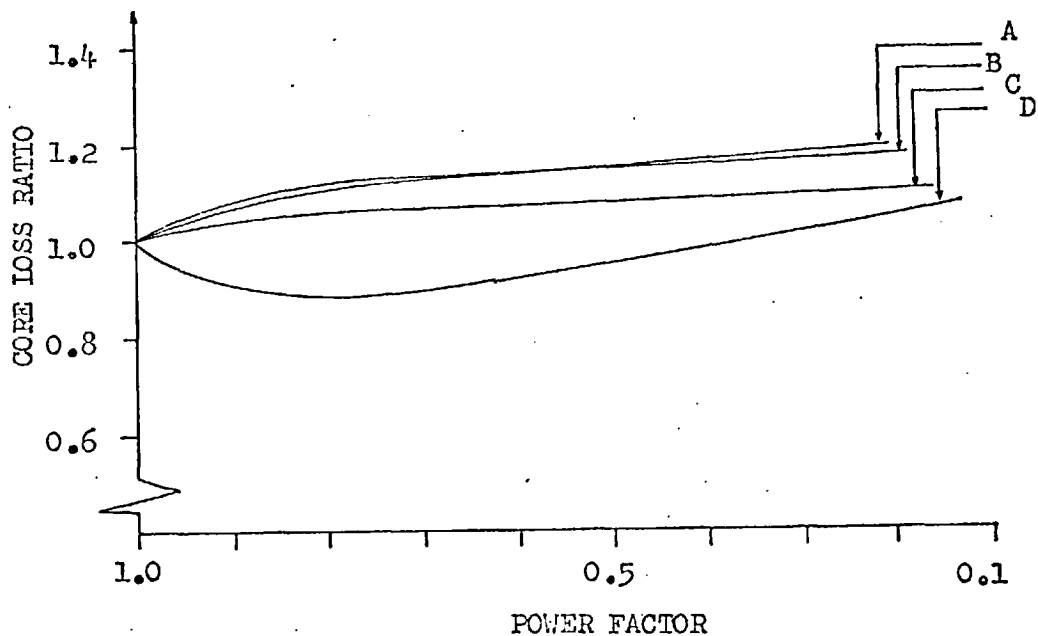


FIG. 6.13

Comparison of core loss ratios measured by different methods at leading P.F. load.

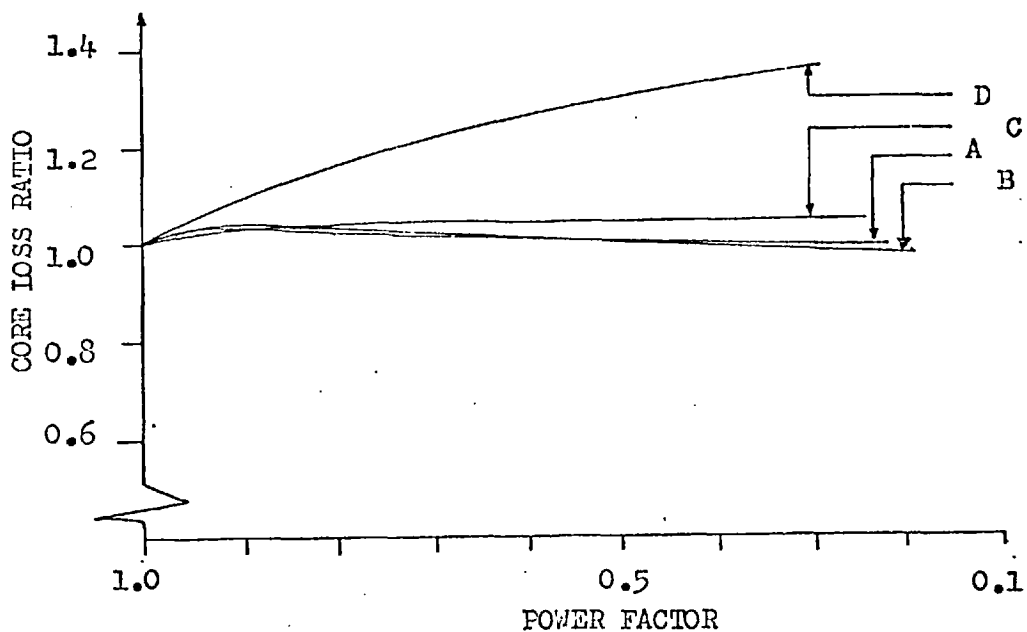


FIG. 6.14

Comparison of core loss ratios measured by different methods at lagging P.F. load.

Load P.F.	%age loss variation with respect to U.P.F.	
	VAW meter measurement	Hall effect wattmeter measurement
Leading:		
.95	5.0	4.0
.9	9.0	8.0
.8	11.5	11.0
.7	13.0	13.0
.6	14.0	14.0
.5	15.0	15.5
.4	16.0	16.5
.3	17.0	18.0
.2	19.0	20.0
.1	20.0	21.0
Lagging		
.95	4.0	4.0
.9	4.5	3.5
.8	3.5	3.0
.7	2.5	2.5
.6	1.5	1.5
.5	.5	1.0
.4	0	0.5
.3	(-)1.0	0
.2	(-) 2.0	(-)0.5
.1	(-)2.5	(-)1.0

(-) shows loss less than U.P.F.

TABLE 6.1

Comparison of core loss measurement by VAW meter and Hall effect wattmeter.

6.6 ADDITIONAL RESULTS

Since the series resistance differential method proved to be more realistic for the extraction of the excitation current from the input and output currents of the transformer under loaded conditions, some additional investigations were made while measuring the core loss and a few of the useful observations are discussed below.

6.6.1 Excitation current and load power factor

In the case of the no-load test, Chapter 2, it was observed that the ratio of excitation currents taken by each winding to provide the required induction in the core was 1.0:0.69:1.0 (R:Y:B). Under loaded condition in three-phase three-limb transformer this ratio does not remain the same and the phase excitation currents tend to equalise. The middle limb current is increased over its open circuit value and the ratio at U.P.F. is 1.0:0.725:0.98. As the power factor becomes more leading, the increase in the excitation current experienced by the middle limb is relatively greater than by the outer limbs.

The ratio measured at .43 P.F. leading is 1.0:0.76:0.98. With lagging load power factor as the power factor decreased the middle limb current tended to reduce more rapidly than the outer limbs and the ratio of the currents approached more closely to the no-load ratio, typically at .36 P.F. lagging it was 1.0:0.7:1.05.

This confirms that the total requirement of excitation current at leading power factor is greater than at lagging power factor. If the average excitation current, taken as the sum

divided by 3, is plotted against load power factor on a dimensionless basis, a gradual increase in this current can be seen as power factor becomes more leading.

6.6.2 The magnetizing current and load power factor

Dependence of the reactive component of the excitation current, i.e. the magnetizing current, on the load power factor, was checked by multiplying (using the VAW meter) the signal extracted with a constant current vector taken from the phase shift unit and shifted into quadrature with the induced voltage of the respective phase of the transformer. The results which represent the reactive magnetizing power showed practically no change over the entire range of load power factor. The maximum change observed was 1.5%. This shows that the magnetizing current remains constant as long as the induction (proportional to the induced voltage) remains constant. This, however, is based on experimental results of a transformer which has negligible leakage reactance compared to winding resistance, a case untypical of actual generator transformers which have 10-15% leakage reactance. It is therefore possible that the small leakage m.m.f. may not have produced any measureable change which could affect the results.

6.6.3 The core material characteristic angle and load power factor

The core material characteristic angle, i.e. the phase angle between the excitation current and its core loss component, which is a function of flux density, should remain unchanged for a fixed value of induction. Since core loss and thus the core loss current

has shown its dependence on load power factor, variation in the above angle over the range of load power factor was checked. It was observed that for lagging power factors the change in this angle was quite symmetrical in all phases. The variation with leading power factor was not, however, symmetrical in all phases and was greater in the case of the middle phase. This asymmetric change, if interpreted in terms of its effects on core loss current amplitudes, shows that the amplitude change in the case of middle phase is more than for the outer phases.

6.6.4 The input current and load power factor

Since input current is the vectorial sum of the excitation and load currents, any change in their magnitudes with load phase angle will be due to their relative phasor positions when the magnitude of the latter is kept constant. This is the condition under which the on-load core loss measurement tests were performed. As the transformer's secondary was connected to a three-phase balanced load and equal change in load phase angle was made on all the three phases, for each set of readings the percentage change in the magnitude of the excitation currents should be the same in all the three phases. A set of measurements was taken over the range of load power factor and percentage variation in the magnitude of the input currents (referred to U.P.F.) was computed and plotted against lagging and leading power factors as shown in Fig. 6.15 and Fig. 6.16 respectively.

It is interesting to note that the percentage variation in each phase is not the same. The middle phase experienced a smaller percentage fall in the input current than the outer phases as power

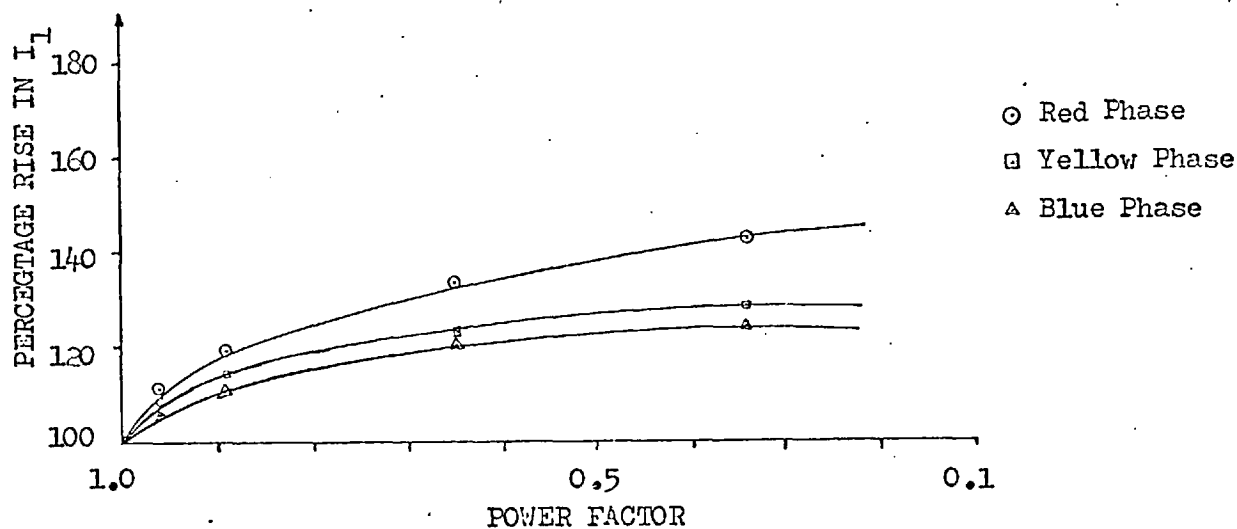


FIG. 6.15 Percentage change in input current with lagging load power factor.

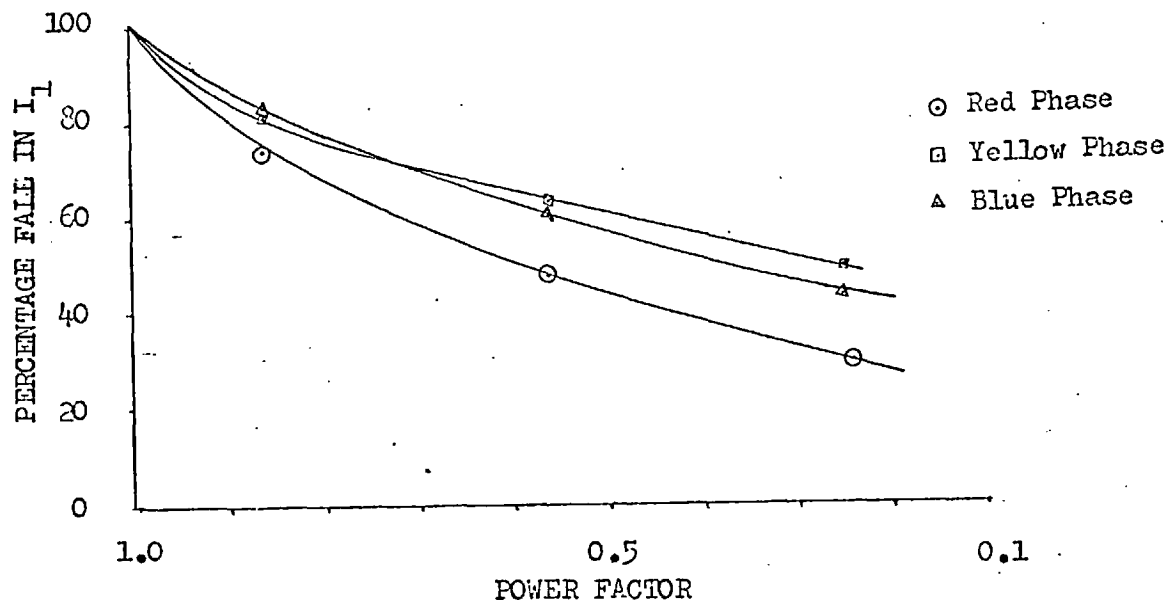


FIG. 6.16 Percentage change in input current with leading load power factor.

factor became more leading. Since the load current was not changed, the change in the input current can only be due to the excitation current and thus in the core loss component of current as there is no change in magnetizing current (section 6.6.2). This means that at leading power factor, the iron loss current of the middle phase increases as compared to the outer phases. As this current meets the energy losses of the core, it is evident that these losses are more at leading power factor. On the other hand, at lagging power factor the percentage rise in the input current of the red phase (outer one) is more than the other two. This phase actually shows a negative loss, i.e. the return of power to the supply. Explained on the above basis, this means that the total requirement of core loss current at low lagging power factor is less. This has already been confirmed by on-load core loss measurements.

6.7 ADDITIONAL TESTS

6.7.1 Simulation of operating conditions

As well as obtaining the core loss measurements given in Section 6.5, some other tests were performed for core loss measurements with different input/output parameters. Initially a test was performed keeping constant both the load current and output voltage. In the case of a transformer coupling a generator with a system, any change in the excitation current of the generator only changes the active and reactive components of VA but does not make any change in the terminal voltage of the generator^{6.2} and hence the transformer core induction remains constant. Using the present test arrangements when the power factor of the secondary side was changed, the secondary terminal voltage changed also. To keep the

secondary terminal voltage constant, adjustment had to be made to the input voltage, thereby changing the core induction. The measurements thus made did not give realistic results as the core losses were changing due to changing induction as well as to load power factor.

6.7.2 Short circuit and impedance test

Other tests were performed to measure equivalent winding impedances and resistances. Figs. 6.17 and 6.18 show the results for the test made with winding no. 2 excited and no. 3 short circuited. These tests were performed on all the windings in pairs to compute equivalent impedances and resistances. The resistances were divided in the ratio of conductor lengths, since the same conductor was used in all the windings.

The resistances thus computed are:

$$\text{Resistance of winding no. 1} = 7.92 \times 10^{-2} \Omega$$

$$\text{Resistance of winding no. 2} = 10.25 \times 10^{-2} \Omega$$

$$\text{Resistance of winding no. 3} = 12.24 \times 10^{-2} \Omega$$

The equivalent reactance was computed from the short circuit tests and also from the geometrical parameters of the transformer.

The resolution of the reactance into its components associated to each winding was tried by the method specified by Stirzaker^{6.3}, but with little success as the equivalent reactances of the transformer were too small compared to equivalent resistances.

The method specified by Boyajian^{6.4} was also tried to divide the equivalent impedance and thus reactance calculated from short circuit test and the results are:

FIG. 6.17

Measurement of equivalent resistance of windings nos. 2 and 3 of three-phase transformer.

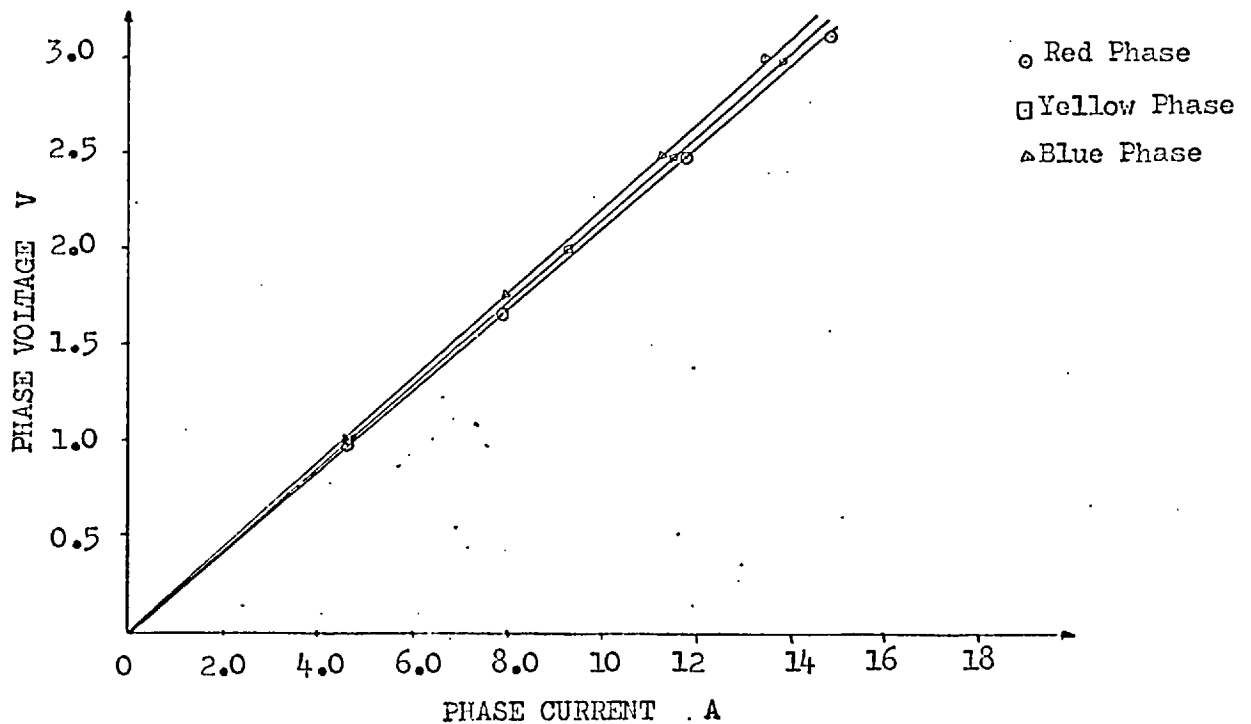
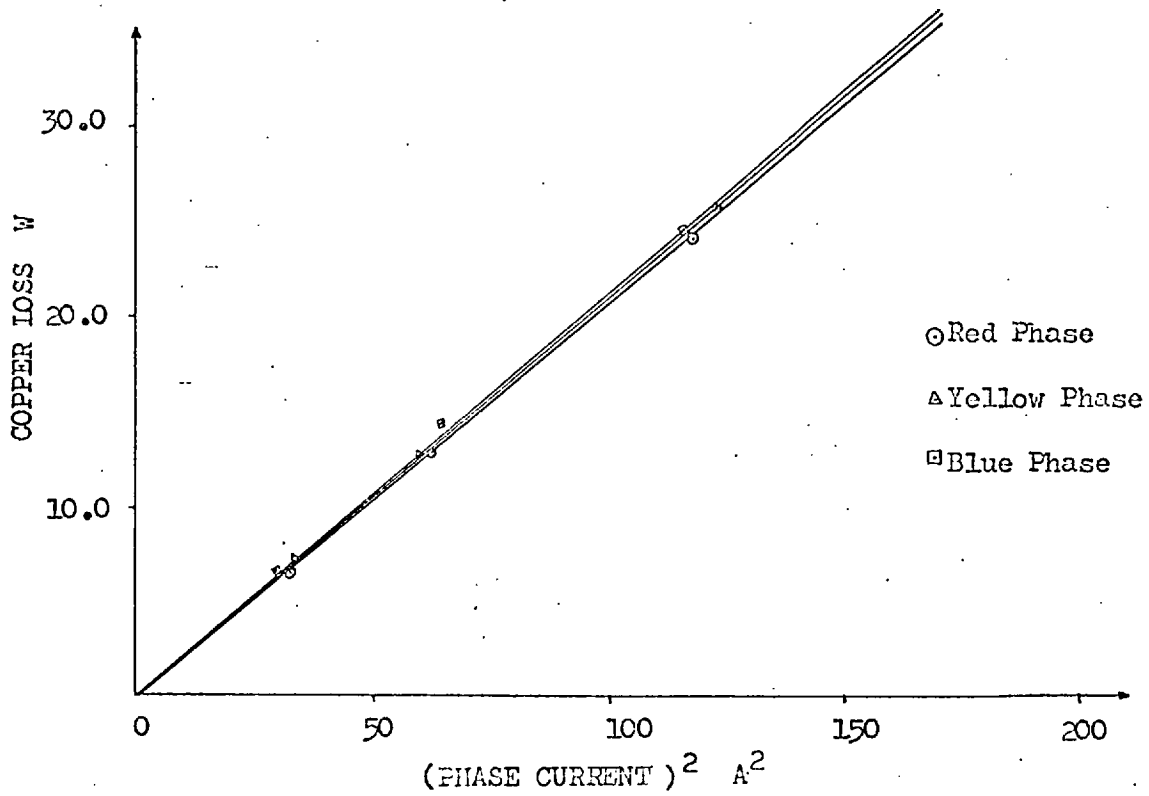


FIG. 6.18

Measurement of equivalent impedances of windings nos. 2 and 3 of three-phase transformer.

$$\text{Reactance of winding no. 1} = 2.41 \times 10^{-2} \Omega$$

$$\text{Reactance of winding no. 2} = 0.23 \times 10^{-2} \Omega$$

$$\text{Reactance of winding no. 3} = 5.81 \times 10^{-2} \Omega$$

Test specified by O'Kelly^{6.5} was also tried to check the above results, but the values obtained did not match presumably due to very small leakage reactance.

CHAPTER SEVENSYNTHETIC LOADING OF TRANSFORMER AND MEASUREMENT
OF LOSSES7.1 INTRODUCTION

The commercially accepted methods for the measurement of losses in a transformer are:

1. Open circuit test - to measure core loss.
2. Short circuit test - to measure copper loss and leakage reactances.
3. Equivalent short circuit heat run test - to dissipate copper plus core losses.
4. Load back or back to back (Sumpner) test - to measure copper plus core losses in one test (specially suitable for single-phase bank transformers but not accurate for high reactance transformers^{7.1}).

Although these tests give a close approximation to the actual losses, and can be performed without any special test equipment, except no. 4, which requires a transformer identical to that being tested, they have a major drawback: none simulates the actual conditions in the transformer under load. Certain other modified versions of these tests can be employed, such as the Delta/Delta test^{7.2} for three-phase transformer. Full excitation voltage can be employed on one set of windings connected in closed delta and rated current can be circulated by a single-phase source connected in series with the other winding connected in delta. By appropriate metering the losses of each circuit can represent the core and copper loss of the

transformer but the limitation would be that these losses would represent a particular condition of loading. As shown in Chapter Six, the core losses in a highly fluxed transformer also become a function of the load power factor, so this test for measurement of core losses in such transformers cannot be said to be representative of loss conditions over the range of load power factor.

The above methods have the advantage of minimum energy loss in the tests but any method which does not produce the exact conditions experienced by the transformer while in actual operation cannot be said to be perfect. The only realistic method would seem, therefore, to be an actual load test. This, however, also has certain problems:

1. Loading device and supply equipment must have equal or larger capacity than the unit to be tested.
2. Energy consumed during the tests is wasted in heat, which is equal to the power rating of the unit under test and losses of the supply source.
3. Facilities must be available to change the power factor of the load, either by a static load containing resistors, capacitors and inductors, or a synchronous machine of suitable capacity. Both present difficulties in terms of capital expenditure and extra test area.

The problems become increasingly important as the rating of the units to be tested increases.

If, however, different components of loss can be investigated under the conditions which the transformer experiences while

loaded, the test can be said to be more realistic. By maintaining such conditions until the temperature stabilises, much better and more extensive results can be obtained. In addition, development rigs for extensive investigations of the distribution of core loss and core flux can be excited in a realistic manner.

In view of the above, a new testing method was investigated which incorporates the above features plus facility of control of load angle. The test named the "synthetic load test" is detailed in this chapter, together with results obtained on three-phase transformers used in the work discussed in Chapter 6. Another single-phase "micro" transformer, the data of which is given in this chapter, was also subjected to actual load test and synthetic load test for the measurement of core loss for which results are also given in this chapter.

7.2 THEORETICAL CONSIDERATIONS

A transformer in steady state operation is considered to be under three main m.m.f's:

1. Magnetomotive force produced by the magnetizing current, sufficient to keep the resultant mutual flux in the core of such a magnitude ^{as} to satisfy the primary voltage equation, i.e. the sum of the primary resistance drop, primary leakage inductance drop and the counter e.m.f. induced must equal the primary impressed voltage.
2. Magnetomotive force produced by the load current, the tendency of which is to magnetise the core in the reverse sense to that of the magnetising current.

3. Magnetomotive force produced by the component of the primary current to balance the demagnetising action of the load current.

Strictly speaking, the m.m.f. as given by 1 above is not wholly attributable to one current only but is due to the combined effect of instantaneous primary and secondary currents producing approximately, though not exactly, counter magnetomotive forces, the phase relations of which depend on the nature of the secondary load, as well as on the characteristics of the transformer. The mutual flux is also considered to be entirely confined within the core, and the leakage flux as so small compared to the resultant mutual flux that its effect on the mutual flux is usually ignored. This assumption is, however, not entirely correct and leakage flux does increase the main flux in some parts of the core and reduce it in the others. If these second order leakage effects are neglected, the primary and secondary m.m.f.'s can be considered equally effective in producing the mutual flux distributed uniformly throughout the core irrespective of their arrangements with respect to each other and with respect to the core.

The instantaneous value of the resultant m.m.f. responsible for producing the resultant mutual flux in the core to satisfy the primary voltage equation can be expressed as:

$$F_R = F_1 - F_0 \quad (7.1)$$

where, F_R = resultant m.m.f.,

F_1 = m.m.f. produced by the primary current = $i_1 N_1$,

F_2 = m.m.f. produced by the secondary current = $i_2 N_2$.

In view of the above, a two-winding transformer can be considered as having two windings producing equal magnetomotive forces in

opposition to each other and a third fictitious winding producing a m.m.f. of such magnitude and direction as to satisfy the primary voltage equation. This division of magnetomotive forces in three components can be considered to exist in a transformer in steady state operation but their separation in physical sense is difficult.

The best physical realisation of this concept can be constructed if the fictitious winding is replaced by an actual winding producing a magnetomotive force of the magnitude which will satisfy the above conditions where the two original windings producing m.m.f.'s of magnitudes proportional to full load current of the transformer but in opposite senses.

Fig. 7.1 shows the equivalent circuit to represent this condition for a unity ratio three-winding transformer. Here

$$E_1 = E_2 = E_3$$

$$V_1 = I_e (R_1 + jX_{1l}) + E_1 \quad (7.2)$$

$$P_1 = \frac{E_1^2}{R_c} \approx \frac{V_1^2}{R_c} \quad (7.3)$$

$$V_2 = I_L (R_2 + R_3 + jX_{2l} + jX_{3l}) + E_2 - E_3 \quad (7.4)$$

$$= I_L [(R_2 + R_3) + j(X_{2l} + X_{3l})] \quad (7.5)$$

$$P_2 = I_L^2 (R_2 + R_3) \quad (7.6)$$

7.3 EXPERIMENTAL RESOLUTION

Consideration of the physical system reveals that a transformer should have one winding suitable for the production of the required m.m.f. and the two other windings able to carry full load current. If these two windings are of 1:1 ratio, the test

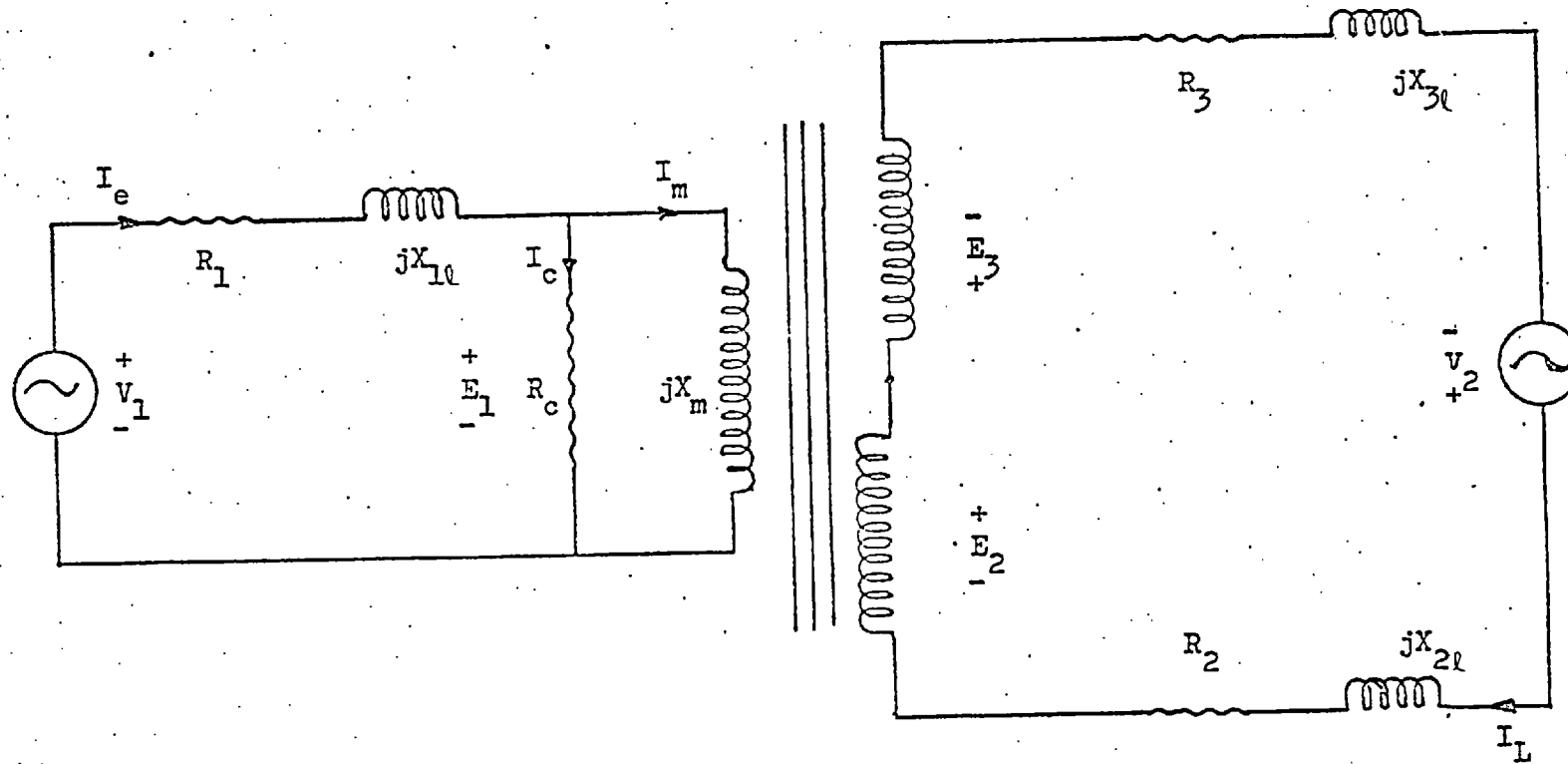


FIG. 7.1

Equivalent circuit for 'Synthetic Load' test; 1:1 ratio transformer.

arrangement could be convenient and simple; alternatively, a secondary central tap can provide this facility, e.g. if any winding is distributed equally between two limbs so as to form one winding (sometimes the case with single-phase bank transformers). However, for a transformer other than central tapped secondary or unity ratio, a suitable current transformer can be used to maintain ampere turn balance in both windings connected in opposition. If this test is adopted as a type test by manufacturers, a suitable rig to provide such facility will be required. For this purpose, a two-winding adjustable ratio transformer can be included in the rig to circulate the load currents through the windings of the test transformers of any transformation ratio.

The load windings when connected in series opposition will produce a zero m.m.f. condition around the main magnetic circuit of the transformer irrespective of the magnitude of the current flowing through them as m.m.f. produced by one winding will be cancelled out by the other. The sense of connections will of course depend on the actual positioning of these windings in relation to the magnetic circuit. If they encircle the same limb, the series opposition connections will produce this zero m.m.f. condition. If these windings are positioned on two different limbs of the same cross-section area, this condition can be achieved as above or by connecting in parallel opposition. The third winding is then energised to the rated voltage and will pass the current required to maintain the magnetising flux in the core.

The core loss at a given frequency can roughly be given by:

$$P_c = K_1 \hat{B}^Y$$

and since the peak induction \hat{B} in the magnetic circuit is proportional

to the impressed voltage on the winding, the relation can be rewritten as:

$$P_c = K_2 \hat{E}^Y$$

where K_1 and K_2 are the constants and Y is the exponent which has a fixed value depending on the type of core material and structure within narrow limits of induction^{7.3}. As the impressed voltages are kept fixed, the power metered in this circuit will represent the core loss plus a very small amount of copper loss due to the winding resistance. The other two windings connected in opposition will give the ohmic and stray losses of the load circuit (copper loss). This circuit has to be energised by a separate adjustable source, isolated from the source providing excitation^{7.4}. A wattmeter connected in this circuit can measure these losses. Either of the two circuits can be connected to the source through a phase shifting unit and thus the phase relation between the load current and the voltage in the magnetizing winding can be adjusted. The iron loss measured in this way will be attributable to a specific load angle, which can be changed by the phase shift and can be computed as discussed in 7.4.

The connection arrangement for the three-phase three-winding transformer is shown in Fig. 7.2. The sum of wattmeter readings W_{c1} and W_{c2} will give the total copper loss while the sum of wattmeter readings W_{i1} , W_{i2} and W_{i3} will give the total core loss.

7.4 CONCEPT OF LOAD POWER FACTOR

In this test arrangement, the secondary current and secondary voltage do not bear the same relation as in the case of an actually loaded transformer. This voltage is just sufficient

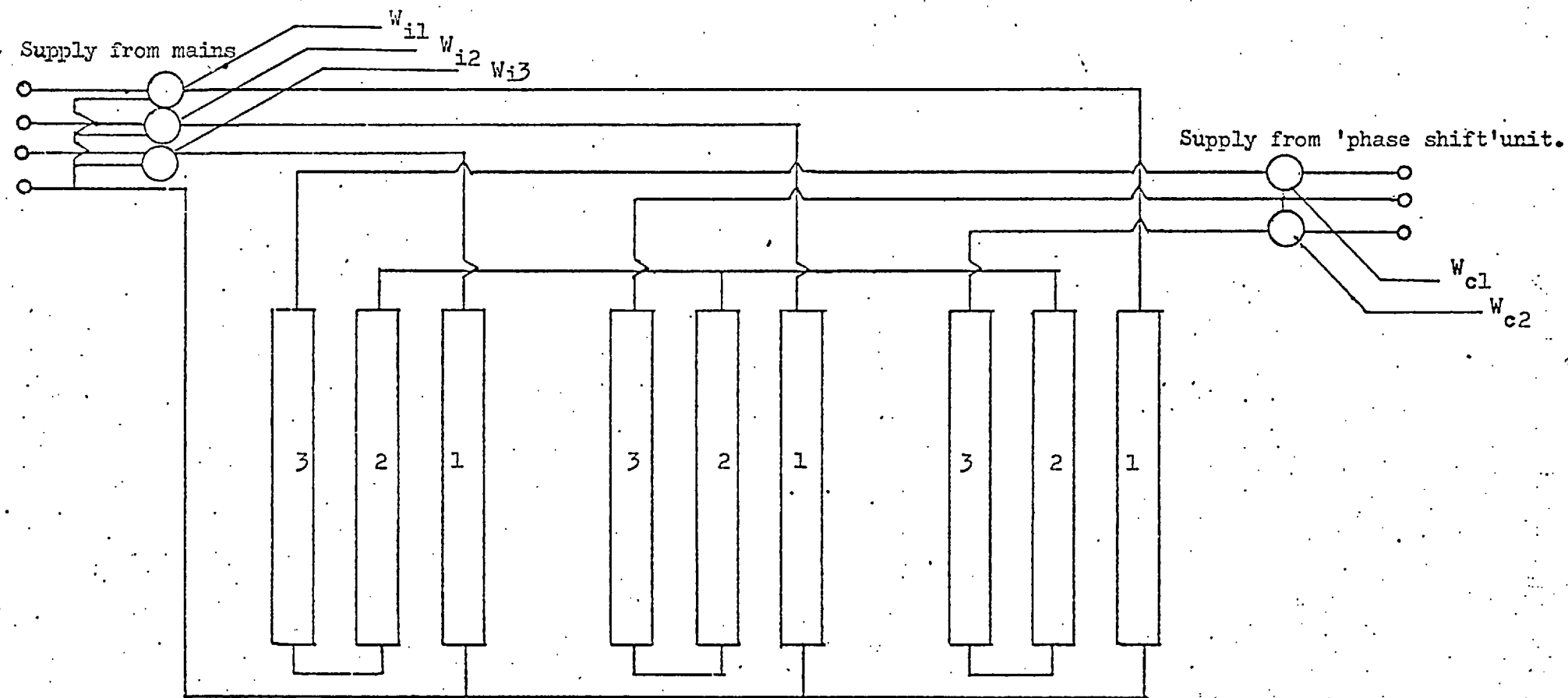


FIG. 7.2

Synthetic load test circuit for a unity ratio transformer.

to circulate the load current through the windings. Any shift in load current with respect to excitation circuit current or vice versa will not make any significant change in the phase relation of the load current to load voltage. However, a thorough investigation reveals that some other datum has to be fixed to measure the power factor of the load.

The load power factor is the cosine of the angle between the load current and the voltage driving this current, i.e. the load side terminal voltage. This voltage has a certain relationship with the induced voltage, which depends on the impedance of the secondary winding and the type of load. For a particular loading condition the relation can be given by:

$$V_2 = E_2 - I_2(R_2 + jX_{2l})$$

where R_2 and X_{2l} are the resistance and leakage reactance of the secondary winding through which a current I_2 is flowing.

The induced voltage has a quadrature relationship with the magnetizing flux which in turn is in phase with the reactive component of the excitation current, i.e. the magnetizing current. The relationship between the excitation current and counter e.m.f. can therefore be established, i.e. the excitation current lags the counter e.m.f. by very nearly 90° and this angle approaches to 90° as flux density increases. As shown in 2.2 this angle can be different for each phase in a highly fluxed three-phase three-limb transformer. On the basis of the above, the induced voltage can be made as datum as its position is being shifted with the excitation current if the latter is supplied through a phase shift unit. The induced voltage in an open circuited secondary transformer winding is considered to

be very nearly equal to the impressed primary voltage times the turns ratio due to small impedance and low current in the winding. In the case of the present test the excitation winding would have the same relationship in the transformer as an open circuited secondary, although windings nos. 2 and 3 will be circulating the full load current but the resulting m.m.f. around the main magnetic circuit due to their combined effect will be zero. The impressed voltage of winding no. 1 can therefore be considered as equal to the induced voltage and thus will have a similar relation to the secondary output voltage. The power factor of the load thus can be measured if the current coil of a phase angle meter is connected in series with the load current circuit of windings 2 and 3 and potential coil to the impressed voltage of winding no. 1.

7.4.1 Correction factor for phase angle meter reading

For more accurate computation of the load power factor, correction to the reading of the phase angle meter can be made. Figs. 7.3 and 7.4 show phasor diagrams of a unity ratio transformer for lagging and leading load angles respectively. Angle ϕ_1 can be measured by open circuit test. Angle ϕ_2 can be computed from the circle diagram of the transformer. A correction chart on this basis was made to correct the phase angle meter reading in this test. As shown in these phasor diagrams the angles ϕ_1 and ϕ_2 must be added to the phase angle meter reading for the capacitive load and be subtracted from it for the inductive load to get correct load power factor. The phase angle meter reading can also be corrected from input/output and impedance characteristics of the transformer and thus power factor of the load. E.g.

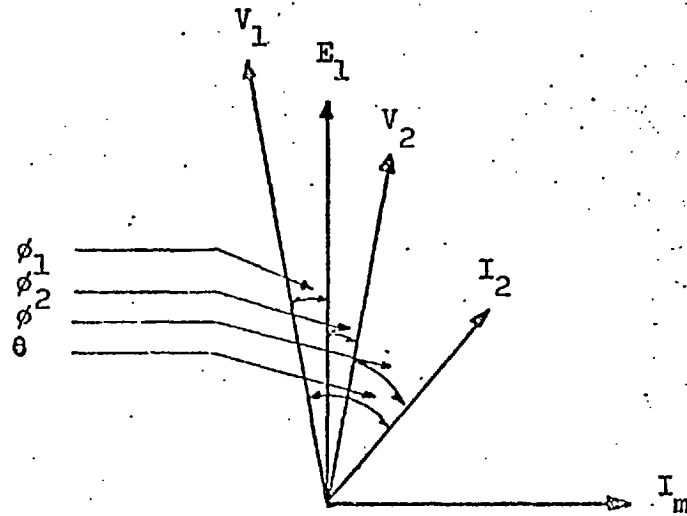


FIG. 7.3

Phasor diagram of a unity ratio transformer with lagging power factor load. (Vectors used to compute load p.f. are only shown.) (θ = phase angle meter reading.)

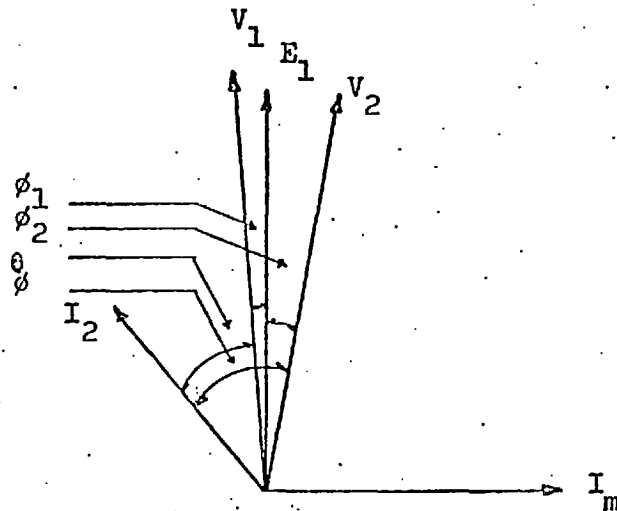


FIG. 7.4

Phasor diagram of a unity ratio transformer with leading power factor load. (Vectors used to compute load p.f. are only shown.) (θ = phase angle meter reading.)

1. Let ϕ_1 be the angle between the open circuit impressed voltage V_1 and induced voltage E_1 and let the open circuit impedance drop be given by $I_1 Z_1$, the angle ϕ_1 can be given by:

$$\phi_1 = \cos^{-1} \left[\frac{V_1^2 + E_1^2 - (I_1 Z_1)^2}{2V_1 E_1} \right]$$

2. Let ϕ_2 be the angle between the output terminal voltage V_2 and the secondary induced voltage E_2 and let $I_2 Z_2$ be the secondary impedance drop at rated secondary current, the angle ϕ_2 can be given by:

$$\phi_2 = \cos^{-1} \left[\frac{V_2^2 + E_2^2 - (I_2 Z_2)^2}{2V_2 E_2} \right]$$

The above condition is for lagging power factor or leading power factor near unity where $V_2 > E_2$.

The load phase angle ϕ can thus be computed from the above angles and the phase angle meter reading θ by:

$$\phi = \theta - (\phi_1 + \phi_2)$$

In the case of capacitive load when $V_2 < E_2$, the angle ϕ_2 can be given by:

$$\phi_2 = \cos^{-1} \left[\frac{V_2^2 + E_2^2 + (I_2 Z_2)^2}{2V_2 E_2} \right]$$

and load phase angle by:

$$\phi = \theta + (\phi_1 + \phi_2)$$

In the above, Z_1 and Z_2 are obtained from measured winding resistances and the components of leakage reactances, the latter being divided between the two windings as the square of the number of turns^{-7.5}.

7.5 TEST ARRANGEMENTS

The synthetic load test to measure the core loss and to study its variation with load angle was performed on the same three-phase test transformers which were used in the actual load tests detailed in Chapter 6.

Since this transformer has a set of three windings of the same size of conductor and number of turns around each limb, together with shadow winding for each main winding, it was considered to be an ideal unit for such a test. The experimental arrangement for this test has been shown in Fig. 7.2. Winding no. 1 was connected to the mains through three single-phase autotransformers and iron loss per phase was metered by a low power factor wattmeter connected in compensated mode to exclude error due to its potential circuit consumption. The sum of per phase readings less copper loss of winding no. 1 due to excitation current was taken as core loss against each load angle position.

Windings nos. 2 and 3 were connected in series opposition and the load current was circulated from the mains through a set of induction regulators wired as phase shifting unit. The ohmic and stray loss due to load current was metered by a standard dynamometer wattmeter (Cambridge A.C. Test Set Type 44371) connected in this circuit. A two-wattmeter method was used to measure this power loss.

The power factor was measured with a phase angle meter, the potential circuit of which was connected to the shadow coil of winding no. 1 of the respective phase and current coil to the load current circuit. The phase angle meter reading was corrected as per Section 7.4 and power factor computed.

7.5.1 Computation of core loss

It was anticipated on theoretical grounds and from the results of previous tests performed on this transformer that the change in the angular relationship between the load current and the excitation current would give a change in the power consumed in the excitation circuit only and there would be no change in the power loss metered on the load side of the circuit.

It was, however, observed that the change in the relationship of the excitation current to the load current influences the readings of wattmeters in both the directions. The possible reason for this variation of power flow in the load circuit and hence an associated change in the excitation current are discussed in Section 7.7.2. The computation of core loss in this condition is made as under:

The total power flow in both circuits is the sum of the core and winding copper losses. Since a.c. resistances of all the windings used in the test are known, and the current in each circuit can be metered, the total copper loss of all the windings employed can be computed. The core loss can thus easily be worked out by subtracting the total copper loss from the total power measured in both circuits.

$$\text{Core loss} = \text{Power supplied by the excitation circuit} + \text{Power supplied by the load current circuit} - \text{Total copper loss of the windings (excitation and load current)}$$

On the basis of the above, the core losses computed are plotted against power factor in Fig. 7.5.

A dimensionless graph on the basis of unity power factor comparing the core loss computed by the synthetic load test and with

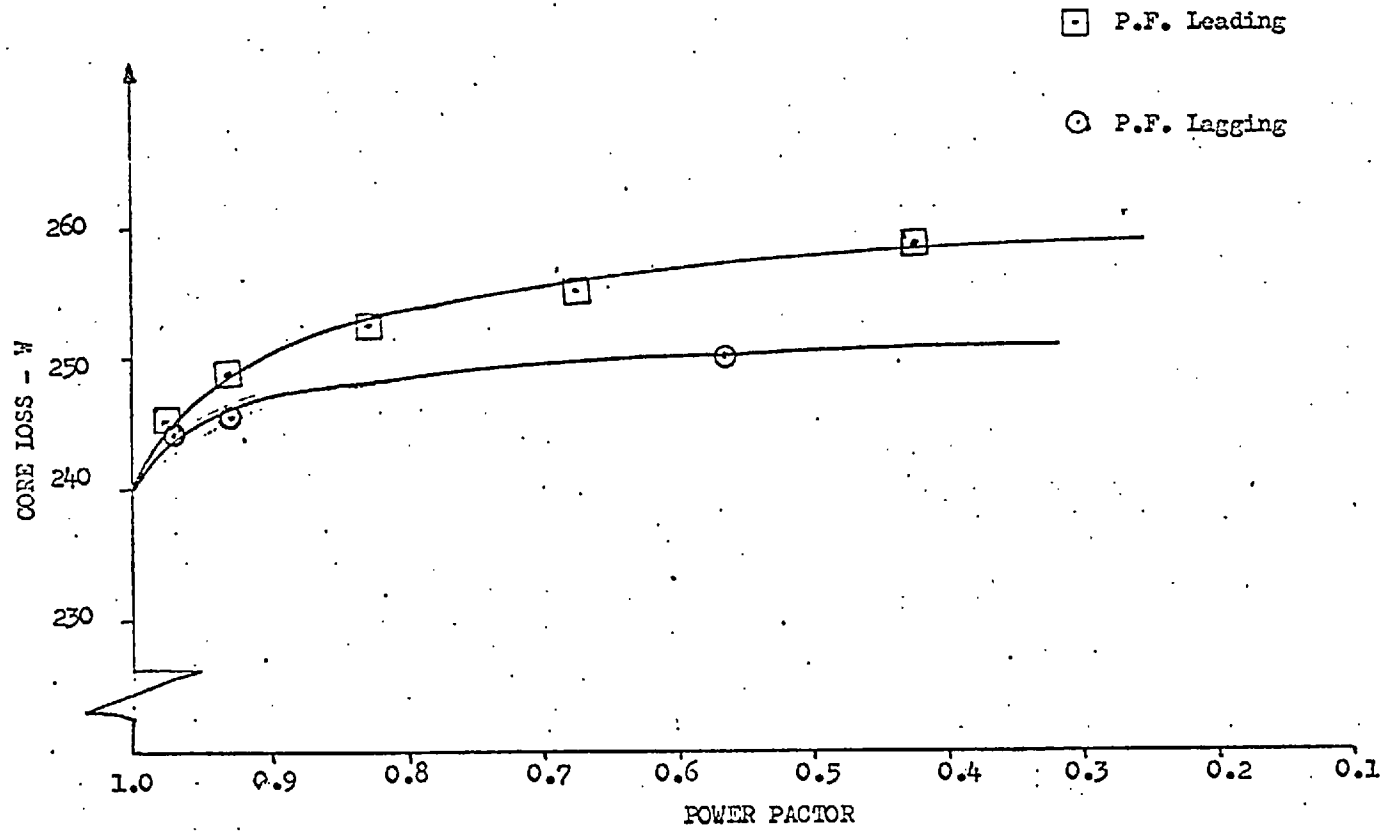


FIG. 7.5

On-load core loss of a three-phase transformer measured by dynamometer wattmeter on synthetic loading.

the actual load test for the measurements made by VAW meter has been plotted against power factor in Figs. 7.6 and 7.7, for leading and lagging power factors, respectively.

The p.u. leakage reactance of this transformer was very small compared to resistance, also the ratio of leakage reactance between winding 1 and 2 to that of winding 1 and 3 was 1:3 which is too large compared to a power transformer and also the p.u. leakage reactance is usually considerably higher in the latter units.

The results plotted do show the dependence of core loss on load power factor and the trend is similar to that noticed in actual load loading. The percentage variation is, however, not even approximately the same. Apart from the factors discussed in 7.7, a further limitation was the capacity of phase shifting unit due to which only 60% of the rated current was circulated in the windings. The transformer having a large thermal time constant might not have attained a steady working temperature, and thus the winding resistance may not be stabilized. If a large current had been circulated, the percentage effect of the inequality of the reactance would have been far less and better results could have been obtained.

On the basis of the nature of these positive qualitative results, it was decided to perform this test on a "micro" transformer having p.u. leakage reactance characteristics and therefore relative excitation and load current m.m.f.'s more representative of an actual high rating transformer.

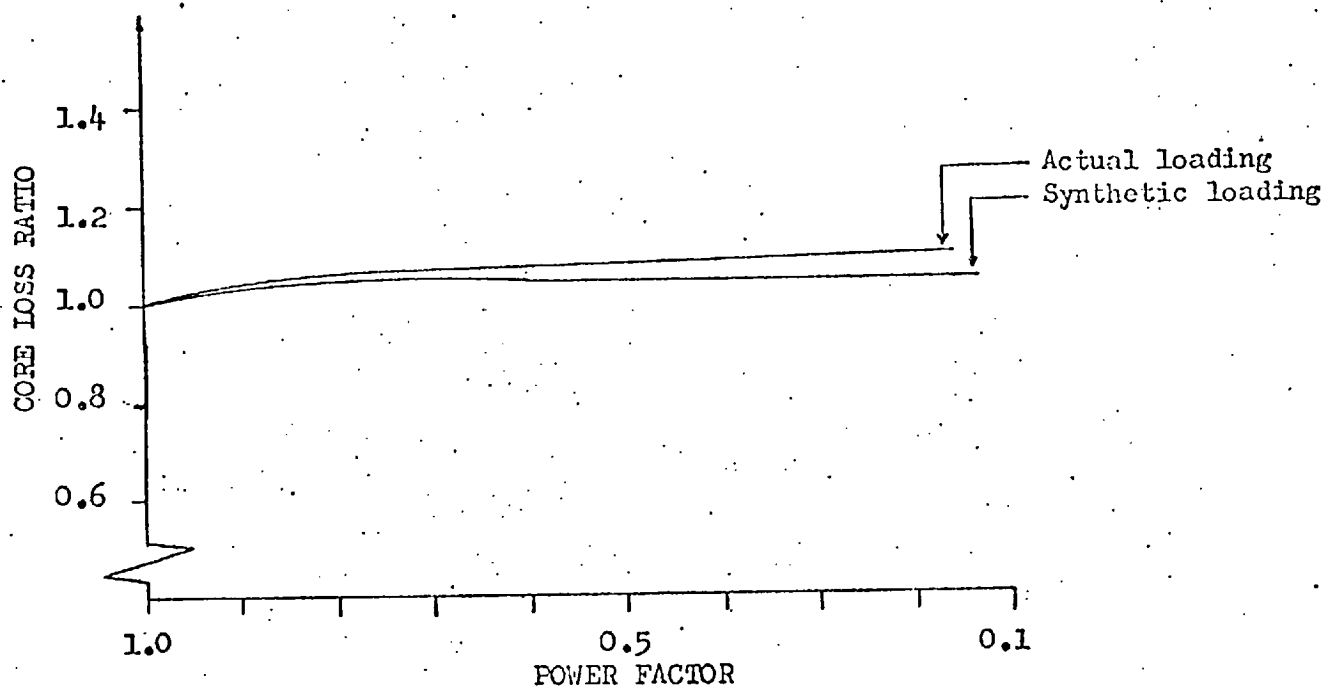


FIG. 7.6

Comparison between core loss ratios of actual loading and synthetic loading of three-phase transformer with leading power factor load.

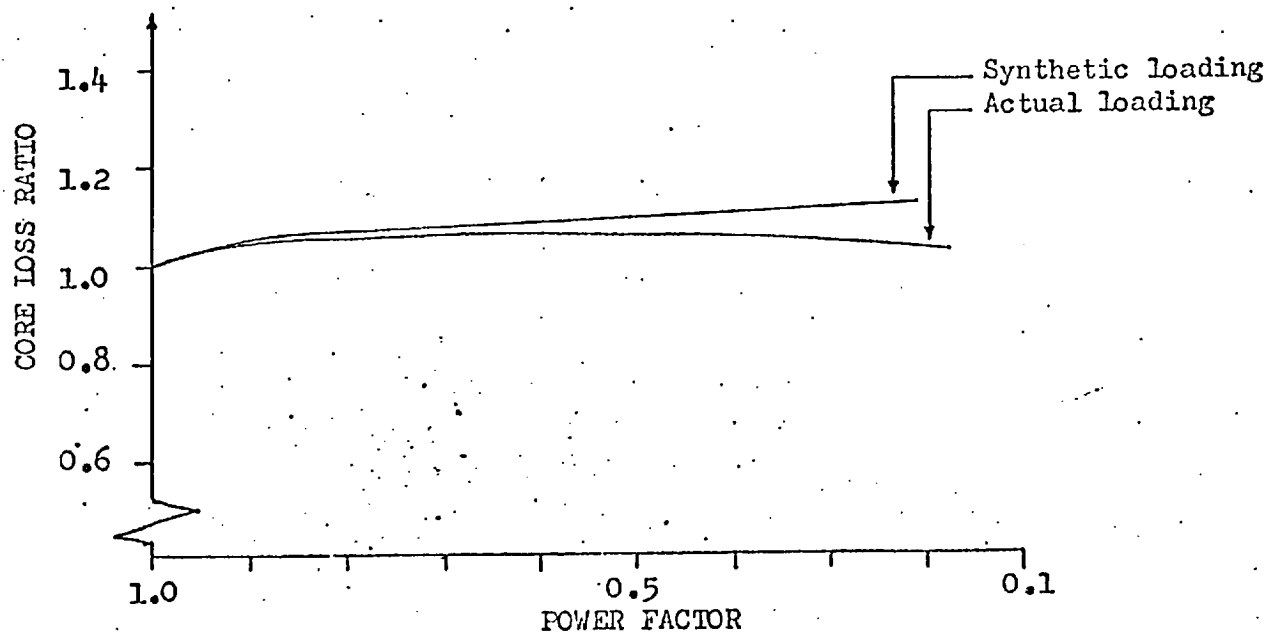


FIG. 7.7

Comparison between core loss ratio as Fig. 7.6 but with lagging power factor load.

7.6 TESTS ON MICRO TRANSFORMER

The single-phase micro transformer was taken from the bank of a 6-phase/3-phase system^{7.6}. This unit was selected for the following reasons:

1. The designed working peak flux density was 1.7 T, thus very near to that of three-phase unit on which the previous tests were made.
2. The per unit impedance characteristics were more nearly equivalent to those of an actual generator transformer.
3. The arrangement and the number of windings enable it to be connected as a unity ratio transformer.

The transformer data are given in Table 7.1 and the physical arrangement of windings is shown in Fig. 7.8.

The following tests were performed on this transformer to measure its core loss:

1. Open circuit test.
2. On load test for core loss measurement with varying load power factor.
3. Synthetic load test for core loss measurement.

7.6.1 Winding connections

Since winding pairs nos. 3 and 6, and 2 and 5 both have the same number of turns and are symmetrical around the inner main limbs, either can be used as magnetizing windings or load windings.

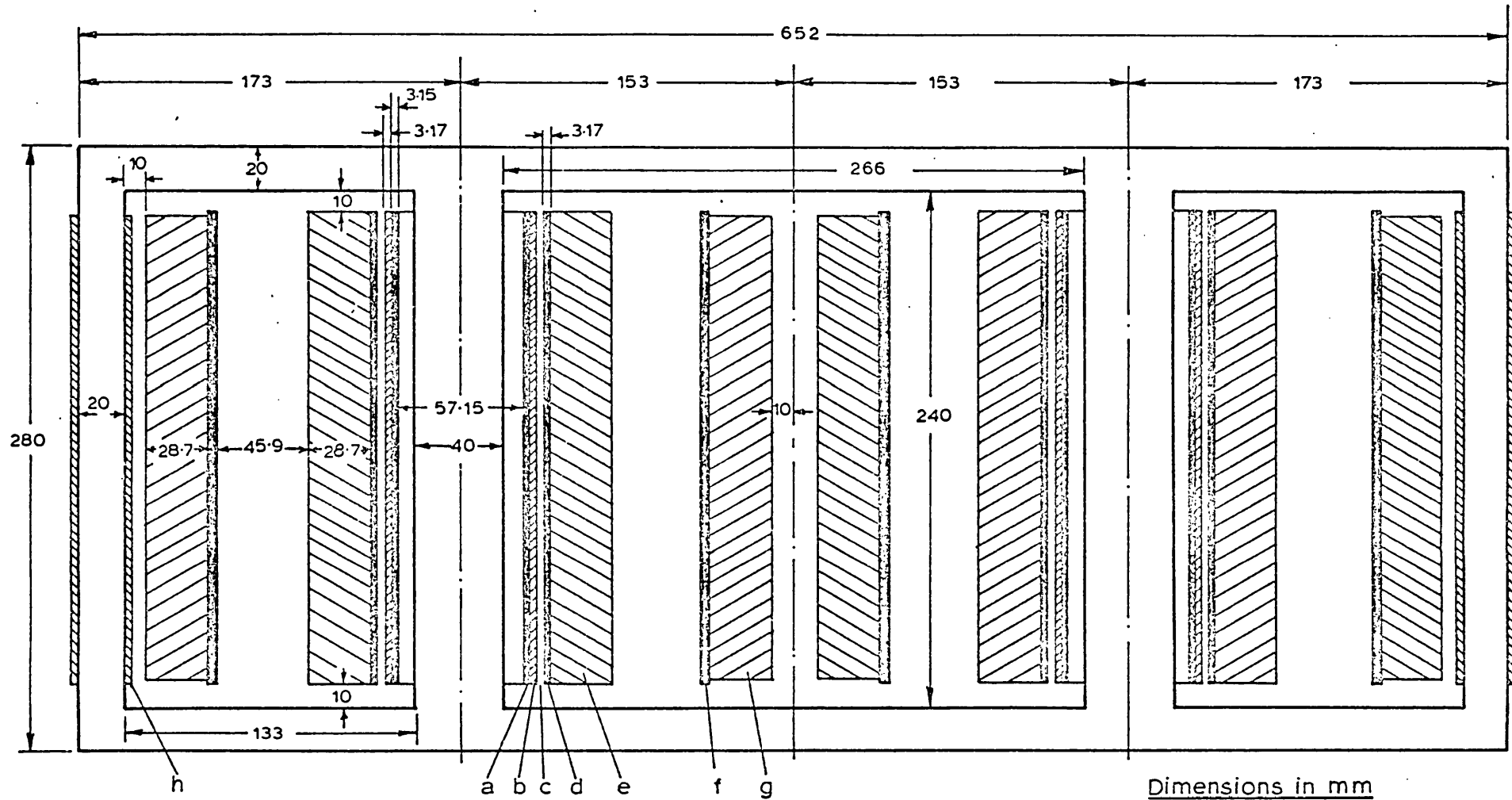


Fig. 7.8 Design of 1000 VA single unit micro-transformer with four windings.
*a - First base cylinder b- Tertiary winding c- Spacing for cooling the tertiary, d- Second base cylinder
 e- First low voltage winding f- Third base cylinder g- Half h.v. winding h- Search coil*

Winding No.	Number of Turns	Nominal Current Rating	Rated Voltage	Terminal Marking
1	104	8.6	60	c_1-c_2
2	26	8.6	15	$3c_1-3c_2$
3	208	4.8	120	c_3-c_4
4	180	5	104	f_1-f_2
5	26	8.6	15	$4c_1-4c_2$
6	208	4.8	120	c_1-c_2

TABLE 7.1

Micro transformer terminal marking and data.

Tests were performed to find the best combination such that when the magnetizing windings are excited to the rated voltage, the induced voltage in the other two windings should be equal. This condition is necessary to eliminate the circulating currents within the winding due to any differential voltage when the windings are connected in opposition. The reason for unequal induced voltage has been discussed in 7.7.2. Four possible combinations were available and each was tested with one pair of windings excited to produce the designed flux density in the core and the other open circuited. The percentage difference in the induced voltages was checked on a digital voltmeter and the best combination selected was:

Windings 3 and 6 connected in series, induced voltage percentage difference = 0.13% in windings 2 and 5. The above pair of windings was considered as magnetizing windings and excited to 240 volts to produce a flux density of 1.7 T in the core. Windings nos. 2 and 5 were connected in opposition to circulate the rated current (8.6 A) in the case of a synthetic load test.

7.6.2 Open circuit test

The standard procedure for this test was adopted. Windings nos. 3 and 6 were connected in series and supplied through a "Variac" while all other windings open circuited. The core loss thus obtained is plotted in Fig. 7.9.

7.6.3 Core loss measurement under load conditions

The method used to extract a signal proportional to excitation current was that given in 3.4.3.1. The measurement of

core loss was effected by multiplying this signal by a constant magnitude current signal taken from phase shifting unit and shifted in phase with the primary induced voltage. This was done using VAW meter as explained in 4.6.2.

Since the primary and secondary windings had a turns ratio of 8:1, the input to output current ratio was therefore 1:8. To obtain correctly proportional voltage drop signals, the series resistors inserted in both the circuits were having resistance ratio inverse to the current ratio. This was obtained through two linear track resistors of 1Ω , 20 A rating calibrated by a Kelvin Bridge to $.848\Omega$ and $.106\Omega$ respectively for primary and load circuits.

The output of the VAW meter was calibrated by multiplying the no-load current signal taken across primary side resistor ($.848\Omega$) and amplifying the same through a 1:10 ratio isolating transformer with the current vector of the same magnitude as taken in the above test and shifted in phase to the induced voltage. The calibration was made with respect to a low power factor wattmeter connected in this circuit measuring the actual core loss. The calibration factor obtained was 6.4. The correction factors of both the wattmeters were taken into account. The core loss thus computed from the reading of the VAW meter taken over the range of load power factor and plotted against the latter is shown in Fig. 7.10.

7.6.4 Computation of core loss from instantaneous power loss

As discussed in 4.6.4, the core loss derivation can be done from the instantaneous power signal obtainable from VAW wattmeter. In the present setup this signal was taken on an oscilloscope on a

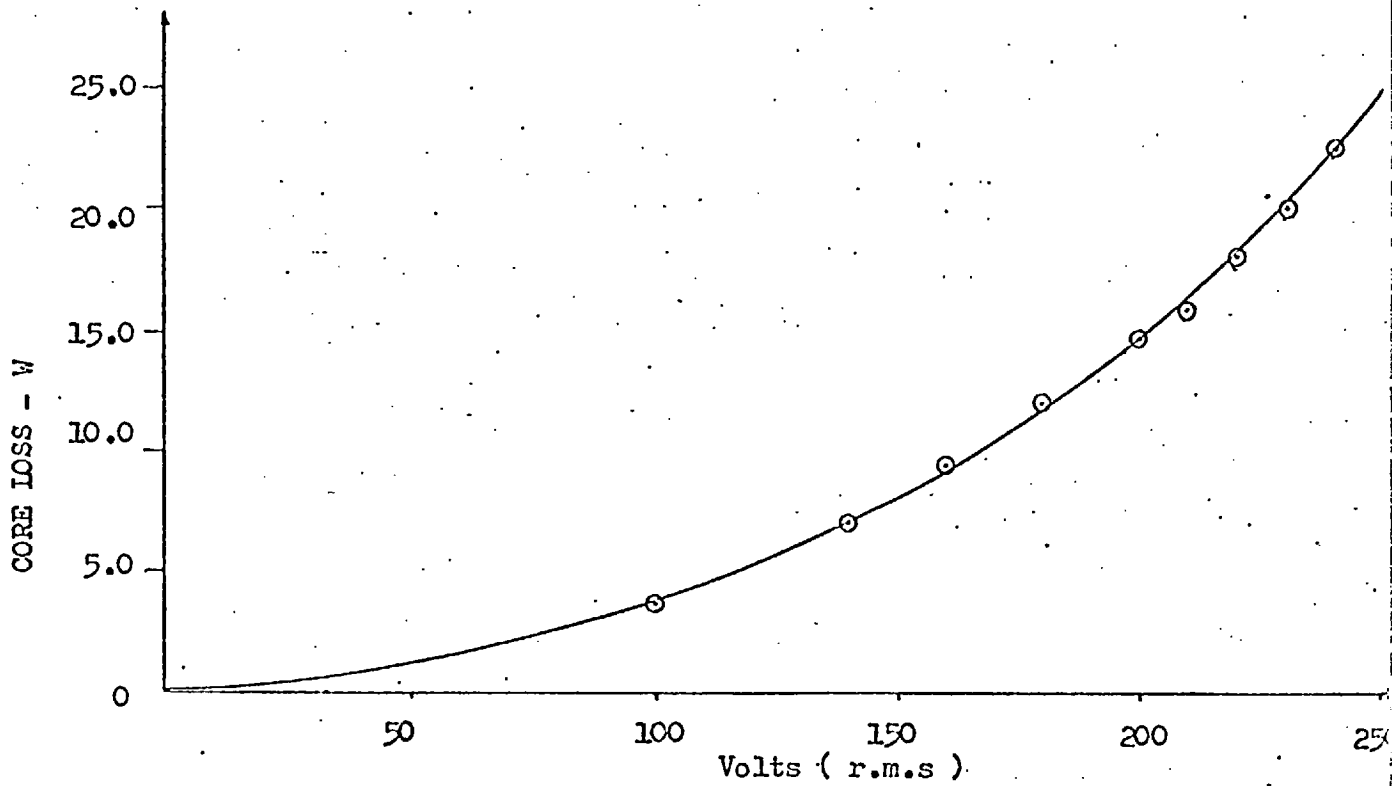


FIG. 7.9

No load core loss of 'micro transformer' with open circuited secondary.

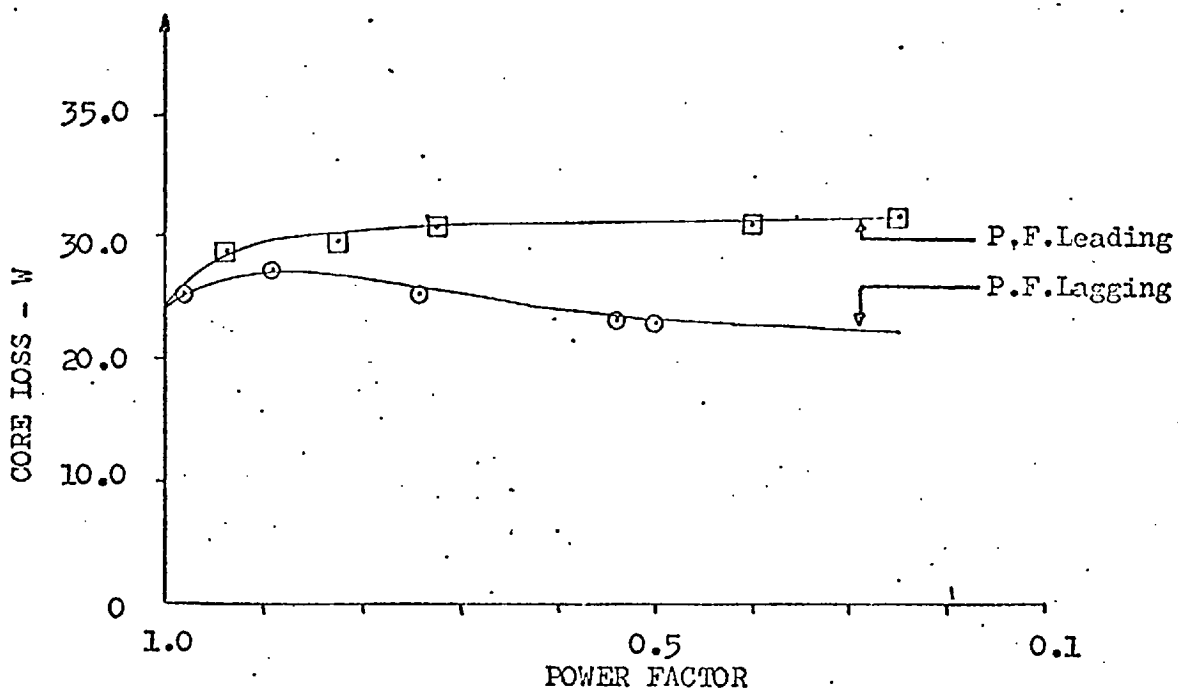


FIG. 7.10

On-load core loss of 'micro transformer' measured by VAW meter on actual loading.

suitable scale and photographed for three different load P.F. (Table 7.2) The areas under the positive half cycle and negative half cycle were measured with a planimeter calibrated in cm^2 with a constant factor of 16.537. The computation was referred to U.P.F. and compared with VAW readings also referred to U.P.F. for the same load angle. This comparison is given in Table 7.2. The comparison shows a close agreement in both methods of measurement. The waveforms of instantaneous power loss used in the computation are given in Fig. 7.11.

7.6.5 Dynamic hysteresis loops

The dynamic hysteresis loss loops for different load P.F. (Table 7.2) were formed for this transformer as given in 4.6.5. Since it was a single phase transformer, each loop can be directly related to the power loss. These have been shown in Fig. 7.12, which very clearly shows the dependence of the core loss on the load power factor.

7.6.6 Synthetic load test

The synthetic load test was performed in a similar way as on three-phase transformer. The full load current was, however, circulated in the load windings nos. 2 and 5 connected in opposition to the mains through the phase shifting unit.

It was anticipated that the only change will occur in the wattmeter connected in the excitation circuit, but it was observed that the indication of the wattmeter connected in the load circuit too was changing with the variation in load power factor. The change in the latter case is mainly attributed to the difference in

Measurement made by VAW meter:

Power factor	VAW meter reading	Core loss [*] W	Variation from U.P.F., W	% variation from U.P.F.
Unity	3.75	24.00	-	-
.54 Lagging	3.57	22.59	1.408(-)	5.86(-)
.88 Leading	4.45	28.48	4.48(+)	18.66(+)

* VAW meter reading x 6.4

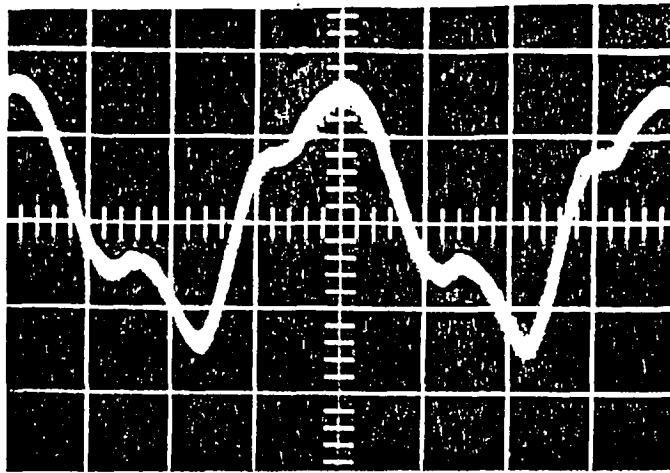
Measurement made by planimeter:

Power factor	Planimeter measurement		Difference	Difference [*] in area (cm ²)	% variatio from U.P.F
	+ve $\frac{1}{2}$ cycle	-ve $\frac{1}{2}$ cycle			
Unity	.6	.47	.13	.21498	-
.54 Lagging	.52	.397	.123	.2034	5.38(-)
.88 Leading	.67	.515	.155	.2563	19.2(+)

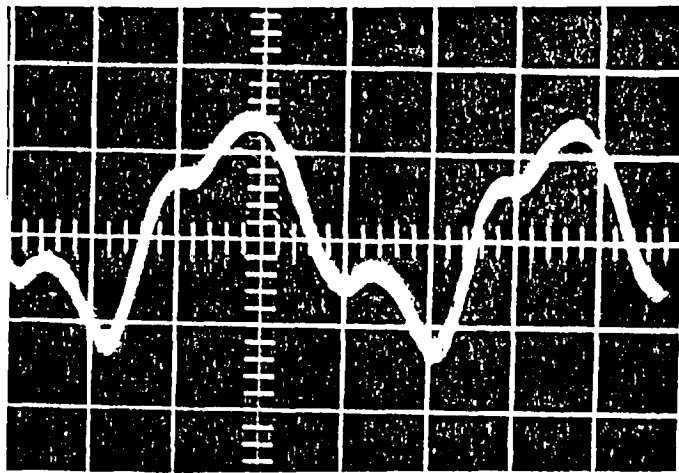
* Planimeter reading x 1.6537

TABLE 7.2

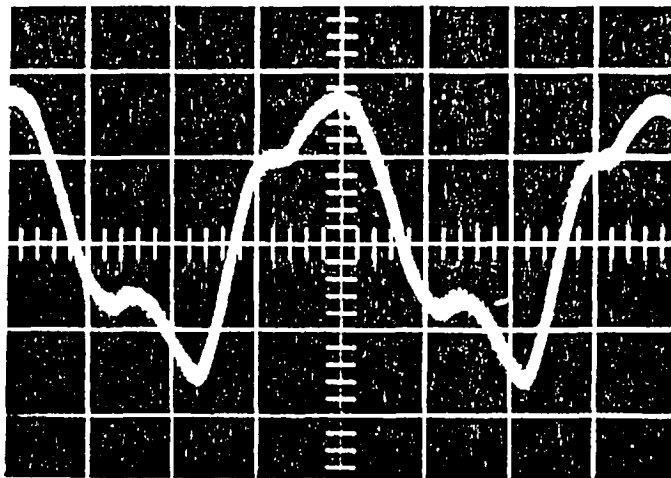
Comparison between VAW meter measurements and derivation of losses from instant power curves.



(a)



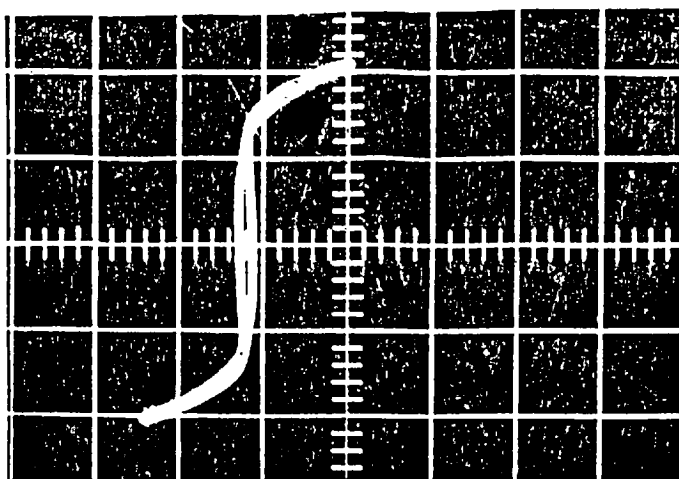
(b)



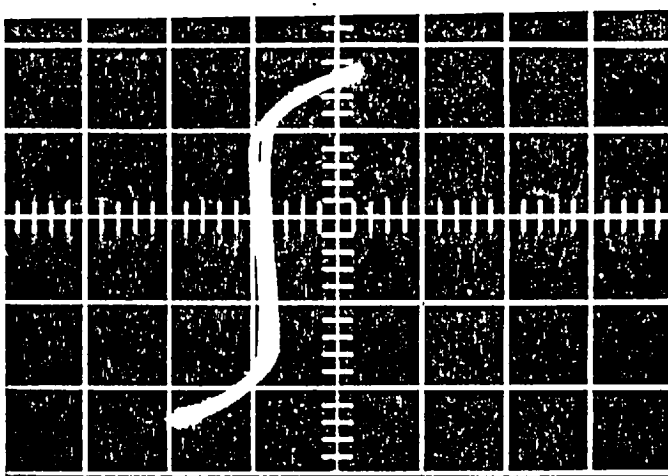
(c)

FIG. 7.11

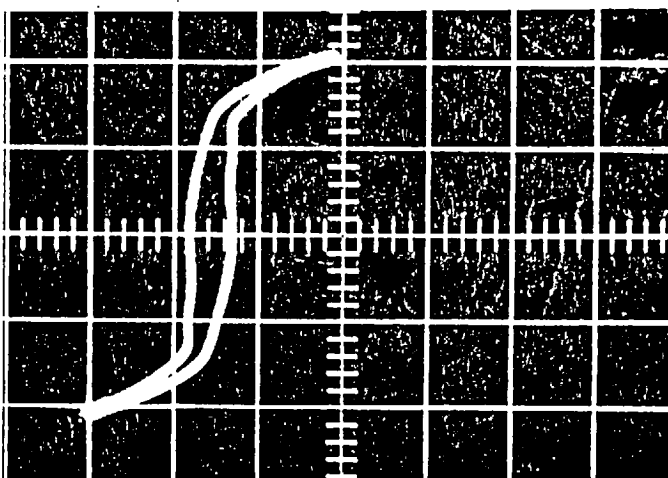
Instantaneous power for 'micro transformer' derived from the output of VAW meter. Oscillograms (a), (b) and (c) correspond to load p.f. of unity, 0.54 lagging and 0.88 leading respectively.



(a)



(b)



(c)

FIG. 7.12

Dynamic hysteresis loops of 'micro transformer' at load factors corresponding to (a), (b) and (c) of Fig. 7.11.

the leakage reactances of both load windings which causes an additional circulating current within the system due to difference in the induced voltage (see 7.6.1). It is possible that the difference in the induced voltage at certain load angles due to redistribution of leakage flux might have been increased enough to affect the system significantly and thus the indication of the wattmeter.

The inequality of the magnetic circuit due to the unequal reluctances of the outer limbs can also be associated with this change in the load circuit. A part of the current flowing in the load circuit of either winding might be contributing towards maintaining the resultant m.m.f. in the core, being produced primarily by the excitation winding. An attempt was made to reduce this inequality in the magnetic circuit by eliminating the outer limbs, i.e. open circuiting these limbs magnetically by providing heavy copper short circuiting rings around these limbs, thus limiting the flux to the central part of the core only. Since, however, the yoke had an area one-half of that of the main limbs, it was not possible to keep the same flux density in both of these parts of the core. The working flux density in the limbs drives the yoke into saturation. As both components of the core loss are flux density dependent, the contribution by the yoke in the total core loss would be increased in this condition and thus the above idea was abandoned.

The results obtained in the synthetic test have been plotted against load power factor and shown in Fig. 7.13. The comparison of these results was made with the results obtained by VAW meter measurements by plotting both on dimensionless basis with

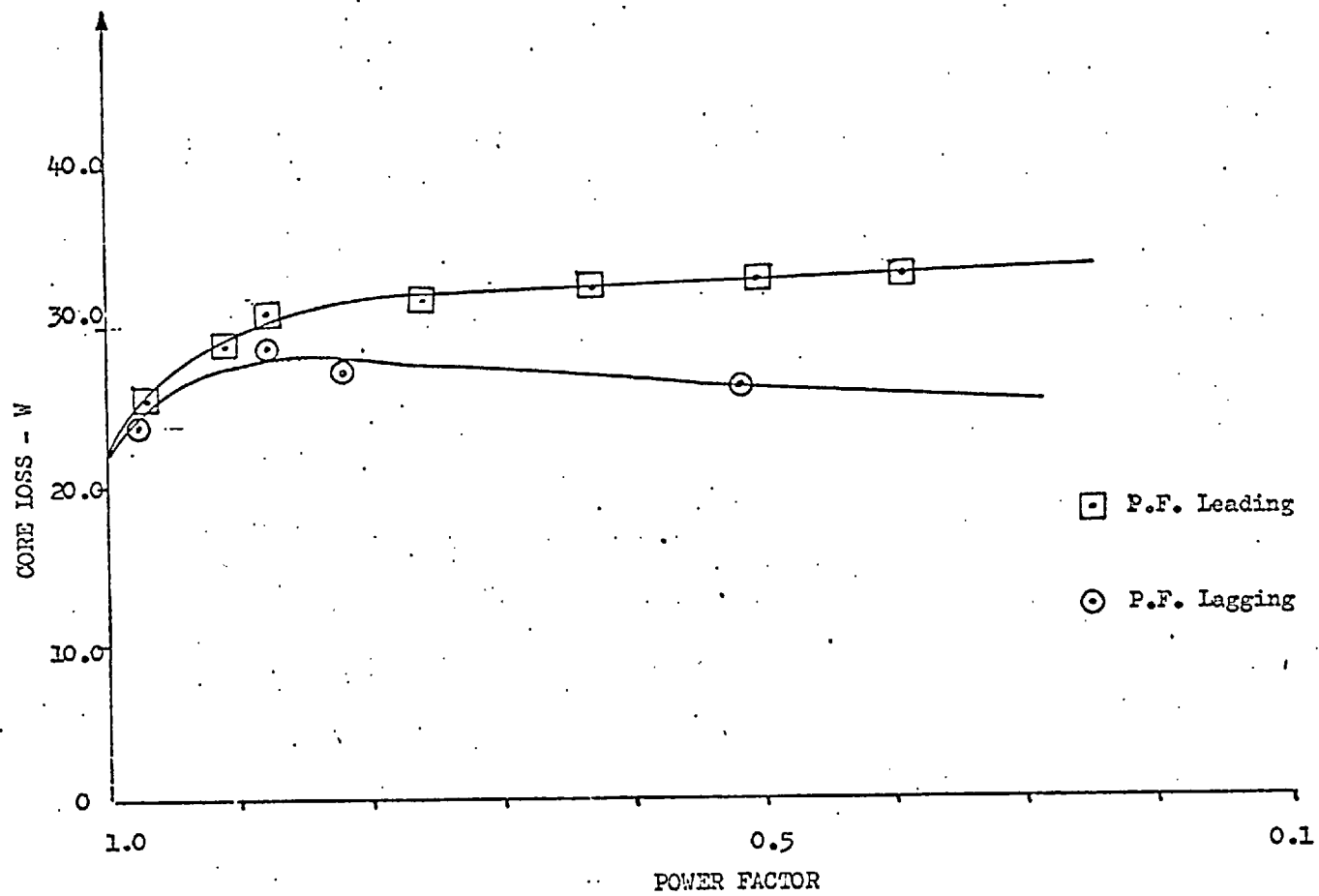


FIG. 7.13

On-load core loss of 'micro-transformer' measured by dynamometer wattmeter on synthetic loading.

reference to U.P.F. against load power factor. The synthetic load results show a slight increase over the VAW meter results but the trend of variation of both with respect to load power factor is very much similar. These plots have been shown in Figs. 7.14 and 7.15 for leading and lagging power factors respectively.

7.7 FACTORS AFFECTING SYNTHETIC LOADING AND THE COMPUTATION OF CORE LOSS

7.7.1 Geometrical considerations

The basis of the synthetic load test is the realisation of the simultaneous presence of the magnetomotive forces of the same magnitude and phase relation as in the case of an actual loading in a transformer. In practice it is not, however, possible to achieve this condition due to shift in the geometrical position of either:

- a) The source of excitation current with respect to the core (when the excitation is provided by some winding other than the winding which would have been the source of excitation current under actual loading), or
- b) The source of counter m.m.f. to balance the m.m.f. produced by the load current (when the excitation is provided by the same winding as under actual loading but the primary current winding is shifted from its original place).

In any production transformer to be tested by synthetic loading, one of the above two conditions would inevitably apply which will differentiate this loading from the actual load. However, test transformers for development purposes can be made having a shadow

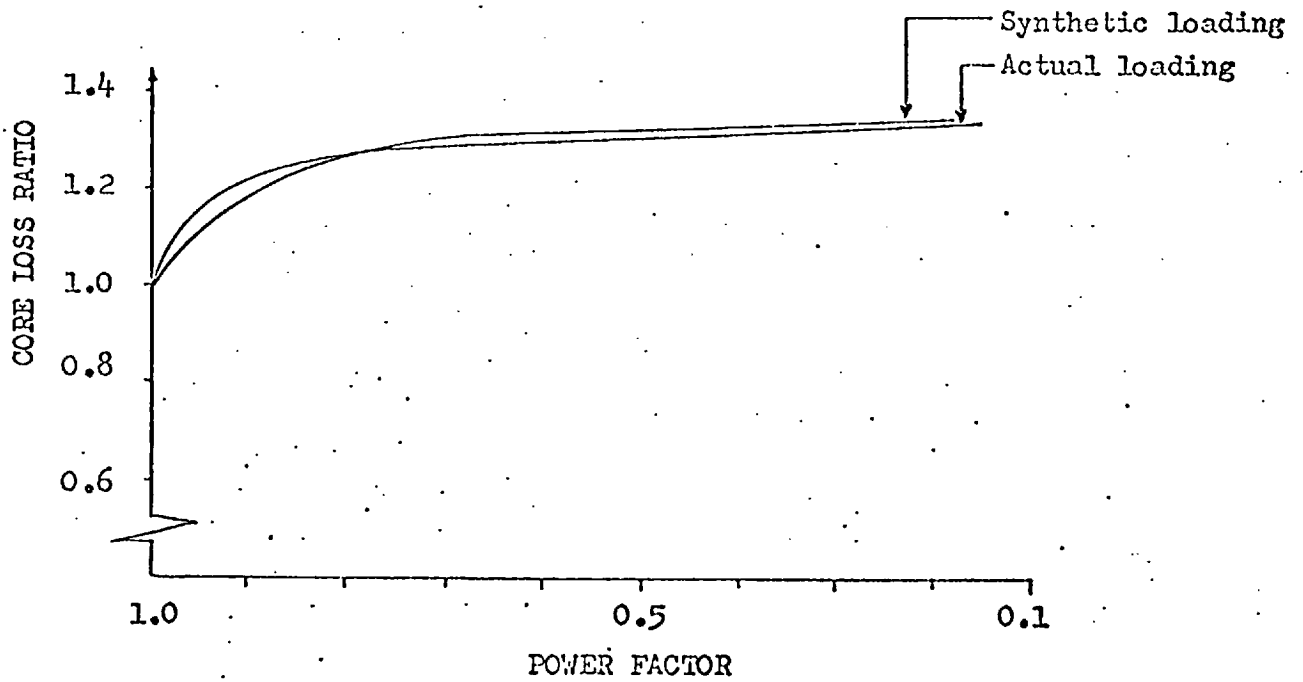


FIG. 7.14

Comparison between core loss ratio of actual loading and synthetic loading of 'micro transformer' with leading power factor load.

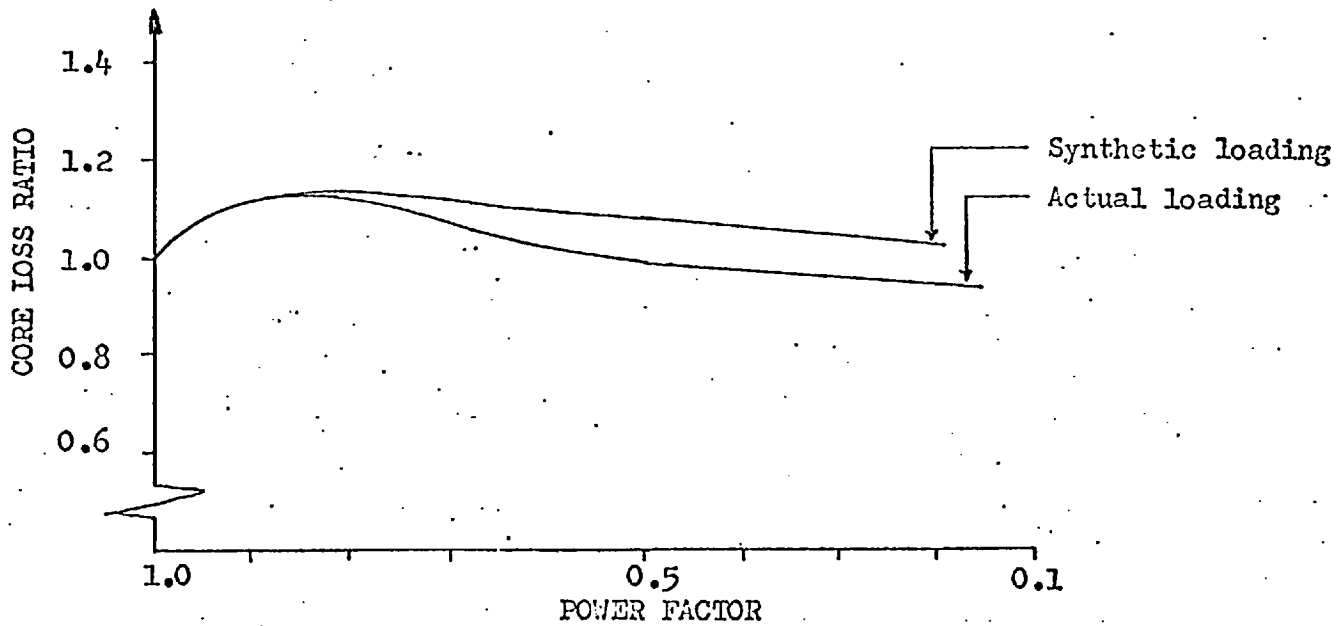


FIG. 7.15

Comparison between core loss ratios as Fig. 7.14 but with lagging power factor load.

winding along with the primary winding of such a rating that the excitation current can be circulated through it, thus maintaining the geometrical position of all the applied magnetomotive forces in synthetic load tests as in the case of actual load tests.

This geometrical displacement of m.m.f.'s is considered responsible for producing the discrepancies in the computed losses that have been observed in these tests. In micro transformer, windings 2 and 5 are physically close to actual load windings; results agree better.

7.7.2 Transfer of power between two circuits

As stated earlier, both wattmeters experience a change in their indications, although the wattmeter connected in the load circuit will only meter the copper and stray losses of load windings. Since the current in this circuit is kept fixed and as the a.c. resistance is stabilized, the indication of the wattmeter should remain constant as the transformer reaches its steady working conditions. It was further observed that at certain load angles the power metered in this circuit is even less than that required to meet the ohmic loss of the windings. This condition provides an indication as to whence the additional power is coming to make up these losses, evidently from the excitation circuit, a situation presumably not present in actual loading. Similarly, this circuit reads much higher than the ohmic loss of the windings at certain other load power factors, it must be then contributing towards maintaining the excitation in the core to the rated value. Thus was also apparent from the reduction in the reading of the wattmeter connected in the excitation circuit.

The above leads to the conclusion that the m.m.f.'s produced in antiphase by the load current windings do not cancel each

other at every point exactly around the core but some resultant m.m.f. remains and its effect on the core excitation is either additive, in which case the excitation current reduces or subtractive, in which case additional current has to flow in the excitation circuit. In either case there is a transfer of energy between the two circuits and thus the core loss has to be computed as shown in 7.5.1.

The reasons for the resultant m.m.f. around the core when the windings are connected in opposition and carrying the same flux could be:

1. These windings in the case of the three-phase test transformer do not occupy exactly the same geometrical position with respect to each limb and thus have differences in resistance due to different conductor lengths and also in leakage reactance. These inequalities may give rise to a small resultant m.m.f.
2. A small difference in the voltage balance (as in the case of micro transformer) can cause a circulating current within the windings when they are connected in parallel. This circulating current is another source of m.m.f. and thus may give rise to a small resultant m.m.f. around the core.

7.7.3 Waveform distortion of current and voltage

When the waveform of the excitation current and the induced voltage were checked for the effective change in the load angle, it was found that some distortion occurred in them as compared with the open circuit conditions and under actual load test. This distortion in the waveform can be due to the influence of differential

m.m.f. on the magnetizing m.m.f. of the core.

In the case of a sinusoidal voltage and a non-sinusoidal current (as in the case of the actual load test), the dynamometer wattmeter responds to the fundamental component of current only. Here, however, the response to the harmonics is also included in the reading. This explains the fact that the core loss measured by synthetic load test is somewhat greater in the case of a microtransformer.

7.8 EFFECTIVENESS OF SYNTHETIC TEST

From the results obtained and plotted, it is clear that this test shows the variation of core loss with load power factor which is qualitatively similar to that measured under actual loading of the transformer. For the purpose of the quantitative comparison, both of the transformers used were not adequate. The three-phase transformer had a relatively small leakage reactance and thus could not truly represent a large unit, while the micro transformer had more magnetic asymmetry in the outer limbs than a full size transformer although, generally, it gave a better representation of a larger unit.

The results as a whole prove the usefulness and suitability of this test for manufacturers' development and also standard type test for transformers designed to operate at high flux densities.

CONCLUSIONS AND SUGGESTIONS FOR FUTURE WORK

This work was carried out on three different topics which although interconnected, have their own applications. The conclusion, therefore, reached in each case is stated separately.

8.1 OPEN CIRCUIT TEST

The open circuit test for a highly fluxed three-phase, three-limb core type transformer shows that:

1. The excitation currents lose their symmetry and therefore the phase angle between phase current and voltage is not the same for all three phases. This is in addition to the magnitude difference due to differences in the magnetic path length associated with each phase. One of the outer phases has in fact a phase angle greater than 90° and the other, a phase angle less than the material phase angle. The middle phase current and voltage, however, have a phase angle equal to the material phase angle.
2. The two-wattmeter method used for core loss measurement can give significantly erroneous results. One reason is the phase angle error of the wattmeter as one wattmeter works under lagging power factor conditions and the other with leading power factor. The other reason is on account of each individual meter's high reading with a relatively small difference representing the core loss. The three-wattmeter method is relatively the best as all three wattmeters work at lagging power factor.

Also, the reading of each individual wattmeter is not as large as the two-wattmeter method, relative to their algebraic sum which represents the core loss.

3. If the use of the two-wattmeter method is unavoidable, the commonly adopted method of connecting the wattmeter current coils in the outer limb circuit should not be used as this arrangement gives the maximum error due to very large wattmeter readings with relatively small difference. The best connection method in the two-wattmeter measurement case is that where individual wattmeters give a comparatively small reading relative to their difference, i.e. connection shown in Fig. 2.1c.

8.2 EXTRACTION OF EXCITATION CURRENT AND ON LOAD CORE LOSS MEASUREMENT

1. The best method of extracting the excitation current is the ohmic potential drop method although, in this case, for core loss measurements special wattmeters are required as the differential current thus obtained is not the actual excitation current but a signal proportional in magnitude and in phase to this current. The direct differential method of excitation current extraction has the advantage that any low power factor dynamometer wattmeter can be used to measure the core loss but it is limited to unity ratio transformer only. The current transformer differential method has the attractions of flexibility and low energy loss associated with the circuit but the shift in phase angle of the extracted current made the core loss measurements unrealistic.

2. The core loss measurements show their dependence on the load power factor and this loss is more sensitive to leading than to lagging reactive loads (see Figs. 6.11 and 6.12).
3. A further investigation revealed that under leading power factor load the increase in the excitation current of the middle limb is greater than the outer limbs. This is further confirmed by the change in the phase angle between the excitation current and voltage of the limb (material characteristic phase angle) which behaves in a similar manner to excitation current. As no change in the magnetization component of the excitation current is observed (see Section 6.4.2), the entire change is due to the core loss component of the excitation current. This shows that, due to redistribution of flux at leading load power factor, the overall change in the core loss component of the excitation current is positive, i.e. giving more core loss. Since this change is greatest in the middle limb, it indicates that this limb is actually dissipating a greater loss than the outer ones at leading reactive loads. An earlier test^{8.1} made to detect the change in leakage flux distribution in the region of middle limb joint and yoke by differentially connecting the search coil nos. 3 and 5 (Fig. 6.1) showed that the leakage flux increases in the region of middle limb joint at leading power factor load. It is a well known fact that a rotating magnetic field is produced at T-joint of the three limb core and the iron loss in the T-joint is dependent on the magnitude and rotating speed of this flux^{8.2}. The magnitude of the same has been checked against a number of factors, but has not so far been checked against load power

factor. It is evident from the present work that there is an increase in the leakage flux with the leading load power factor in the region of T-joint and there is every possibility that the rotating field experiences an increase in the magnitude under this condition, thus the middle limb joint works at higher flux density and absorbs more power. There is a possibility that adjustment in the cross-section area of the core around this region may reduce the overall percentage increase in the core loss if the working flux density of the same is kept substantially near to the rest of the core under conditions when the load power factor is leading.

4. The Hall effect wattmeter constructed for this project gives very good results even at very low power factor. The results are virtually identical with those obtained by VAW meter. The meter performance can be made even better by using better quality operational amplifiers and its range can be extended by the provision of additional circuitry containing switchable resistors for current and voltage channels.

5. The derivation of core loss from the instantaneous power loss curve and the display of dynamic hysteresis loops of the transformer core could have academic interest as it would be fascinating to demonstrate these to students and show them the actual change in the loop area with the load power factor.

8.3 SIMULATION OF THE ON LOAD CONDITIONS IN THE TRANSFORMER BY SYNTHETIC TEST

The synthetic load test results made on the micro transformer to measure the core loss show a sufficient agreement with those

under an actual load by VAW meter. Since the test can be made to simulate full load conditions without handling the rated VA of the transformer, it is hoped that further development in the method will lead to establishing its validity as manufacturer's type test and a good tool for development purposes. The improvement in its results can well be checked if a shadow coil suitable to take the excitation current of the test transformer is wound along with one of the main windings, thus keeping the geometrical positions of all the applied m.m.f.s. in synthetic load test as in the case of actual loading.

REFERENCESCHAPTER ONE

- 1.1 Nakata, T., Ishihara, Y. and Nakano, M., "Analysis of magnetic characteristics of three-phase core-type transformer with triple layer core". Elec. Eng. in Japan, Vol. 91, No. 3, p. 17, 1971.
- 1.2 Rele, A. and Palmer, S., "Cooling large transformer cores". Trans. IEE (PAS), Vol. 91, No. 4, p. 1527, 1972.
- 1.3 Nakata, T., "Analysis of flux distribution of three-phase, three-limb transformer core". As Ref. 1.1, Vol. 95, No. 3, p. 43, 1975.
- 1.4 Kawaguchi, Y., "Design of electrostatic shielding rings installed at the corner of the transformer". Ibid, Vol. 91, No. 1, p. 1, 1971.
- 1.5 Stigant, S.A. and Franklin, A.C., "J & P Transformer Book". Newnes-Butterworth, London, p. 31, 1973.
- 1.6 Davis, E.J., "Should we build slot-less machines". International Conference on Electrical Machines, City University, 1974.
- 1.7 Minutes CEGB - Imperial College meeting: "To discuss modelling a transformer with the intention of examining over-fluxing". January 1967.
- 1.8 Private discussion with Mr. A.C. Hall.

- 1.9 Campbell, A., "On the magnetic properties of silicon iron (Stalloy) in alternating magnetic field of low value".
Proc. Phys. Soc., 32, p. 779, 1920.
- 1.10 Stewart, K.H., "Losses in electrical sheet steel".
Proc. IEE, 97, Part II, p. 121, 1950.
- 1.11 Brailsford, F. and Fogg, R., "Anomalous iron loss in cold reduced grain oriented transformer steel".
Proc. IEE, Vol. III, No. 8, p. 1463, 1964.
- 1.12 Wilkins, F.J., "Measurement and interpretation of power losses in electrical sheet steel". Proc. IEE, Vol. 112, No. 4, 1965.
- 1.13 Wilkins, F.J., "Instrument for measuring local power losses in uncut electrical sheet steel". Proc. IEE, Vol. 112, No. 4, 1965.
- 1.14 Blomberg, H. and Karattunen, "A ferrometer for the determination of a.c. magnetization curve and iron losses of small ferromagnetic sheet sample".
- 1.15 Brailsford, F. and Bradshaw, C.G., "Iron loss at high flux densities in electrical sheet steel". Proc. IEE, p. 463, February 1955.
- 1.16 Nakata, T., Ishihara, Y. and Nakano, M., "Iron losses of silicon core produced by distorted flux".
Elec. Eng. in Japan, Vol. 90, No. 1, 1970.
- 1.17 MacFarlane, J. and Harris, M.J., "The control of flux waveform in iron testing by application of a feedback amplifier technique". Proc. IEE, Vol. 105, p. 390, 1958.

- 1.18 Cocks, F.D. and Nagy, F.N., "Measurement of iron loss in a single lamination at high flux densities with a Hall effect wattmeter". IEE Conference on Magnetic Materials and their Application, No. 33, p. 17.
- 1.19 McEachron, K.B., "Magnetic flux distribution in transformers". Trans. AIEE, p. 247, 1922.
- 1.20 Mankin, E.A. and Morozov, D.W., "Stray losses in large power transformer cores". Proc. CIGRE, paper no. 128, 1964.
- 1.21 Sato, T., Suzuki, Y., Saito, S. and Inui, Y., "Calculation of magnetic field taking into account eddy current and non-linear magnetism". Elec. Eng. in Japan, Vol. 96, p. 96, 1976. (July-August)
- 1.22 Nakano, S., Manura, T. and Iwamoto, M., "Three dimensional analysis of leakage field of power transformer". Ibid, Vol. 96, p. 55, 1976 (September-October).
- 1.23 Carpenter, C.J. and Lowther, D.A., "Losses due to transverse fluxes in laminated iron cores". IEE Conf. on advances in magnetic materials and applications, September 1976.
- 1.24 Carpenter, C.J., "Theory of flux penetration into laminated iron and associated losses". Proc. IEE, Vol. 124, p. 659, 1977.
- 1.25 Carpenter, C.J., "Heating in transformer cores due to radial leakage flux-computed results". Ibid, Vol. 124, p. 1181, 1977.

- 1.26 Hemmings, R.F. and Wale, G.D., "Heating in transformer cores due to radial leakage flux - experimental model and test results". Ibid, Vol. 124, p. 1064, 1977.
- 1.27 Swampillai, C.R., "The measurement of localised losses in magnetic cores using a Hall probe". DIC Dissertation, 1968. Imperial College, University of London.
- 1.28 Allen, P.H.G., "Loss measurement survey by Poynting vector wattmeter". Electrical Journal, December 1958. P. 1735.
- 1.29 Ali, M., "Generation of excessive losses in generator transformer core under leading power factor conditions". M.Sc. Report, Imperial College, London, 1970.
- 1.30 Hanna, R.A., "The six-phase two-circuit synchronous generator and its associated transformer". Ph.D. Thesis. London University, 1978.

CHAPTER TWO

- 2.1 Buckingham, H. and Price, E.M., "Principles of electrical measurements". The English University Press, p. 62, 1970.
- 2.2 Brailsford, F., "Current and power relationships in the measurement of iron losses in a three-limb transformer core". IEE Measurement Section paper no. 1550, p. 409, 1954.
- 2.3 MacFadyen, K.A., "Vector permeability". JIEE, Vol. 94, Part III, p. 407, 1947.

- 2.4 Stigant, S.A. and Franklin, A.C., "J & P Transformer Book".
Newnes-Butterworth, London, p. 227, 1973.
- 2.5 Blume, L.F. and others, "Transformer engineering". John Wiley
and Sons Inc., New York, p. 129, 1938.

CHAPTER THREE

- 3.1 American Standard C.42.15, "Definition of electrical terms
group 15". p. 9, 1958.
- 3.2 Members of MIT Staff, "Magnetic Circuits and Transformers".
MIT Press, Massachusetts, USA, p. 338, 1965.
- 3.3 Ali, M., "Generation of excessive losses in generator
transformer cores under leading power factor conditions".
M.Sc. Report, Imperial College, London, 1970.
- 3.4 Course notes, "Power system equipment course". Department of
Electrical Engineering, Imperial College, London, 1971
(Dr. P.H.G. Allen).
- 3.5 Jenkins, B.D., "Introduction to instrument transformers".
George Newnes Ltd., London W.C.2, pp.12-18, 1967.
- 3.6 National Physical Laboratories. Used to give ratio error employing
a R.C.F. but are following B.S. practice at present.
- 3.7 Jenkins, B.D., Reference 3.5, p. 7.
- 3.8 Jenkins, B.D., Ibid, pp. 59-60.
- 3.9 Mallinger, J. and Gewecke, H., "Zum Diagramm des Stromwandlers".
Elekt. Zeitsch., Vol. 53, p. 270, 1912.

- 3.10 Hague, B., "Instrument transformers". Sir Isaac Pitman and Sons Ltd., London, pp. 74-78, 1936.
- 3.11 Hague, B., Ibid, pp. 80-87.
- 3.12 Hague, B., Ibid, p. 105.
- 3.13 Park, J.H., "Accuracy of high range current transformers". Bureau of Standards, Journal of Research, Vol. 14, p. 367, 1935.
- 3.14 Kusters, N.L. and Moore, W.J.M., "The compensated current comparator; A new reference standard for current transformer calibration in industry". Trans. IEEE, p. 107, 1964.
- 3.15 Frood, T.R., "Current transformer - new method of error measurement". Electrical Review, 9th October, 1970.

CHAPTER FOUR

- 4.1 Steinmetz, C.P., "On the law of hysteresis". Trans. AIEE, Vol. 9, pp. 3-51, 1892.
- 4.2 Buckingham, H. and Price, E.M., "Principles of electrical measurements", The English University Press, p. 56, 1970.
- 4.3 Garret, D.E. and Cole, F.G., "A general purpose electronic wattmeter". Proc. IRE, pp. 165-171, 1952.
- 4.4 Barlow, H.E.M., "The design of semi-conductor wattmeter for power frequency and audio frequency application". Proc. IEE, pp. 186-191, November 1954.

- 4.5 As reference 4.2 above, but p. 61.
- 4.6 "Instruction Book", Weston Wattmeters Models S.67-S.99
Sangamo Weston Ltd., Enfield, Middlesex, England.
- 4.7 "Operating Instructions", AC Test Set Type 44371, Cambridge
Industrial Instruments Ltd., Sydney Road, London N.10
- 4.8 "Data Sheets", Vav Meter Model 102. John Fluke Manufacturing
Inc., P.O. Box 7428, Seattle 33, Washington.

CHAPTER FIVE

- 5.1 Hall, E.H., "The new action of magnetism on a permanent
electric current". Philosophical Magazine, p. 301, 1880.
- 5.2 Hollitscher, H., "Hall probe application for the design and
development of rotating machines". Solid-State
Electronics, Pergamon Press, p. 581, 1966.
- 5.3 Gregory, B.A., "An introduction to electrical instrumentation".
The Macmillan Press, p. 206, 1973.
- 5.4 Frank, E., "Electrical measurement analysis".
McGraw-Hill Book Co., USA, 1959.
- 5.5 Barlow, H.E.M., "The application of Hall effect in a semi-
conductor to the measurement of power in an
electromagnetic field". Proc. IEE, p. 179, 1954.
- 5.6 Kuhrt, F., "Eigenschaften der Hallgeneratoren". Siemens
Zeitschrift, 28, p. 370, 1954.

- 5.7 Billings, A.R. and Lloyd, D.J., "The sources of error in Hall effect multiplier". Proc. IEE, p. 706, 1960.
- 5.8 Barlow, H.E.M., "The design of semi-conductor wattmeters for power-frequency and audio-frequency applications". Proc. IEE, p. 186, 1954.
- 5.9 Pedder, D.A.G., Issawi, A.M. and Bolton, H.R., "A solid state variable frequency three-phase power source with individual harmonic control". Trans. IEEE Electronics and Control, p. 100, 1977.

CHAPTER SIX

- 6.1 Rippen, E.C., "Power plant for 1970's", Proc. IEE, Vol. 115, p. 103, 1968.
- 6.2 Adkins, B., "Transient theory of synchronous generators connected to a power system". Proc. IEE, Vol. 92(II), p. 510, 1951.
- 6.3 Stirzaker, E.G., "Determination of separate leakage reactance of transformer from no load test". Bull. Elec. Eng. Educ., No. 2 June 1960.
- 6.4 Boyajian, A., "Resolution of transformer reactances into primary and secondary reactances". Journal AIEE, p. 842, 1925.
- 6.5 O'Kelly, D., "Measurement of transformer winding leakage reactance". IEEE Trans. on Education. September 1968.

CHAPTER SEVEN

- 7.1 Rapson, E.T.A., "Experimental electrical engineering".
Sir Isaac Pitman and Sons Ltd., p. 128, 1964.
- 7.2 Stigant, S.A. and Franklin, A.C., "J & P Transformer Book".
Newnes-Butterworth, London, p. 299, 1973.
- 7.3 Reed, E.G., "The essentials of transformer practice".
Chapman & Hall Ltd., London, p. 34, 1927.
- 7.4 Hunt, W.L. and Stein, R., "Static electromagnetic devices".
Allyn and Bacon Inc., Boston, USA, p. 189, 1968.
- 7.5 Hunt, W.L. and Stein, R., Ibid, p. 165.
- 7.6 Hanna, R.A., "The six-phase two-circuit synchronous generator
and its associated transformer". Ph.D. Thesis,
London University, January 1978.

CHAPTER EIGHT

- 8.1 Ali, M., "Generation of excessive losses in generator
transformer cores under leading power factor conditions".
M.Sc. Report, Imperial College, London, 1970.
- 8.2 Nakata, T., "Analysis of flux distribution of three-phase
three-limbed transformer cores". Elec. Eng. in
Japan, Vol. 95, No. 3, p. 43, 1975.